

5-1-2013

Neuropathogenesis of highly pathogenic avian influenza in ferrets following intranasal instillation or aerosol exposure to low doses

Jennifer Plourde

Follow this and additional works at: https://digitalrepository.unm.edu/biom_etds

Recommended Citation

Plourde, Jennifer. "Neuropathogenesis of highly pathogenic avian influenza in ferrets following intranasal instillation or aerosol exposure to low doses." (2013). https://digitalrepository.unm.edu/biom_etds/139

This Dissertation is brought to you for free and open access by the Electronic Theses and Dissertations at UNM Digital Repository. It has been accepted for inclusion in Biomedical Sciences ETDs by an authorized administrator of UNM Digital Repository. For more information, please contact disc@unm.edu.

Jennifer Rose Plourde

Candidate

Biomedical Sciences Graduate Program

Department

This dissertation is approved, and it is acceptable in quality and form for publication:

Approved by the Dissertation Committee:

Brian Hjelle, M.D., Chairperson

Michelle Ozbun, Ph.D.

Bryce Chackerian, Ph.D.

Larry Davis, M.D.

Kevin Harrod, Ph.D.

**NEUROPATHOGENESIS OF HIGHLY PATHOGENIC AVIAN
INFLUENZA IN FERRETS FOLLOWING INTRANASAL
INSTILLATION OR AEROSOL EXPOSURE TO LOW DOSES**

by

JENNIFER ROSE PLOURDE

B.S., Biochemistry, University of Tampa, 2003
M.S., Operations Research, Air Force Institute of Technology, 2005

DISSERTATION

Submitted in Partial Fulfillment of the
Requirements for the Degree of

**Doctor of Philosophy
Biomedical Sciences**

The University of New Mexico
Albuquerque, New Mexico

May 2013

ACKNOWLEDGEMENTS

I thank my husband, Mike, and our sons, Tommy and James, for their understanding and support. With the birth of our second son in the middle of my first semester and my husband's six-month deployment to Afghanistan during my third year, I could only describe this experience as a challenge. It was worth it and my love for you is "for always."

Without the help and guidance of all members, past and present, of the Harrod Lab at Lovelace Respiratory Research Institute and my amazing classmates, especially Sarah Vaughan and Zac Karim, I would not be at this point in my life - concluding my formal education. Additionally, the support of all scientists and technicians, regardless of whose lab they worked in, was instrumental in my success.

I would like to thank all the members of my committee, especially my mentor Dr. Kevin Harrod, who challenged me at every meeting and made it clear that they supported me and wanted to see the best research they knew was within my capabilities. The entire faculty at UNM Health Sciences Center demonstrated their passion for research to new students and allowed some of their passion to rub off on us. The Biomedical Sciences Graduate Program office at UNM was fantastic in making sure I met all the mileposts of the program and helped to ensure my success. Thank you Ignacio, Natalie, and Mary!

Last but not least, I would like to thank my parents and brothers for always pushing me to do my best and supporting my seemingly odd decisions in life. From moving away from Connecticut for college, to joining the Air Force, to getting a Master's degree, and then leaving my Air Force career to return to school for this degree, they have been my longest and biggest supporters. I love you all.

**NEUROPATHOGENESIS OF HIGHLY PATHOGENIC AVIAN INFLUENZA IN
FERRETS FOLLOWING INTRANASAL INSTILLATION OR AEROSOL
EXPOSURE TO LOW DOSES**

BY

Jennifer Rose Plourde

B.S., Biochemistry, University of Tampa, 2003
M.S., Operations Research, Air Force Institute of Technology, 2005
Ph.D., Biomedical Sciences, University of New Mexico, 2013

ABSTRACT

Highly pathogenic avian influenza (HPAI), subtype H5N1, has continued to infect humans every year since its initial outbreak in 1997. The overall mortality is approximately 60% and while the emergence of this avian influenza virus has yet to reach the Western Hemisphere, its high lethality and pandemic potential warrant attention from the research community to better understand HPAI disease. Neuroinvasiveness of H5N1 virus is poorly understood and using two HPAI strains of varying lethality in the ferret model provide a basis for comparing differences in neuropathogenesis and its contribution to lethality. The studies described herein used two methods of HPAI exposure in ferrets to elucidate the neuropathogenesis of the virus and its correlation between neurological signs of infection and lesions within the central nervous system (CNS). Following both methods of exposure to low doses of a lethal strain of H5N1, we observed 100% lethality in conjunction with the neurological signs of infection that correlated with lesions within the CNS. Furthermore, we showed that an H5N1 strain that does not cause neurological signs does not replicate in the brain and has attenuated

lethality. We concluded that CNS involvement leads to a poor outcome following H5N1 infection. The increased understanding of the temporal-spatial kinetics of neuroinvasion and the correlation of neuroanatomical locations of lesions with the neurological signs observed during these studies could be useful for identifying routes of neuroinvasion and identifying targets for therapeutics to block CNS entry of HPAI. Finally, understanding the neurological sequelae of HPAI infection could aid clinicians in a more rapid diagnosis of influenza infection when patients present with atypical symptoms.

Table of Contents

ACKNOWLEDGEMENTS	iii
ABSTRACT.....	iv
List of Figures	viii
List of Tables	x
Chapter 1: Introduction.....	1
Background.....	1
Influenza virus structure	2
Influenza A virus replication	4
Highly pathogenic avian influenza in humans	7
HPAI pathogenesis in animal models of infection	12
Viral determinants of increased pathogenesis of HPAI.....	15
Genetic analysis of A/Vietnam/1203/2004 and A/HongKong/483/1997	17
Neuropathogenesis of influenza A	17
Purpose of study	20
References	22
Figure.....	33
Tables.....	34
Chapter Two: Neurovirulence of H5N1 infection in ferrets is mediated by multifocal replication in distinct permissive neuronal cell regions ...	36
Abstract.....	37
Introduction	38
Materials and Methods	39
Results	44
Discussion.....	54

Acknowledgments	58
References	60
Figure Legends	63
Figures	67
Table	75
Chapter Three: Aerosol Exposure to Low Doses of H5N1 Results in Widespread Infection and Neuroinflammation in the Ferret	76
Abstract.....	77
Introduction	78
Materials and Methods	79
Results	84
Discussion.....	90
Acknowledgements	93
References	95
Figure Legends	98
Figures	102
Table	110
Chapter Four: Discussion	111
Summary of Studies.....	111
Routes of H5N1 infection in the CNS	113
Correlation of neurological signs of infection with lesions in the CNS	116
Limitations of the Study	118
Future Studies	119
Conclusions	121
References	123

List of Figures

Chapter One

Figure 1. Cartoon representation of an influenza virus.....	33
---	----

Chapter Two

Figure 1. VN1203 was more lethal than HK483 in ferrets despite similar weight loss in non-survivors.	67
Figure 2. VN1203 induced significant pathology despite similar nasal turbinate titers in ferrets infected with either virus.....	63
Figure 3. Viral titers and histopathology were similar in the lung of H5N1 infected ferrets.	69
Figure 4. High viral titers were measured in the brain of VN1203 infected ferrets.	70
Figure 5. VN1203 infection in the ferret brain was multifocal and evident in the olfactory tract.	71
Figure 6. VN1203 infection resulted in multifocal infection in the cerebral cortex of ferrets.	72
Figure 7. VN1203 infected and replicated in Purkinje cells and deep cerebellar nuclei of the cerebellum.....	73
Figure 8. VN1203 resulted in severe and widespread brain lesions compared with HK483.	74

Chapter Three

Figure 1. Survival, temperature, and bodyweight of ferrets following aerosolized H5N1 exposure.....	102
Figure 2. Ferrets suffer from severely damaged lungs following aerosol exposure to H5N1.	103

Figure 3. Pathological findings and H5N1 nucleoprotein are detected in the olfactory bulb of ferrets following aerosol exposure at a low dose.	104
Figure 4. Widespread distribution of H5N1 and inflammation in the frontal lobe following aerosol exposure in ferrets.	105
Figure 5. Aerosol exposure to H5N1 results in perivascular cuffing, karyorrhexis, and widespread viral infection in the neocortex and hippocampus.	106
Figure 6. Aerosolized H5N1 results in widespread infection and pathological observations in the thalamus.	107
Figure 7. Viral antigen and cell death are detected in the cerebellum of ferrets following aerosol exposure.	108
Figure 8. Aerosol exposure to H5N1 results in significant destruction in the brain stem of ferrets.	109

List of Tables

Chapter One

Table 1. Influenza RNA segments and known functions of each translated protein. 34

Table 2. Genetic analysis of VN1203 and HK483. 35

Chapter Two

Table 1. Clinical observations in ferrets post-challenge with VN1203 or HK483. 75

Chapter Three

Table 1. Prevalence of neurological signs in ferrets. 110

Chapter 1: Introduction

Background

Influenza viruses cause global epidemics annually and the occasional pandemic, such as the 1918 “Spanish influenza” and the more recent 2009 H1N1 “Swine flu” pandemic (1). Three to five million humans are infected with seasonal strains of influenza worldwide each year with an estimated 250,000 to 500,000 deaths (2). This highly contagious virus is easily transmissible among humans and an incubation time of approximately one to five days assists in the widespread transmission of the disease (2, 3). The virus typically causes a mild or severe respiratory illness that commonly presents as a sudden onset of fever, myalgia, dry cough, headache, sore throat, runny nose, anorexia, and generally feeling unwell (2, 3). Vaccines are available for the expected circulating strains of seasonal influenza at the beginning of the influenza season each year and vaccination has been estimated to prevent approximately 60% of influenza infections and varies each season (4). Unfortunately, only about 40% of Americans were vaccinated annually over the past four influenza seasons (2009-2010, 2010-2011, 2011-2012, 2012-present) leaving the majority of the population vulnerable to disease (5).

While seasonal influenza viruses are well studied and vaccines are available for prevention, highly pathogenic avian influenza (HPAI) emerged in humans in 1997 without any reassortment with a human influenza strain (6-19). Vaccines are under development but are not readily available and early vaccines have been shown to be ineffective without the addition of an adjuvant (20-22). As of 15 February 2013, the World Health Organization (WHO) confirmed cases of H5N1 infection in 620 humans resulting in 367 deaths (59%) in twelve countries since 2003 (23). Infection with this highly lethal virus manifests in humans

as fast-progressing pneumonia, respiratory distress syndrome, symptoms in the intestinal tract and central nervous system (CNS), multi-organ failure, and in fatal cases, death occurred within ten days of symptom onset (24-27).

As seen with the 2009 swine origin H1N1 pandemic, the introduction of a reassortant novel virus with unique epitopes to an immunologically naïve population can result in rapid dissemination (28). The high incidence rate of seasonal influenza coupled with the emergence of HPAI in humans and the possibility of reassortment suggest HPAI has the potential to become a highly lethal transmissible virus that could reach pandemic proportions. Research must continue to further illuminate characteristics of HPAI infection and viral determinants of lethality in an effort to better identify highly pathogenic emerging strains and to develop better therapeutics and vaccines to increase the survival of those infected with or susceptible to HPAI.

Influenza virus structure

Influenza viruses, commonly referred to as “the flu,” are of the Family *Orthomyxoviridae* and are enveloped, negative sense, segmented, single stranded RNA viruses (**Figure 1**). There are three types of influenza viruses: A, B, and C; where type A and B commonly infect humans and cause seasonal epidemics; and type C causes mild respiratory infections and is not believed to cause epidemics. Influenza A viruses are further subtyped according to the phylogeny of the hemagglutinin (HA) and neuraminidase (NA) surface glycoproteins. There are 16 distinct HAs and 9 NAs, all found in avian hosts, for a total of 144 possible subtypes. Typically, H3N2 and H1N1 along with influenza B virus comprise the seasonal strains that currently circulate in humans while the HPAI subtype H5N1 is generally restricted to avian species.

The influenza virus is a Baltimore class V virus, enveloped with a helical capsid, and contains eight single stranded negative sense RNA genomes. The eight genomic segments range in size from 800 to 2,300 nucleotides and encode up to eleven proteins that each have specific functions. Each viral RNA segment is encapsidated by nucleoprotein (NP) and has a ribonucleoprotein (RNP) associated with it. The RNP consists of NP and the three polymerase proteins: polybasic polymerase 1 (PB1), polybasic polymerase 2 (PB2), and polymerase acid (PA). The envelope is acquired as the virus buds from the host cell and the surface glycoproteins (*i.e.*, hemagglutinin (HA) and neuraminidase (NA)) protrude from the envelope in a ratio of 4:1 (HA:NA). These glycoproteins also encompass the epitopes for antibody recognition and humoral immunity and are the targets of current antiviral treatments. The glycoproteins also function in viral entry to and exit from the cell. The M2 protein is translated from the matrix (M) segment and is an integral membrane protein that projects from the envelope and functions as an ion channel necessary for virus uncoating. Immediately below the lipid bilayer is the matrix protein, M1, known for its interactions with RNPs and the non-structural protein 2 (NS2). Finally, the nuclear export protein/NS2 (NEP/NS2) is also associated with the virus. The nonstructural protein 1 (NS1) is a multi-functional protein largely known to be an interferon antagonist and can inhibit the host innate immune response during infection, suppressing host immune and apoptotic responses, and activating phosphoinositide 3-kinase (PI3K) (29, 30). While the NS1 protein has been shown to enhance viral mRNA export in later stages of infection, as well as increase viral mRNA translation, it has also been shown inhibit cellular mRNA export (reviewed in 30, 31). The functions of each influenza A protein are summarized in **Table 1**.

The mRNAs of the M and NS segments are each spliced to generate the M2 and NEP/NS2 proteins, respectively. Additionally, an 11th protein, PB1-F2 is encoded in an alternate open reading frame near the 5' end of PB1. This protein is not present in all influenza A virus strains but has been shown to contribute to virulence in mammals (32, 33). PB1-F2 was suggested to have pro-apoptotic activity during infection by killing host immune cells responding to infection with A/Puerto Rico/8/1934 (PR8) (29, 34, 35). Further research found that the pro-apoptotic activity was restricted to the laboratory strain, PR8, but the PB1-F2 protein of the three pandemic influenza strains during the 20th century, as well as an HPAI H5N1 subtype, functions to enhance the lung inflammatory response and induces increased pathology in a mouse model. McAuley *et al.* suggest this additional protein increases the virulence of pandemic strains when the PB1 segment is derived from an avian influenza strain (33).

Influenza A virus replication

Replication of influenza viruses begins with attachment to host cells expressing specific receptors. It has been shown that the surface glycoproteins bind to neuraminic acids (*e.g.*, sialic acids) on the cell's surface to initiate infection and replication. Generally, human influenza viruses preferentially bind to an *N*-acetylneuraminic acid that is attached to the ending galactose sugar by an $\alpha 2,6$ linkage (SA $\alpha 2,6$ Gal) commonly found in the upper respiratory tract while avian influenza viruses preferentially attach to sialic acids with an $\alpha 2,3$ linkage which are found in the lower respiratory tract of humans (36). While human influenza virus receptors(Sa $\alpha 2,6$ Gal) are prominent in the respiratory tract and lungs, receptors for avian influenza (SA $\alpha 2,3$ Gal) have been found on type II pneumocytes, bronchi, bronchioli, trachea, a few epithelial cells in the upper respiratory tract, and cells outside the

respiratory tract, Kupfer cells, glomerular cells, splenic T cells, and neurons in the brain and intestine (37). The absence of avian influenza receptors in the upper airway could explain the lack of efficient human-to-human transmission of H5N1.

After attachment to the host cell, influenza virus is internalized into endocytic compartments via clathrin-mediated endocytosis (38) or nonclathrin, noncaveolae-mediated endocytosis (39). The viral HA undergoes a structural change after the HA0 precursor is cleaved into HA1 and HA2. It has been suggested that the cleavage of human influenza virus HA proteins is completed by type II transmembrane serine proteases and human airway trypsin-like protease. HPAI viruses, however, do not require these specific proteases and the HA protein can be cleaved by ubiquitously expressed subtilisin-like proteases (reviewed in 40). Several cleaved HA molecules undergoing conformational changes in the acidic environment of the endosome results in uncoating and releasing contents of the virion into the cytoplasm (41). The first few steps of the viral replication cycle occur quickly with the majority of virus particles entering the cytoplasm from the endosome about 25 minutes after internalization and RNP complexes reaching the nucleus only ten minutes later (42).

The viral RNP (vRNP) consists of viral RNA, which is coated by NP and has the PB1, PB2, and PA proteins bound to the partially complementary ends of the viral RNA. The vRNP enters the nucleus where viral RNA synthesis occurs. The vRNPs are too large for passive diffusion and use active nuclear import mechanisms of the cell to reach the nucleus. While all proteins in the vRNP have nuclear localization signals, it has been shown that the signals on the NP are both sufficient and necessary for viral RNA import into the nucleus (29).

Once the negative sense viral RNA is imported into the nucleus, replication occurs following a two-step process. A full-length positive-sense copy, termed complementary RNA (cRNA), of the viral RNA is made from the negative sense strand. The cRNA is used as a template to generate more viral genomic RNA. Additionally, the negative sense viral RNA is also transcribed into viral messenger RNA (mRNA) by a primer-dependent mechanism. The mRNA are not full copies of the viral RNA and are capped and polyadenylated. The reaction of viral RNA to mRNA, viral RNA to cRNA, and cRNA to viral RNA are all catalyzed by the same RNA-dependent RNA polymerase (RdRp) complex comprised of the influenza PB1, PB2, and PA proteins and is packaged within the virion (29).

Influenza RdRp is used to replicate the viral genome and transcribe its mRNA. Through a process known as “cap-snatching,” a 5’ capped primer is taken from host pre-mRNA transcripts and used to initiate mRNA synthesis (43, 44). The same polymerase used for transcription is used for polyadenylation of the mRNA transcripts. A stretch of five to seven uracil residues and an adjacent double-stranded region of the viral RNA promoter are required for polyadenylation (45-47). In addition to translation of eight influenza proteins from the eight mRNAs generated through transcription, the translation of M and NS mRNA can result in two proteins each due to splicing (*i.e.*, M1 and M2, and NS1 and NEP/NS2, respectively) (29).

In addition to acting as a template for mRNA synthesis, viral RNA is also used as a template for cRNA, which is full length and is not capped or polyadenylated. The RdRp used for mRNA synthesis in a primer-dependent manner is also used to generate cRNA independent of a primer (29, 44, 48). Soon after the virion contents are released and imported to the nucleus, the RNPs are only capable of transcription (29). If the process is interrupted at

this step, there will be an accumulation of mRNA in the cell. The switch from mRNA synthesis to cRNA synthesis is not fully understood and several hypotheses have been suggested (29, 44, 48). One hypothesis is that an accumulation of NP is required to produce full-length cRNA, which only occurs after translation (29). An alternate model is that a switch does not occur, but NP and the polymerase have a stabilization role and both mRNA and cRNA are made early during infection but cRNA is degraded until enough NP exists to encapsidate the cRNA (48). More recently, it has been shown that the concentrations of capped cellular mRNA, the 5'-end of the viral RNA, and the RdRp regulate the switch between transcription and replication (44).

Once copied viral RNA has been synthesized from cRNA, it must be exported from the nucleus. However, before export to the cytoplasm, the newly generated viral RNA must be encapsidated by NP and form an RNP complex with PB1, PB2, and PA. These complexes are then exported through the functions of M1 and NEP/NS2. The M1 protein has been shown to associate with the lipid membrane and interact with vRNP and NEP/NS2. Following export to the cytoplasm, influenza viruses are packaged and assembled at the apical plasma membrane of polarized cells where they can bud out of the host cell. Budding will not occur in the absence of M1. Additionally, once the virus particle buds from the cell, its envelope remains attached to the cell membrane and NA is required to remove the sialic acid from the carbohydrate to complete the budding process. Without NA, the particle cannot be released from the cell (29).

Highly pathogenic avian influenza in humans

Birds are the reservoir for influenza A viruses with three subtypes having emerged in humans as pandemic strains: H1N1 (1918 and 2009), H2N2 (1957), and H3N2 (1968) (49).

Generally, influenza viruses are species-specific and inter-species transmission is not common. However, some avian influenza viruses have been shown to jump the species barrier and infect other mammals such as horses (50), pigs (51), and whales (52) without reassortment with circulating human influenza strains. The influenza strains that caused the 1957 and 1968 human pandemics were reassortant strains of both human and avian viruses believed to have been generated in pigs. Reassortant strains can arise when a host, such as a pig, acquires two or more influenza strains concurrently. Following replication of multiple strains, progeny virions can contain segments from one or more strain of influenza and continue to spread among new hosts (28).

An avian influenza H5N1 not previously known to infect humans infected eighteen people in Hong Kong between May and December of 1997. The first case was a previously healthy three-year-old boy who was hospitalized six days after the onset of fever, sore throat, and cough, and died six days after hospitalization. Death was attributed to acute respiratory distress secondary to viral pneumonia, multi-organ failure, disseminated intravascular coagulation, and complications from Reye's syndrome (9, 53). The second case was a two-year-old boy with congenital heart disease that presented with the same symptoms, was hospitalized, and survived. Subsequent cases included previously healthy individuals ranging in age from 1 to 60 years old who presented with typical flu-like symptoms as well as vomiting in one case (9). H5N1 influenza virus was isolated or seroconversion to H5N1 virus was detected by a neutralization assay in each of the confirmed cases. Overall, 18 individuals were confirmed to have H5N1 infection in 1997 and six cases were fatal (33%) (8, 9, 54, 55).

Following the initial avian influenza outbreak in humans, an epidemiological investigation was performed with serum samples from 502 people who may have had contact

with the initial case or with poultry. Samples included serum from family members, neighbors, children and staff of the child-care center, health-care workers, poultry workers, and workers on pig farms. Control samples from 218 healthy children and 201 healthy adult residents of Hong Kong were also collected. All serum samples were tested for antibody to H5N1 using micro-neutralization assays. Of the 502 samples, 9 (2%) had elevated titers suggesting they were exposed to H5N1 though they may have been asymptomatic. The positive results included 5 poultry workers, and 1 each from the health care workers, neighbors, lab workers, and child care center contacts. The remaining samples and all the control samples were negative (9, 54, 56).

Antigenic and genetic analysis of the viral isolates from seven confirmed cases indicated two closely related but distinguishable groups of H5N1 suggesting multiple introductions in humans from poultry sources. Genetic reassortment between avian and human influenza viruses likely did not occur since all eight RNA genomic segments were from an avian virus (9, 54, 56).

The first case of H5N1 infection in humans in 1997 was determined to be the result of direct exposure to infected poultry (57). More recent patients however, fell ill following plucking and preparing diseased birds, handling fighting cocks, playing with infected poultry, and consuming undercooked infected poultry (58). While human-to-human contact is not common, there have been isolated reports of limited household clusters of infection (59) and a case of child-to-mother transmission (60). Serologic studies of health care workers and social contacts of infected humans suggested inefficient transmission (61) although further studies with RT-PCR detected mild cases, more infection in older adults, and more clusters in families in Vietnam causing concern that H5N1 may be adapting to humans (58).

Following the initial outbreak of H5N1 in humans in 1997, H5N1 did not appear again in humans until its re-emergence in 2003 (17, 62-64). The first new cases of avian influenza infection were confirmed in a family of five that had visited mainland China where they had contact with live chickens. Three members of the family (ages 7, 8, and 33) became ill and the previously healthy 7 year old and 33 year old died of the disease. The 8 year old recovered and was confirmed to also have been infected with influenza A, subtype H5N1 (17).

Generally, HPAI presents in healthy young children or adults and presentation of initial symptoms include: high fever and “influenza-like” illness with lower respiratory tract symptoms (58). Some patients also experienced diarrhea, vomiting, abdominal pain, pleuritic pain, and bleeding from the nose and gums (59, 65-67). Atypically, patients presented with encephalopathy and diarrhea in the absence of respiratory symptoms (68). Illness presentation began with lower respiratory tract manifestations and respiratory distress, tachypnea, and inspiratory crackles (66). Pneumonia was apparent in nearly all patients and radiographic abnormalities were observed at a median of seven days following fever onset (66). The illnesses progressed to respiratory failure and acute respiratory distress syndrome (ARDS) manifested around six days after illness onset (66). Additionally, multi-organ failure with signs of renal dysfunction and cardiac compromise (59, 65-67) were also common as well as pulmonary hemorrhage, pneumothorax, pancytopenia, Reye’s syndrome, ventilator-associated pneumonia, and sepsis syndrome without bacteremia (58).

As of January 2013, the WHO reported the fatality rate among hospitalized patients to be approximately 59% (23). It is important to note that the 59% fatality rate may be accurate only for patients who are hospitalized and may not account for individuals who are infected

with H5N1 although asymptomatic or who have only a mild illness and do not seek medical attention. A seroprevalence study of H5N1 infection in humans showed that 1 to 2% of more than 12,500 individuals in 20 separate studies had seroevidence for H5N1 infection suggesting that H5N1 infects more humans than are reported (69). While the initial emergence of H5N1 in humans in 1997 resulted in most deaths among patients older than 13, more recent H5N1 strains have resulted in a case fatality rate of 89% in patients younger than 15 and increased fatalities in infants and young children (59, 66). This fast progressing disease results in death nine to ten days following illness onset with progressive respiratory failure as the cause of death (58, 59, 66).

Although H5N1 has continued to diversify since the H5 hemagglutinin gene was sequenced in 1997, the HA has remained relatively unchanged providing a basis for comparing emerging strains. This has also permitted the development of a standard nomenclature system based on clades that group H5 isolates by their HA sequence (70). This system has formally identified 20 distinct clades of virus since 2008 (71, 72) and clades are defined by an isolate meeting these specific criteria: 1) share a common clade-defining node in the phylogenetic tree, 2) the grouping is monophyletic with a bootstrap of > 60 at the node (after 1000 neighbor-joining bootstrap replicates, and 3) the average percentage pair-wise nucleotide distances between and within clades of $> 1.5\%$ and $< 1.5\%$ respectively. Sub-lineages, or sub-clades, are added as the viruses evolve within these identified clades until they meet the three criteria for forming a new clade. While 20 clades have been identified, 13 of these have been considered inactive and have not been detected since 2008 (70). The eradication of the 13 strains could have been the result of being out-competed by other emerging strains or high mortality in the host and thereby prohibiting efficient spread.

HPAI pathogenesis in animal models of infection

Experimental infections of influenza A virus in animal models are often used to study virus characteristics and pathogenesis as well as the host immune response. The mouse model is commonly used to study infectious diseases and has been used to elucidate the pathogenesis of H5N1. Unlike human influenza A viruses, avian influenza A viruses such as H5N1 can replicate in the mouse without requiring prior adaptation (73-75). In mice, H5N1 viruses are classified as either lethal (A/HongKong/483/1997-like) or nonlethal (A/HongKong/486/1997-like). H5N1 viruses that are “HK483-like” result in systemic spread, cytokine dysregulation, severe tissue pathology, and death. Conversely, infection with an “HK486-like” virus results in replication limited to the respiratory tract, and mice cleared the virus 7-9 days post-infection (74, 76). Research with these two viruses suggests that differences in inflammatory and innate immune responses may be the mechanism of increased pathogenesis of the “HK483-like” viruses (74, 76). Specifically, infection with a lethal virus results in a significant reduction of circulating lymphocytes (74, 77) and an increase in apoptosis in the lung and spleen compared with less virulent strains (74).

Interestingly, H5N1 has been shown to spread to the brain of infected mice and this characteristic also separates “HK483-like” viruses from “HK486-like” viruses (74, 78, 79). Similar to what was observed in the lung, the innate immune response in the central nervous system (CNS) also differentiated virulent from non-virulent strains of H5N1. The lethal strains resulted in the synthesis of pro-inflammatory cytokines in the brain, which resulted in anorexia, weight loss, and death (80). Viruses isolated from later outbreaks in 2004, can also be characterized as highly virulent or lowly virulent with infection of highly virulent strains resulting in systemic spread in mice (81). Unlike the strains isolated in 1997, which required

high inoculating doses to induce lethality, Maines *et al.* demonstrated 20-60 infectious virions were sufficient to cause lethality in BALB/c mice with an isolate from 2004 (81).

HK483 has been shown to result in higher neurotropism than other 1997 isolates of H5N1 (82) and has been used to identify routes of infection in the CNS (78). Following intranasal inoculation of 10^4 LD₅₀ of HK483, BALB/cA Jcl mice were examined one to six days post-infection and immunohistochemistry (IHC) and *in situ* hybridization were used to detect viral infection in the brain. Virus was detected in the nasal cavity as early as one day post-infection and in the lung by two days post-infection. The first detection of virus in the CNS was in the pterygopalatine ganglia, trigeminal ganglia, and spinal cord at three days post-infection. By five days post-infection, virus was detected in the olfactory bulb, cerebrum, brain stem, and vagal ganglia in addition to the nasal cavity and lung. The *in situ* hybridization results were similar to the IHC results for both tissue and day of detection for the CNS (78).

While mice are often used to study infectious diseases, ferrets have become a standard for studying the pathogenesis of influenza viruses due their ability to closely model influenza infection in humans. Ferrets sneeze, cough, experience fever and nasal discharge, as well as become lethargic (reviewed in 83). The similarities in pathogenesis and viral distribution may be due to the sialic acid distribution in their respiratory tract, which is similar to that in humans. Both ferrets and humans have predominantly $\alpha(2-6)$ -linked sialic acids on the upper airway epithelia and $\alpha(2-3)$ -linked sialic acids on the lower airway epithelia (83).

In contrast to the mouse model, the dichotomy of “HK483-like” and “HK486-like” viruses is not valid in the ferret model of HPAI infection (75, 84). In ferrets, infection with

either of these viruses results in disease that includes lethargy, clinical signs of respiratory disease, weight loss, lymphopenia, and at high doses, neurological signs (85). Both of these H5N1 isolates from 1997 can spread systemically in ferrets reaching the spleen, intestine, liver, and peripheral blood (81).

H5N1 isolates from the 2004 outbreak have also been used to study pathogenesis in the ferret model, and similar to what was observed in mice, these strains exhibit increased virulence compared to strains isolated in 1997 (81, 86). These isolates, that include A/Vietnam/1203/2004 (VN1203) and A/Thailand/16/2004 (Thai16) routinely spread to the brain, spleen, and intestine and resulted in a faster mean time-to-death when compared with H5N1 isolates from 1997 (81). Additionally, increased inflammation was observed in the brains of ferrets infected with the 2004 isolates, as was diffuse interstitial inflammation in the lungs (81, 86). Wang and colleagues found that VN1203 infection in ferrets could be characterized by high viral titers in the brain and low levels in the ileum using real-time PCR. Importantly, they found that viral RNA could be detected in the blood one to two days post-infection suggesting viremia could be an important marker of fatal infection in ferrets (87).

HPAI H5N1 preferentially attaches to nonciliated cuboidal epithelial cells, type II pneumocytes, and alveolar macrophages. It rarely attaches to the upper respiratory tract and most often results in lesions in the alveoli and bronchioles, not in the trachea or bronchi (reviewed in 88). Additionally, H5N1 has been found in human brain, intestine, liver, lymph nodes, placenta, and fetal lung and it is believed to be spread systemically by viremia (88) or via the peripheral nervous system (89).

Viral determinants of increased pathogenesis of HPAI

Since the emergence of H5N1 in humans in 1997, HPAI has been widely studied to identify virulence mechanisms that contribute to increased pathogenesis and lethality in humans as well as identify markers of possible human-to-human transmission. The HA0 of influenza viruses must be cleaved post-translationally into the subunits HA1 and HA2 at a conserved arginine residue for infectivity to occur through the activation of the membrane fusion potential of HA (90). Research on H5N1 strains isolated in 1997 identified a multi-basic cleavage site present on the HPAI HA that permitted the cleavage to be activated by multiple intracellular proteases, including furin-like proteases that are ubiquitously expressed. This is in contrast to the presence of a single cleavage site common in human influenza strains that require extracellular trypsin-like proteases to cleave the HA0 into HA1 and HA2 (91-93). It subsequently has been shown that removal of the multi-basic amino acid cleavage site reduces virulence (94); however, the possession of the site is not sufficient for virulence since not all H5 or H7 viruses with this sequence are lethal in mammals (74, 81, 95). This multi-basic cleavage site has also been shown to be essential in the systemic spread of H5N1 along the olfactory and hematogenous routes in ferrets (96).

Neuraminidase (NA) is a glycoprotein in addition to HA that is present on the surface of influenza virus particles and is essential for release of the virus particle during the budding process following replication. The anti-influenza agents zanamivir and oseltamivir block the NA from cleaving the sialic acid residues and therefore inhibit the progeny virions from budding (97). Wagner *et al.* revealed a correlation between the avidity of HA and the strength of NA activity. When HA exhibits weak binding, the NA is likely to have weakened activity (98, 99). Importantly, it has been shown that when the active sites of these proteins

are mutated, the binding activities are altered and insertions and deletions in the NA stalk regions that alter its length can modify its activity (100, 101). Specifically, NA stalk deletions prominent in H5N1 viruses increase virulence in the mouse model (102). While virulence determinants have been identified in the HA and NA of H5N1 viruses, these glycoproteins are not the only determinants of pathogenicity. Experimentally generated reassortant viruses containing the HA and NA from virulent HPAI strains with the remaining six genes from non-virulent influenza viruses were not lethal to mice or ferrets (77, 103).

Subsequent to fusion of the virus to the host cell, the ion channel activity of matrix 2 (M2), an integral membrane protein, induces the virus to dissociate the ribonucleoprotein (RNP) complex from the virus. Additional roles of the M2 protein include assembly, budding, and the ratio of filamentous and spherical particles (104-106). This protein is highly conserved and is believed to be a good target for developing a universal influenza vaccine (107). The antiviral medicines amantadine and rimantidine target the influenza A M2 protein to inhibit viral uncoating or disassembly of the virion during endocytosis. New antiviral treatments need to be developed because influenza A viruses have now acquired resistance to amantadine through mutations in the M2 segment (108, 109).

Experimentally generated reassortant viruses have been used to demonstrate the role of the polymerase complex (PB1, PB2, and PA) in pathogenesis and increased virulence (77, 103). The replacement of these genes in A/Ck/Vietnam/C58/04, a non-virulent strain, with the PB1, PB2, and PA of A/Vietnam/1203/2004, a highly virulent influenza strain, resulted in increased virulence. Conversely, the PB1, PB2, and PA of A/Ck/Vietnam/C58/04 inserted in the A/Vietnam/1203/2004 backbone resulted in an attenuated virus that abolished the increased pathogenicity in mice and ferrets (103). The importance of the polymerase

complex was also shown by inserting the PB1, PB2, and PA of a human H3N2 virus into the backbone of a HPAI H5N1 which resulted in efficient replication but poor transmission (77). This suggests viral replication may be a key determinant of lethality and these proteins should be examined further for their role in virulence.

Genetic analysis of A/Vietnam/1203/2004 and A/HongKong/483/1997

The clade 0, A/HongKong/483/1997 (HK483) and clade 1 virus, A/Vietnam/1203/2004 (VN1203) are often compared to elucidate novel virulence factors through genetic analysis, reverse genetics techniques, and animal studies to compare differences in the pathogenesis of these distinct viruses. Both viruses were isolated from fatal human cases; however, they have been shown to have differing lethality in animal models with VN1203 exhibiting 100% lethality in ferrets and HK483 resulting in up to 33% lethality (81). A multiple sequence alignment of the ten proteins encoded by the VN1203 and HK483 genomes identified the NS1 segment as the most different (19% different) between these two strains while the remaining nine proteins were only 2.2-9.5% different (**Table 2**).

Interestingly, both HK483 and VN1203 contain the multi-basic amino acid cleavage site in the HA and both lack the E158G mutation in PB2 that has been shown to confer virulence. Not surprisingly, neither virus possesses the D701N mutation in PB2 that enhances transmission (110).

Neuropathogenesis of influenza A

Influenza is often considered to cause disease in the respiratory tract; however there has been evidence of CNS involvement in twelve influenza A pandemics or epidemics over the last century (1). The neurological sequelae have not been extensively studied and the

recurrence of these symptoms with each pandemic should be considered when studying newly emergent influenza strains such as HPAI H5N1.

Case reports from the 1918 “Spanish Influenza,” which was caused by an H1N1 virus that contained avian influenza segments, describe the frequent observation of delirium – sudden severe confusion and rapid changes in brain function - despite the absence of meningitis (111). Post-mortem examination of the CNS revealed several cases where degeneration was observed in nerve cells, particularly in the motor nuclei in the pons. General congestion of the brain was also found; however, inflammation was not observed in the brain or meninges (112). In addition to acute effects of influenza on the CNS during the 1918 pandemic, long-term (6 to 12 months) effects in patients that recovered were also described as follows: depression, neurasthenia – weakness in the nerves, fatigue, anxiety, depression, and headache, neuritis – inflammation in the nerves, impaired sensation, strength, and reflexes, abnormal circulation, inability to sweat, and other “nervous ills.” Researchers at the time hypothesized that the pandemic strain specifically infected nerve centers and justified it by the clear and extensive neurological sequelae. They also speculated the pneumogastric nerve (now commonly referred to as the vagus nerve) was the origin due to the complications principally involving the stomach and lung (113). Other instances of neurological involvement following the 1918 pandemic included cerebro-spinal fever, poliomyelitis, and polio-encephalitis (114). Finally, a link between encephalitis lethargica – high fever, ophthalmoplegia, mental confusion, and lethargy – during influenza infection and post-encephalitic Parkinsonism was described (reviewed in 1).

The H1N1 influenza strain that caused the 1918 pandemic was not the only subtype to induce neurological manifestations of disease. The H2N2 pandemic in 1957 consisted of

reported cases of encephalitis, seizures, muscle paralysis, and Guillain-Barré-like syndrome (1, 115) and the H3N2 pandemic in 1968 had reported cases of amyotrophy, flares of multiple sclerosis, encephalitis, encephalopathy, myelopathy, polyneuropathy, and Guillain-Barré-like syndrome. During the 1968 pandemic however, one researcher suggested the encephalitis was not due to viral infection but due to fulminating staphylococcal septicemia (116).

The most recent pandemic in 2009 as a result of the novel swine origin H1N1 strain of influenza also caused neurological sequelae in infected individuals. A study of primary neurological manifestations of 2009 H1N1 in California were described as encephalopathy/encephalitis, seizures, meningitis, and “other” which referred to one case of Guillain-Barré Syndrome. The study examined 2,069 cases of severe or fatal 2009 H1N1 infections and found neurological signs in 20% of the confirmed cases with 18% of those (~4% of the total) described as “primary influenza-associated neurological complications” and the remainder as secondary neurologic manifestations (117).

Neurotropism of avian influenza has been described in naturally susceptible populations of avian species (118, 119) as well as in mammalian species such as domestic cats, tigers, leopards, mice, and others (52, 119-121). CNS involvement of H5N1 is not limited to avian species and other animals, as it has been described in humans as presentation of encephalitis or encephalopathy and found more often in children than adults (3). In humans, H5N1 has been detected in the brain and cerebrospinal fluid of some patients following clinical presentation of diarrhea, generalized convulsions, seizures, and coma (3, 24, 68, 88, 121-123). The occurrence of symptoms outside the respiratory tract suggests avian H5N1 has a wider tissue tropism than human influenza viruses. Unfortunately, in most

cases, limited autopsy samples were taken and viral replication could not be confirmed in extra-pulmonary tissue (84). In 2005, post-mortem tissue from a fetus and two adult patients that succumbed to H5N1 infection were examined to better understand the pathogenesis of the virus. Viral genomic sequences and antigen were detected in many extra-pulmonary tissues including neurons of the brain. The presence of virus in the brain was confirmed by *in-situ* hybridization and immunohistochemistry (24). A more detailed study also found H5N1 virus in the brain of a patient in 2008 with a history of fever, cough, and dyspnea. Virus was successfully isolated from the cerebral cortex, cerebral medullary substance, cerebellum, brain stem, hippocampus ileum, and other organs outside the respiratory tract (123). These findings suggest H5N1 is reaching the CNS and replicating to high titers following natural infection. More research must be conducted to further explore the route of infection and identify targets to prevent dissemination to the CNS.

Early animal studies after the initial H5N1 outbreak in 1997 sought to characterize the newly emerging strains and found that H5N1, specifically in mice and ferrets intranasally infected with high doses of HK483, could replicate in the brain and cause neurological signs of infection. HK483 was highly lethal in mice, with 100% mortality but lesser so in ferrets at only 5-10% (84). More recently, other strains of H5N1 have also been shown to replicate in the brain of ferrets and result in high lethality suggesting H5N1 does have a wider tropism compared with circulating human influenza strains. Furthermore, they are able to induce severe CNS involvement and lethality in mammals (24, 86, 88, 89, 121-125).

Purpose of study

Increased understanding of neurotropism and clinical signs of CNS involvement may aid clinicians in the earlier diagnosis of H5N1 infection when patients present with atypical

symptoms. Further studies to elucidate the molecular determinants of neurotropism as they contribute to increased lethality could guide development for therapeutics and vaccines that could target aspects that prevent the virus from entering the brain and increasing the mortality rate compared to virus strains that do not reach the CNS.

Preliminary studies in our laboratory and literature reports of neuropathogenesis in mammals suggest H5N1 viruses that disseminate to the brain and replicate in neuronal tissue are more lethal than those confined to the respiratory tract. The studies presented here use the ferret model to examine differences in the neuropathogenesis of HK483 and VN1203 (Chapter 2) and differences between CNS involvement following intranasal instillation and aerosol exposure of VN1203 (Chapter 3).

The ferret model is often used to study the pathogenesis of H5N1 virus and is a good comparison for pathogenesis in humans. While intranasal instillation is the common method of infection in ferrets, the use of nose-only aerosol chambers have recently been introduced as a better model for presenting H5N1 in a more physiologically relevant manner (126, 127). This dissertation includes the results of two original studies that specifically examine the neuropathogenesis of two H5N1 viruses from different clades following intranasal instillation and aerosol exposure to physiologically relevant low doses of H5N1. The first virus, HK483 was isolated during the initial outbreak of H5N1 in 1997 and has been shown to have less lethality than a strain isolated in 2004, VN1203. HK483 and VN1203 are often used to compare differences in pathogenesis to determine viral determinants of lethality (81, 85).

References

1. **Henry, J., R. J. Smeyne, H. Jang, B. Miller, and M. S. Okun.** 2010. Parkinsonism and neurological manifestations of influenza throughout the 20th and 21st centuries. *Parkinsonism Relat Disord.* **16**:566-71.
2. **World Health Organization.** April 2009. Influenza (Seasonal) Fact Sheet. Available from: <http://www.who.int/mediacentre/factsheets/fs211/en/index.html>.
3. **Studahl, M.** 2003. Influenza virus and CNS manifestations. *J Clin Virol.* **28**:225-232.
4. **Centers for Disease Control and Prevention.** 2013. What you should know for the 2012-2013 influenza season. [updated 24 January 2013; cited 28 January 2013]. Available from: <http://www.cdc.gov/flu/about/season/flu-season-2012-2013.htm>.
5. **Centers for Disease Control and Prevention.** 2012. National early season flu vaccination coverage, United States 2012-13 flu season. [updated 3 December 2012; cited 28 January 2013]. Available from: <http://www.cdc.gov/flu/fluview/nifs-estimates-nov2012.htm>.
6. 2010. Summary of human infection with highly pathogenic avian influenza A (H5N1) virus reported to WHO, January 2003-March 2009: cluster-associated cases. *Wkly Epidemiol Rec.* **85**:13-20.
7. 2010. Update on human cases of highly pathogenic avian influenza A (H5N1) infection: 2009. *Wkly Epidemiol Rec.* **85**:49-51.
8. 1997. Influenza A virus subtype H5N1 infection in humans. *Commun Dis Rep CDR Wkly.* **7**:441.
9. 1997. Isolation of avian influenza A(H5N1) viruses from humans--Hong Kong, May-December 1997. *MMWR Morb Mortal Wkly Rep.* **46**:1204-7.
10. **Beigel, J. H., J. Farrar, A. M. Han, F. G. Hayden, R. Hyer, M. D. de Jong, S. Lochindarat, T. K. Nguyen, T. H. Nguyen, T. H. Tran, A. Nicoll, S. Touch, and K. Y. Yuen.** 2005. Avian influenza A (H5N1) infection in humans. *N Engl J Med.* **353**:1374-85.
11. **De Martin, S., and A. Nicoll.** 2005. H5N1 avian influenza: update on the global situation. *Euro Surveill.* **10**:E051215 1.
12. **Ducatez, M. F., C. M. Olinger, A. A. Owoade, S. De Landtsheer, W. Ammerlaan, H. G. Niesters, A. D. Osterhaus, R. A. Fouchier, and C. P. Muller.** 2006. Avian flu: multiple introductions of H5N1 in Nigeria. *Nature.* **442**:37.
13. **Joseph, T., and K. Subbarao.** 2005. Human infections with avian influenza viruses. *Md Med.* **6**:30-2.

14. **Lye, D. C., D. H. Nguyen, S. Giriputro, T. Anekthananon, H. Eraksoy, and P. A. Tambyah.** 2006. Practical management of avian influenza in humans. *Singapore Med J.* **47**:471-5.
15. **Malik Peiris, J. S.** 2009. Avian influenza viruses in humans. *Rev Sci Tech.* **28**:161-73.
16. **Parry, J.** 2004. Mortality from avian flu is higher than in previous outbreak. *BMJ.* **328**:368.
17. **Peiris, J. S., W. C. Yu, C. W. Leung, C. Y. Cheung, W. F. Ng, J. M. Nicholls, T. K. Ng, K. H. Chan, S. T. Lai, W. L. Lim, K. Y. Yuen, and Y. Guan.** 2004. Re-emergence of fatal human influenza A subtype H5N1 disease. *Lancet.* **363**:617-9.
18. **Subbarao, K., and J. Katz.** 2000. Avian influenza viruses infecting humans. *Cell Mol Life Sci.* **57**:1770-84.
19. **Yu, H., Y. Shu, S. Hu, H. Zhang, Z. Gao, H. Chen, J. Dong, C. Xu, Y. Zhang, N. Xiang, M. Wang, Y. Guo, N. Cox, W. Lim, D. Li, Y. Wang, and W. Yang.** 2006. The first confirmed human case of avian influenza A (H5N1) in Mainland China. *Lancet.* **367**:84.
20. **Wu, J., S. Z. Liu, S. S. Dong, X. P. Dong, W. L. Zhang, M. Lu, C. G. Li, J. C. Zhou, H. H. Fang, Y. Liu, L. Y. Liu, Y. Z. Qiu, Q. Gao, X. M. Zhang, J. T. Chen, X. Zhong, W. D. Yin, and Z. J. Feng.** 2010. Safety and immunogenicity of adjuvanted inactivated split-virion and whole-virion influenza A (H5N1) vaccines in children: a phase I-II randomized trial. *Vaccine.* **28**:6221-7.
21. **Layton, R. C., A. Gigliotti, P. Armijo, L. Myers, J. Knight, N. Donart, J. Pyles, S. Vaughan, J. Plourde, N. Fomukong, K. S. Harrod, P. Gao, and F. Koster.** 2011. Enhanced immunogenicity, mortality protection, and reduced viral brain invasion by alum adjuvant with an H5N1 split-virion vaccine in the ferret. *PLoS One.* **6**:e20641. doi: 10.1371/journal.pone.0020641; 10.1371/journal.pone.0020641.
22. **Layton, R. C., N. Petrovsky, A. P. Gigliotti, Z. Pollock, J. Knight, N. Donart, J. Pyles, K. S. Harrod, P. Gao, and F. Koster.** 2011. Delta inulin polysaccharide adjuvant enhances the ability of split-virion H5N1 vaccine to protect against lethal challenge in ferrets. *Vaccine.* **29**:6242-6251. doi: 10.1016/j.vaccine.2011.06.078; 10.1016/j.vaccine.2011.06.078.
23. **World Health Organization.** 2013. Cumulative number of confirmed human cases of avian influenza A(H5N1) reported to WHO. [update 15 February 2013; cited 22 February 2013]. Available from: http://www.who.int/influenza/human_animal_interface/EN_GIP_20130215CumulativeNumberH5N1cases.pdf
24. **Gu, J., Z. Xie, Z. Gao, J. Liu, C. Korteweg, J. Ye, L. T. Lau, J. Lu, Z. Gao, B. Zhang, M. A. McNutt, M. Lu, V. M. Anderson, E. Gong, A. C. H. Yu, and W. I. Lipkin.**

2007. H5N1 infection of the respiratory tract and beyond: a molecular pathology study. *The Lancet*. **370**:1137-1145.
25. 2008. Update on Avian Influenza A (H5N1) Virus Infection in Humans. *N Engl J Med*. **358**:261-273. doi: 10.1056/NEJMra0707279.
26. **Ng, W. F., and K. F. To.** 2007. Pathology of human H5N1 infection: new findings. *The Lancet*. **370**:1106-1108.
27. **Ashour, M. M., A. M. Khatab, R. F. El-Folly, and W. A. Amer.** 2012. Clinical features of avian influenza in Egyptian patients. *J Egypt Soc Parasitol*. **42**:385-396.
28. **Wang, T. T., and P. Palese.** 2009. Unraveling the Mystery of Swine Influenza Virus. *Cell*. **137**:983-985.
29. **Knipe, D. M., and P. M. Howley (eds.),** 2007. *Fields Virology, Volume 2*. Lippincott, Williams, & Wilkins, Philadelphia, PA.
30. **Hale, B. G., R. E. Randall, J. Ortin, and D. Jackson.** 2008. The multifunctional NS1 protein of influenza A viruses. *J Gen Virol*. **89**:2359-2376. doi: 10.1099/vir.0.2008/004606-0; 10.1099/vir.0.2008/004606-0.
31. **Schneider, J., and T. Wolff.** 2009. Nuclear functions of the influenza A and B viruses NS1 proteins: do they play a role in viral mRNA export? *Vaccine*. **27**:6312-6316. doi: 10.1016/j.vaccine.2009.01.015; 10.1016/j.vaccine.2009.01.015.
32. **Zamarin, D., M. B. Ortigoza, and P. Palese.** 2006. Influenza A virus PB1-F2 protein contributes to viral pathogenesis in mice. *J Virol*. **80**:7976-7983. doi: 10.1128/JVI.00415-06.
33. **McAuley, J. L., J. E. Chipuk, K. L. Boyd, N. Van De Velde, D. R. Green, and J. A. McCullers.** 2010. PB1-F2 proteins from H5N1 and 20 century pandemic influenza viruses cause immunopathology. *PLoS Pathog*. **6**:e1001014. doi: 10.1371/journal.ppat.1001014; 10.1371/journal.ppat.1001014.
34. **Lamb, R. A., and M. Takeda.** 2001. Death by influenza virus protein. *Nat Med*. **7**:1286-1288. doi: 10.1038/nm1201-1286.
35. **Chen, W., P. A. Calvo, D. Malide, J. Gibbs, U. Schubert, I. Bacik, S. Basta, R. O'Neill, J. Schickli, P. Palese, P. Henklein, J. R. Bennink, and J. W. Yewdell.** 2001. A novel influenza A virus mitochondrial protein that induces cell death. *Nat Med*. **7**:1306-1312. doi: 10.1038/nm1201-1306.
36. **Connor, R. J., Y. Kawaoka, R. G. Webster, and J. C. Paulson.** 1994. Receptor specificity in human, avian, and equine H2 and H3 influenza virus isolates. *Virology*. **205**:17-23. doi: 10.1006/viro.1994.1615.

37. **Yao, L., C. Korteweg, W. Hsueh, and J. Gu.** 2008. Avian influenza receptor expression in H5N1-infected and noninfected human tissues. *FASEB J.* **22**:733-740. doi: 10.1096/fj.06-7880com.
38. **Matlin, K. S., H. Reggio, A. Helenius, and K. Simons.** 1981. Infectious entry pathway of influenza virus in a canine kidney cell line. *J Cell Biol.* **91**:601-613.
39. **Sieczkarski, S. B., and G. R. Whittaker.** 2002. Influenza virus can enter and infect cells in the absence of clathrin-mediated endocytosis. *J Virol.* **76**:10455-10464.
40. **Bertram, S., I. Glowacka, I. Steffen, A. Kuhl, and S. Pohlmann.** 2010. Novel insights into proteolytic cleavage of influenza virus hemagglutinin. *Rev Med Virol.* **20**:298-310. doi: 10.1002/rmv.657; 10.1002/rmv.657.
41. **Stegmann, T., H. W. Morselt, J. Scholma, and J. Wilschut.** 1987. Fusion of influenza virus in an intracellular acidic compartment measured by fluorescence dequenching. *Biochim Biophys Acta.* **904**:165-170.
42. **Martin, K., and A. Helenius.** 1991. Transport of incoming influenza virus nucleocapsids into the nucleus. *J Virol.* **65**:232-244.
43. **Krug, R. M.** 1981. Priming of influenza viral RNA transcription by capped heterologous RNAs. *Curr Top Microbiol Immunol.* **93**:125-149.
44. **Olson, A. C., E. Rosenblum, and R. D. Kuchta.** 2010. Regulation of influenza RNA polymerase activity and the switch between replication and transcription by the concentrations of the vRNA 5' end, the cap source, and the polymerase. *Biochemistry.* **49**:10208-10215. doi: 10.1021/bi101011j; 10.1021/bi101011j.
45. **Robertson, J. S., M. Schubert, and R. A. Lazzarini.** 1981. Polyadenylation sites for influenza virus mRNA. *J Virol.* **38**:157-163.
46. **Li, X., and P. Palese.** 1994. Characterization of the polyadenylation signal of influenza virus RNA. *J Virol.* **68**:1245-1249.
47. **Luo, G. X., W. Luytjes, M. Enami, and P. Palese.** 1991. The polyadenylation signal of influenza virus RNA involves a stretch of uridines followed by the RNA duplex of the panhandle structure. *J Virol.* **65**:2861-2867.
48. **Vreede, F. T., T. E. Jung, and G. G. Brownlee.** 2004. Model suggesting that replication of influenza virus is regulated by stabilization of replicative intermediates. *J Virol.* **78**:9568-9572. doi: 10.1128/JVI.78.17.9568-9572.2004.
49. **Stevens, J., O. Blixt, J. C. Paulson, and I. A. Wilson.** 2006. Glycan microarray technologies: tools to survey host specificity of influenza viruses. *Nat Rev Microbiol.* **4**:857-864. doi: 10.1038/nrmicro1530.

50. **Webster, R. G., and Y. J. Guo.** 1991. New influenza virus in horses. *Nature*. **351**:527.
51. **Kundin, W. D.** 1970. Hong Kong A-2 influenza virus infection among swine during epidemic in Taiwan. *Nature*. **228**:857.
52. **Hinshaw, V. S., W. J. Bean, J. Geraci, P. Fiorelli, G. Early, and R. G. Webster.** 1986. Characterization of two influenza A viruses from a pilot whale. *J Virol*. **58**:655-656.
53. **Claas, E. C., A. D. Osterhaus, R. van Beek, J. C. De Jong, G. F. Rimmelzwaan, D. A. Senne, S. Krauss, K. F. Shortridge, and R. G. Webster.** 1998. Human influenza A H5N1 virus related to a highly pathogenic avian influenza virus. *Lancet*. **351**:472-7.
54. 1998. Update: isolation of avian influenza A(H5N1) viruses from humans--Hong Kong, 1997-1998. *MMWR Morb Mortal Wkly Rep*. **46**:1245-7.
55. **Ku, A. S., and L. T. Chan.** 1999. The first case of H5N1 avian influenza infection in a human with complications of adult respiratory distress syndrome and Reye's syndrome. *J Paediatr Child Health*. **35**:207-9.
56. **Centers for Disease Control and Prevention.** 1998. From the Centers for Disease Control and Prevention. Isolation of avian influenza A(H5N1) viruses from humans--Hong Kong, May-December 1997. *J Am Med Assoc*. **279**:263-4.
57. **Mounts, A. W., H. Kwong, H. S. Izurieta, Y. Ho, T. Au, M. Lee, C. B. Bridges, S. W. Williams, K. H. Mak, J. M. Katz, W. W. Thompson, N. J. Cox, and K. Fukuda.** 1999. Case-Control Study of Risk Factors for Avian Influenza A (H5N1) Disease, Hong Kong, 1997. *J Infect Dis*. **180**:505-508. doi: 10.1086/314903.
58. 2005. Avian Influenza A (H5N1) Infection in Humans. *N Engl J Med*. **353**:1374-1385. doi: doi:10.1056/NEJMra052211.
59. **Hien, T. T., N. T. Liem, N. T. Dung, L. T. San, P. P. Mai, N. v. V. Chau, P. T. Suu, V. C. Dong, L. T. Q. Mai, N. T. Thi, D. B. Khoa, L. P. Phat, N. T. Truong, H. T. Long, C. V. Tung, L. T. Giang, N. D. Tho, L. H. Nga, N. T. K. Tien, L. H. San, L. V. Tuan, C. Dolecek, T. T. Thanh, M. de Jong, C. Schultz, P. Cheng, W. Lim, P. Horby, and J. Farrar.** 2004. Avian Influenza A (H5N1) in 10 Patients in Vietnam. *N Engl J Med*. **350**:1179-1188. doi: doi:10.1056/NEJMoa040419.
60. **Unghusak, K., P. Auewarakul, S. F. Dowell, R. Kitphati, W. Auwanit, P. Puthavathana, M. Uprasertkul, K. Boonnak, C. Pittayawonganon, N. J. Cox, S. R. Zaki, P. Thawatsupha, M. Chittaganpitch, R. Khontong, J. M. Simmerman, and S. Chunsutthiwat.** 2005. Probable Person-to-Person Transmission of Avian Influenza A (H5N1). *N Engl J Med*. **352**:333-340. doi: doi:10.1056/NEJMoa044021.
61. **Bridges, C. B., J. M. Katz, W. H. Seto, P. K. S. Chan, D. Tsang, W. Ho, K. H. Mak, W. Lim, J. S. Tam, M. Clarke, S. G. Williams, A. W. Mounts, J. S. Bresee, L. A. Conn,**

T. Rowe, J. Hu-Primmer, R. A. Abernathy, X. Lu, N. J. Cox, and K. Fukuda. 2000. Risk of Influenza A (H5N1) Infection among Health Care Workers Exposed to Patients with Influenza A (H5N1), Hong Kong. *J Inf Dis.* **181**:344-348. doi: 10.1086/315213.

62. **Tran, T. H., T. L. Nguyen, T. D. Nguyen, T. S. Luong, P. M. Pham, V. Nguyen v, T. S. Pham, C. D. Vo, T. Q. Le, T. T. Ngo, B. K. Dao, P. P. Le, T. T. Nguyen, T. L. Hoang, V. T. Cao, T. G. Le, D. T. Nguyen, H. N. Le, K. T. Nguyen, H. S. Le, V. T. Le, D. Christiane, T. T. Tran, J. Menno de, C. Schultsz, P. Cheng, W. Lim, P. Horby, and J. Farrar.** 2004. Avian influenza A (H5N1) in 10 patients in Vietnam. *N Engl J Med.* **350**:1179-88.

63. **Parry, J.** 2004. WHO investigates possible human to human transmission of avian flu. *BMJ.* **328**:308.

64. **Normile, D., and M. Enserink.** 2004. Infectious diseases. Avian influenza makes a comeback, reviving pandemic worries. *Science.* **305**:321.

65. **Chan, P. K. S.** 2002. Outbreak of Avian Influenza A(H5N1) Virus Infection in Hong Kong in 1997. *Clin Infect Dis.* **34**:S58-S64. doi: 10.1086/338820.

66. **Chotpitayasunondh, T., K. Ungchusak, W. Hanshaoworakul, S. Chunsuthiwat, P. Sawanpanyalert, R. Kijphati, S. Lochindarat, P. Srisan, P. Suwan, Y. Osotthanakorn, T. Anantasetagoon, S. Kanjanawasri, S. Tanupattarachai, J. Weerakul, R. Chaiwirattana, M. Maneerattanaporn, R. Poolsavathitkool, K. Chokephaibulkit, A. Apisarnthanarak, and S. Dowell.** 2005. Human Disease from Influenza A (H5N1), Thailand, 2004. *Emerg Infect Dis.* **11**:201-9.

67. **Tam, J. S.** 2002. Influenza A (H5N1) in Hong Kong: an overview. *Vaccine.* **20, Supplement 2**:S77-S81. doi: 10.1016/S0264-410X(02)00137-8.

68. **de Jong, M. D., B. V. Cam, P. T. Qui, V. M. Hien, T. T. Thanh, N. B. Hue, M. Beld, L. T. Phuong, T. H. Khanh, N. V. V. Chau, T. T. Hien, D. Q. Ha, and J. Farrar.** 2005. Fatal Avian Influenza A (H5N1) in a Child Presenting with Diarrhea Followed by Coma. *N Engl J Med.* **352**:686-691. doi: doi:10.1056/NEJMoa044307.

69. **Wang, T. T., M. K. Parides, and P. Palese.** 2012. Seroevidence for H5N1 influenza infections in humans: meta-analysis. *Science.* **335**:1463. doi: 10.1126/science.1218888; 10.1126/science.1218888.

70. **World Health Organization.** 2011. Updated unified nomenclature system for the highly pathogenic H5N1 avian influenza viruses. [updated October 2011; cited 16 January 2013]. Available from: http://www.who.int/influenza/gisrs_laboratory/h5n1_nomenclature/en/index.html.

71. **WHO/OIE/FAO H5N1 Evolution Working Group.** 2009. Continuing progress towards a unified nomenclature for the highly pathogenic H5N1 avian influenza viruses: divergence

of clade 2.2 viruses. *Influenza and Other Respiratory Viruses*. **3**:59-62. doi: 10.1111/j.1750-2659.2009.00078.x.

72. **WHO/OIE/FAO H5N1 Evolution Working Group**. 2012. Continued evolution of highly pathogenic avian influenza A (H5N1): updated nomenclature. *Influenza and Other Respiratory Viruses*. **6**:1-5. doi: 10.1111/j.1750-2659.2011.00298.x.

73. **Gao, P., S. Watanabe, T. Ito, H. Goto, K. Wells, M. McGregor, A. J. Cooley, and Y. Kawaoka**. 1999. Biological Heterogeneity, Including Systemic Replication in Mice, of H5N1 Influenza A Virus Isolates from Humans in Hong Kong. *J Virol*. **73**:3184-3189; 3184.

74. **Tumpey, T. M., X. Lu, T. Morken, S. R. Zaki, and J. M. Katz**. 2000. Depletion of Lymphocytes and Diminished Cytokine Production in Mice Infected with a Highly Virulent Influenza A (H5N1) Virus Isolated from Humans. *J Virol*. **74**:6105-6116. doi: 10.1128/jvi.74.13.6105-6116.2000.

75. **Lu, X., T. M. Tumpey, T. Morken, S. R. Zaki, N. J. Cox, and J. M. Katz**. 1999. A Mouse Model for the Evaluation of Pathogenesis and Immunity to Influenza A (H5N1) Viruses Isolated from Humans. *J Virol*. **73**:5903-5911.

76. **Katz, J., X. Lu, A. Frace, T. Morken, S. Zaki, and T. Tumpey**. 2000. Pathogenesis of and immunity to avian influenza A H5 viruses. *Biomed Pharmacother*. **54**:178-187.

77. **Maines, T. R., L. Chen, Y. Matsuoka, H. Chen, T. Rowe, J. Ortin, A. Falco´n, N. T. Hien, L. Q. Mai, E. R. Sedyaningsih, S. Harun, T. M. Tumpey, R. O. Donis, N. J. Cox, K. Subbarao, and J. M. Katz**. 2006. Lack of transmission of H5N1 avian–human reassortant influenza viruses in a ferret model. *Proc Nat. Acad Sci U S A*. **103**:12121-12126.

78. **Park, C. H., M. Ishinaka, A. Takada, H. Kida, T. Kimura, K. Ochiai, and T. Umemura**. 2002. The invasion routes of neurovirulent A/Hong Kong/483/97 (H5N1) influenza virus into the central nervous system after respiratory infection in mice. *Arch Virol*. **147**:1425-1425-1436.

79. **Tanaka, H., C. Park, A. Ninomiya, H. Ozaki, A. Takada, T. Umemura, and H. Kida**. 2003. Neurotropism of the 1997 Hong Kong H5N1 influenza virus in mice. *Vet Microbiol*. **95**:1-13.

80. **Rothwell, N. J**. 1999. Cytokines – killers in the brain? *J Physiol*. **514**:3-17. doi: 10.1111/j.1469-7793.1999.003af.x.

81. **Maines, T. R., X. H. Lu, S. M. Erb, L. Edwards, J. Guarner, P. W. Greer, D. C. Nguyen, K. J. Szretter, L. Chen, P. Thawatsupha, M. Chittaganpitch, S. Waicharoen, D. T. Nguyen, T. Nguyen, H. H. T. Nguyen, J. Kim, L. T. Hoang, C. Kang, L. S. Phuong, W. Lim, S. Zaki, R. O. Donis, N. J. Cox, J. M. Katz, and T. M. Tumpey**. 2005. Avian Influenza (H5N1) Viruses Isolated from Humans in Asia in 2004 Exhibit Increased Virulence in Mammals. *J Virol*. **79**:11788-11800; 11788.

82. **Nishimura, H., S. Itamura, T. Iwasaki, T. Kurata, and M. Tashiro.** 2000. Characterization of human influenza A (H5N1) virus infection in mice: neuro-, pneumo- and adipotropic infection. *J Gen Virol.* **81**:2503-2510.
83. **Belser, J. A., K. J. Szretter, J. M. Katz, and T. M. Tumpey.** 2009. Use of Animal Models to Understand the Pandemic Potential of Highly Pathogenic Avian Influenza Viruses. *Advances in Virus Research.* **73**:55-97; 55.
84. **Rowe, T., D. S. Cho, R. A. Bright, L. A. Zitzow, and J. M. Katz.** 2003. Neurological Manifestations of Avian Influenza Viruses in Mammals. *Avian Diseases.* **47**:1122-1126.
85. **Zitzow, L. A., T. Rowe, T. Morken, W. Shieh, S. Zaki, and J. M. Katz.** 2002. Pathogenesis of Avian Influenza A (H5N1) Viruses in Ferrets. *J Virol.* **76**:4420-4429; 4420.
86. **Govorkova, E. A., J. E. Rehg, S. Krauss, H. Yen, Y. Guan, M. Peiris, T. D. Nguyen, T. H. Hanh, P. Puthavathana, H. T. Long, C. Buranathai, W. Lim, R. G. Webster, and E. Hoffmann.** 2005. Lethality to Ferrets of H5N1 Influenza Viruses Isolated from Humans and Poultry in 2004. *J Virol.* **79**:2191-2198; 2191.
87. **Wang, X., J. Zhao, S. Tang, Z. Ye, and Hewlett I.** 2010. Viremia associated with fatal outcomes in ferrets infected with avian H5N1 influenza virus. *PLoS One.* **5**:e12099. doi: 10.1371/journal.pone.0012099.
88. **Kuiken, T., J. van den Brand, D. van Riel, M. Pantin-Jackwood, and D. E. Swayne.** 2010. Comparative Pathology of Select Agent Influenza A Virus Infections. *Vet Pathol.* **47**:893-914. doi: 10.1177/0300985810378651.
89. **Jang, H., D. Boltz, K. Sturm-Ramirez, K. R. Shepherd, Y. Jiao, R. Webster, and R. J. Smeyne.** 2009. Highly pathogenic H5N1 influenza virus can enter the central nervous system and induce neuroinflammation and neurodegeneration. *Proc Natl Acad Sci U S A.* **106**:14063-14068; 14063.
90. **Skehel, J., and D. Wiley.** 2000. Receptor binding and membrane fusion in virus entry: the influenza hemagglutinin. *Annu Rev Biochem.* **69**:531-69.
91. **Bosch, F., W. Garten, H. Klenk, and R. Rott.** 1981. Proteolytic cleavage of influenza virus hemagglutinins: primary structure of the connecting peptide between HA1 and HA2 determines proteolytic cleavability and pathogenicity of Avian influenza viruses. *Virology.* **113**:725-35.
92. **Walker, J., S. Molloy, G. Thomas, T. Sakaguchi, T. Yoshida, T. Chambers, and Y. Kawaoka.** 1994. Sequence specificity of furin, a proprotein-processing endoprotease, for the hemagglutinin of a virulent avian influenza virus. *J Virol.* **68**:1213-1218.
93. **Steinhauer, D.** 1999. Role of hemagglutinin cleavage for the pathogenicity of influenza virus. *Virology.* **258**:1-20.

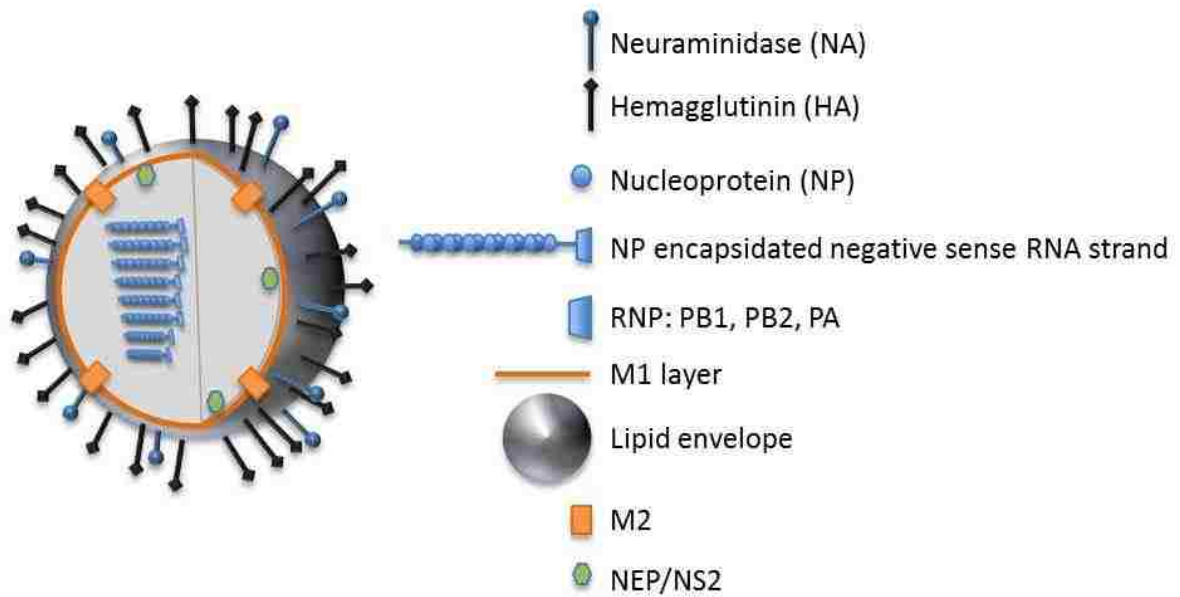
94. **Hatta, M., P. Gao, P. Halfmann, and Y. Kawaoka.** 2001. Molecular basis for high virulence of Hong Kong H5N1 influenza A viruses. *Science*. **293**:1840-1842.
95. **Belser, J., X. Lu, T. Maines, C. Smith, Y. Li, R. Donis, J. Katz, and T. Tumpey.** 2007. Pathogenesis of avian influenza (H7) virus infection in mice and ferrets: Enhanced virulence of Eurasian H7N7 viruses isolated from humans. *J Virol*. **81**:11139-11147.
96. **Schrauwen, E. J. A., S. Herfst, L. M. Leijten, P. van Run, T. M. Bestebroer, M. Linster, R. Bodewes, J. H. C. M. Kreijtz, G. F. Rimmelzwaan, A. D. M. E. Osterhaus, R. A. M. Fouchier, T. Kuiken, and D. van Riel.** 2012. The Multibasic Cleavage Site in H5N1 Virus Is Critical for Systemic Spread along the Olfactory and Hematogenous Routes in Ferrets. *J Virol*. **86**:3975-3984. doi: 10.1128/jvi.06828-11.
97. **McNicholl, I. R., and J. J. McNicholl.** 2001. Neuraminidase inhibitors: zanamivir and oseltamivir. *Ann Pharmacother*. **35**:57-70.
98. **Wagner, R., M. Matrosovich, and H. Klenk.** 2002. Functional balance between haemagglutinin and neuraminidase in influenza virus infections. *Rev Med Virol*. **12**:159-66.
99. **Wagner, R., T. Wolff, A. Herwig, S. Pleschka, and H. Klenk.** 2000. Interdependence of Hemagglutinin Glycosylation and Neuraminidase as Regulators of Influenza Virus Growth: a Study by Reverse Genetics. *J Virol*. **74**:6316-6323. doi: 10.1128/jvi.74.14.6316-6323.2000.
100. **Baigent, S. J., and J. W. McCauley.** 2001. Glycosylation of haemagglutinin and stalk-length of neuraminidase combine to regulate the growth of avian influenza viruses in tissue culture. *Virus Research*. **79**:177--185.
101. **Baigent, S. J., R. C. Bethell, and J. W. McCauley.** 1999. Genetic Analysis Reveals That Both Haemagglutinin and Neuraminidase Determine the Sensitivity of Naturally Occurring Avian Influenza Viruses to Zanamivir in Vitro. *Virology*. **2**:323--338.
102. **Matsuoka, Y., D. E. Swayne, C. Thomas, M. Rameix-Welti, N. Naffakh, C. Warnes, M. Altholtz, R. Donis, and K. Subbarao.** 2009. Neuraminidase Stalk Length and Additional Glycosylation of the Hemagglutinin Influence the Virulence of Influenza H5N1 Viruses for Mice. *J Virol*. **83**:4704-4708. doi: 10.1128/JVI.01987-08.
103. **Salomon, R., J. Franks, E. A. Govorkova, N. A. Ilyushina, H. Yen, D. J. Hulse-Post, J. Humberd, M. Trichet, J. E. Rehg, R. J. Webby, R. G. Webster, and E. Hoffmann.** 2006. The polymerase complex genes contribute to the high virulence of the human H5N1 influenza virus isolate A/Vietnam/1203/04. *Journal of Experimental Medicine*. **203**:689-697; 689.
104. **Roberts, N. A.** 2001. Treatment of Influenza with Neuraminidase Inhibitors: Virological Implications. *Philosophical Transactions: Biological Sciences*. **356**:1895-1897.

105. **Hughey, P., P. Roberts, L. Holsinger, S. Zebedee, R. Lamb, and R. Compans.** 1995. Effects of antibody to the influenza A virus M2 protein on M2 surface expression and virus assembly. *Virology*. **212**:411-421.
106. **Schroeder, C., H. Heider, E. Möncke-Buchner, and Tse-I Lin.** 2005. The influenza virus ion channel and maturation cofactor M2 is a cholesterol-binding protein. *European Biophysics Journal*. **34**:52-66. doi: 10.1007/s00249-004-0424-1.
107. **Fiers, W., M. De Filette, A. Birkett, S. Neiryck, and W. Min Jou.** 2004. A "universal" human influenza A vaccine. *Virus Research*. **103**:173-176.
108. **Pielak, R. M., and J. J. Chou.** 2010. Flu channel drug resistance: a tale of two sites. *Protein Cell*. **1**:246-258. doi: 10.1007/s13238-010-0025-y; 10.1007/s13238-010-0025-y.
109. **Ison, M. G.** 2011. Antivirals and resistance: influenza virus. *Curr Opin Virol*. **1**:563-573. doi: 10.1016/j.coviro.2011.09.002; 10.1016/j.coviro.2011.09.002.
110. **Steel, J., A. C. Lowen, S. Mubareka, and P. Palese.** 2009. Transmission of influenza virus in a mammalian host is increased by PB2 amino acids 627K or 627E/701N. *PLoS Path*. **5**:e1000252.
111. **Abrahams, A.** 1919. Discussion on Influenza. *Proc R Soc Med*. **12**:97-102.
112. **Spilsbury, B. H.** 1919. Discussion on Influenza. *Proc R Soc Med*. **12**:55-57.
113. **Turner, E. B.** 1919. Discussion on Influenza. *Proc R Soc Med*. **12**:76-90.
114. **Hamer, W. H.** 1919. Discussion on Influenza. *Proc R Soc Med*. **12**:24-26.
115. **Kapila, C. C., S. Kaul, S. C. Kapur, T. S. Kalayanam, and D. Banderjee.** 1958. Neurological and hepatic disorders associated with influenza. *BMJ*. **2**:1311-1314.
116. 1970. Neurological complications of influenza. *BMJ*. **1**:248-249.
117. **Glaser, C. A., K. Winter, K. DuBray, K. Harriman, T. M. Uyeki, J. Sejvar, S. Gilliam, and J. K. Louie.** 2012. A population-based study of neurologic manifestations of severe influenza A(H1N1)pdm09 in California. *Clin Infect Dis*. **55**:514-520. doi: 10.1093/cid/cis454; 10.1093/cid/cis454.
118. **Brojer, C., E. O. Agren, H. Uhlhorn, K. Bernodt, D. S. Jansson, and D. Gavier-Widen.** 2012. Characterization of encephalitis in wild birds naturally infected by highly pathogenic avian influenza H5N1. *Avian Dis*. **56**:144-152.
119. **Cardona, C. J., Z. Xing, C. E. Sandrock, and C. E. Davis.** 2009. Avian influenza in birds and mammals. *Comp Immunol Microbiol Infect Dis*. **32**:255-73.

120. **Keawcharoen, J., K. Oraveerakul, T. Kuiken, R. A. Fouchier, A. Amonsin, S. Payungporn, S. Noppornpanth, S. Wattanodorn, A. Theambooniers, R. Tantilertcharoen, R. Pattanarangsarn, N. Arya, P. Ratanakorn, D. M. Osterhaus, and Y. Poovorawan.** 2004. Avian influenza H5N1 in tigers and leopards. *Emerg Infect Dis.* **10**:2189-91.
121. **Zhang, Z., J. Zhang, K. Huang, K. S. Li, K. Y. Yuen, Y. Guan, H. Chen, and W. F. Ng.** 2009. Systemic infection of avian influenza A virus H5N1 subtype in humans. *Hum Pathol.* **40**:735-9.
122. **Korteweg, C., and J. Gu.** 2008. Pathology, molecular biology, and pathogenesis of avian influenza A (H5N1) infection in humans. *Am J Pathol.* **172**:1155-1170. doi: 10.2353/ajpath.2008.070791; 10.2353/ajpath.2008.070791.
123. **Gao, R., L. Dong, J. Dong, L. Wen, Y. Zhang, H. Yu, Z. Feng, M. Chen, Y. Tan, Z. Mo, H. Liu, Y. Fan, K. Li, C. K. Li, D. Li, W. Yang, and Y. Shu.** 2010. A systematic molecular pathology study of a laboratory confirmed H5N1 human case. *PLoS One.* **5**:e13315.
124. **Bodewes, R., J. H. C. M. Kreijtz, G. van Amerongen, R. A. M. Fouchier, A. D. M. E. Osterhaus, G. F. Rimmelzwaan, and T. Kuiken.** 2011. Pathogenesis of influenza A/H5N1 virus infection in ferrets differs between intranasal and intratracheal routes of inoculation. *Am J Pathol.* **179**:30-30-36. doi: 10.1016/j.ajpath.2011.03.026.
125. **Plourde, J. R., J. A. Pyles, R. C. Layton, S. E. Vaughan, J. L. Tipper, and K. S. Harrod.** 2012. Neurovirulence of H5N1 infection in ferrets is mediated by multifocal replication in distinct permissive neuronal cell regions. *PLoS One.* **7**:e46605. doi: 10.1371/journal.pone.0046605; 10.1371/journal.pone.0046605.
126. **Lednicky, J. A., S. B. Hamilton, R. S. Tuttle, W. A. Sosna, D. E. Daniels, and D. E. Swayne.** 2010. Ferrets develop fatal influenza after inhaling small particle aerosols of highly pathogenic avian influenza virus A/Vietnam/1203/2004 (H5N1). *Virology.* **7**:231-422X-7-231. doi: 10.1186/1743-422X-7-231; 10.1186/1743-422X-7-231.
127. **Gustin, K. M., J. A. Belser, D. A. Wadford, M. B. Pearce, J. M. Katz, T. M. Tumpey, and T. R. Maines.** 2011. Influenza virus aerosol exposure and analytical system for ferrets. *Proc Natl Acad Sci U S A.* **108**:8432-8437. doi: 10.1073/pnas.1100768108.

Figure

Figure 1. Cartoon representation of an influenza virus.



Tables

Table 1. Influenza RNA segments and known functions of each translated protein.

RNA segments/proteins	RNA genome length (in nucleotides)	Protein length (in amino acids)	Function
PB2	2341	759	Cap recognition, component of the RNA transcriptase complex
PB1-F2		87	Pro-apoptotic activity
PB1	2341	757	Endonuclease activity, elongation, part of transcriptase complex
PA	2233	716	Protease, part of transcriptase and replicase complex
HA	1778	550	Surface glycoprotein, receptor binding, fusion activity, major antigen
NP	1565	498	RNA binding, RNA synthesis, RNA nuclear import
NA	1413	454	Surface glycoprotein, neuraminidase activity
M1	1027	252	Matrix protein, interaction with vRNPs and surface glycoproteins, nuclear export, budding
M2	366	97	Membrane protein, ion channel activity, assembly
NS1	890	230	Multi-functional protein, viral interferon antagonist
NEP/NS2	418	121	Nuclear export of vRNPs

Table 2. Genetic analysis of VN1203 and HK483.

Segment	Protein	# a.a.	# Same a.a.	# Different a.a.	Percent Similarity
1	PB2	759	733	26	97%
2	PB1	684	669	15	98%
3	PA	716	669	32	93%
4	HA	568	546	22	96%
5	NP	498	487	11	98%
6	NA	450	407	43	90%
7	M1	252	240	12	95%
	M2	97	88	9	91%
8	NS1	230	186	44	81%
	NS2	121	110	11	91%

a.a.: amino acid

Chapter Two: Neurovirulence of H5N1 infection in ferrets is mediated by multifocal replication in distinct permissive neuronal cell regions

Jennifer R. Plourde,^{1,2} John A. Pyles,¹ R. Colby Layton,^{1,3} Sarah E. Vaughan,^{1,2} Jennifer L. Tipper,¹ and Kevin S. Harrod^{1,2,#}

¹Infectious Diseases Program, Lovelace Respiratory Research Institute, 2425 Ridgecrest Dr. SE, Albuquerque, NM 87108

² Department of Pathology, University of New Mexico School of Medicine, 1 University of New Mexico, Albuquerque, NM 87131-0001

³ RC Layton present location: MRIGlobal, Virology & Infectious Disease Animal Models, Energy and Life Sciences Division, 425 Volker Blvd, Kansas City, MO 64110

Email: kharrod@lrri.org

Conceived and designed experiments: JRP, RCL, JLT, KSH. Performed the experiments: JRP, JAP, RCL, SEV. Analyzed the data: JRP, KSH. Wrote the paper: JRP, KSH

Citation:

Plourde JR, Pyles JA, Layton RC, Vaughan SE, Tipper JL, Harrod KS.

Neurovirulence of H5N1 Infection in Ferrets Is Mediated by Multifocal Replication

in Distinct Permissive Neuronal Cell Regions. PLoS One. 2012;7(10):e46605. doi:

10.1371/journal.pone.0046605. Epub 2012 Oct 8. PubMed PMID: 23056366; PubMed

Central PMCID: PMC3466300.

Abstract

Highly pathogenic avian influenza A (HPAI), subtype H5N1, remains an emergent threat to the human population. While respiratory disease is a hallmark of influenza infection, H5N1 has a high incidence of neurological sequelae in many animal species and sporadically in humans. We elucidate the temporal/spatial infection of H5N1 in the brain of ferrets following a low dose, intranasal infection of two HPAI strains of varying neurovirulence and lethality. A/Vietnam/1203/2004 (VN1203) induced mortality in 100% of infected ferrets while A/Hong Kong/483/1997 (HK483) induced lethality in only 20% of ferrets with death occurring significantly later following infection. Neurological signs were prominent in VN1203 infection, but not HK483, with seizures observed three days post challenge and torticollis or paresis at later time points. VN1203 and HK483 replication kinetics were similar in primary differentiated ferret nasal turbinate cells and similar viral titers were measured in the nasal turbinates of infected ferrets. Pulmonary viral titers were not different between strains and pathological findings in the lungs were similar in severity. VN1203 replicated to high titers in the olfactory bulb, cerebral cortex, and brain stem; whereas HK483 was not recovered in these tissues. VN1203 was identified adjacent to and within the olfactory nerve tract and multifocal infection was observed throughout the frontal cortex and cerebrum. VN1203 was also detected throughout the cerebellum, specifically in Purkinje cells and regions that coordinate voluntary movements. These findings suggest the increased lethality of VN1203 in ferrets is due to increased replication in brain regions important in higher order function and explains the neurological signs observed during H5N1 neurovirulence.

Introduction

Highly pathogenic avian influenza A (HPAI), subtype H5N1, has infected humans in 12 countries and has been associated with approximately a 60% mortality rate since 1997 (http://www.who.int/influenza/human_animal_interface/EN_GIP_20111010CumulativeNumberH5N1cases.pdf). Severe disease of H5N1 includes fast-progressing pneumonia, acute respiratory distress syndrome (ARDS), diarrhea, central nervous system (CNS) clinical signs, and multi-organ failure. Death often occurs within ten days of symptom onset (1-3). Studies to identify virulence factors contributing to these phenotypes have been the focus of many recent investigations (4-8). However the mechanisms leading to increased pathogenesis by H5N1, particularly non-pulmonary events, remain to be discovered.

ARDS is a common manifestation of pulmonary influenza infection; however H5N1 has been atypically shown to also infect and damage the CNS. De Jong and colleagues reported acute encephalitis in brains of humans infected with H5N1. These patients did not present with respiratory illness but had severe diarrhea, with early onset of seizures and coma, and death occurring within one to five days post hospital admittance (9). Murine infection models have illustrated that neurotropic H5N1 strains exhibit higher lethality than those that do not replicate efficiently in the brain (10). Several groups have investigated possible routes of viral entry into the brain, including the olfactory system as a major route into the brain of experimentally infected ferrets (10-12). Studies by Park *et al.* suggested that, in addition to the olfactory nerves, HPAI enters the CNS through the vagal, trigeminal, and sympathetic nerves (12). Furthermore, the dissemination of H5N1 through the bloodstream is plausible due to the presence of virus in organs such as the spleen apart from the site of initial infection.

While these possible routes of infection in the brain have been identified, little is known regarding HPAI dissemination within the CNS and its contribution to clinical signs and lethality. Therefore, delineating neurotropic features of H5N1 infection in the ferret model could lead to a better understanding of mechanisms responsible for widespread infection throughout the central nervous system.

Herein, we compare two strains of H5N1 with distinct neurotropism and lethality in ferrets to elucidate the temporal-spatial neuroinvasion leading to death. We show that VN1203 resulted in wider dissemination in the brain and associated with higher morbidity and clinical signs of neurological involvement. By comparison, HK483 infection resulted in low mortality, no viable virus recovered from the brain, and a low incidence of brain lesions limited solely to the olfactory system. Furthermore, we identify brain regions and cell types susceptible to VN1203 that explain the myriad of neurological signs during lethal infection. These findings broaden our understanding of the neurovirulence of H5N1 viruses and support further investigation into therapies leading to CNS protection.

Materials and Methods

Ethics statement

The protocol (FY10-098) for all animal procedures was approved by the Institutional Animal Care and Use Committee (IACUC) and Institutional Biosafety Committee of the Lovelace Respiratory Research Institute, Albuquerque, NM. All facilities were accredited by the Association for Assessment and Accreditation of Laboratory Animal Care International (AAALAC). Ferret experiments were conducted in the Animal Biosafety Level 3 enhanced (ABSL-3+) facility and guidelines for ferret housing, environment, and comfort described in the Guide For The Care and Use of Laboratory Animals, Seventh Edition, National Research

Council, were strictly followed. Euthanasia was performed under the guidance of the American Veterinary Medical Associations (AVMA) Guidelines on Euthanasia.

Virus preparation

Highly pathogenic avian influenza A (HPAI) H5N1 viruses were obtained from the Centers for Disease Control and Prevention (CDC) (Atlanta, GA). A/Vietnam/1203/2004 (VN1203) was isolated from a pharyngeal swab from a ten year old male patient that died of the disease in Vietnam in 2004 (7) and A/Hong Kong/483/1997 (HK483) was isolated from a 13 year old male patient that died of the disease in Hong Kong in 1997 (7). These viruses were propagated from the CDC stock in eggs twice to produce working stocks, aliquoted, titrated by plaque assay on Madin-Darby Canine Kidney (MDCK) cells, and stored at -80°C. All manipulations with these viruses were conducted under Biosafety Level 3 (BSL-3) conditions in the BSL-3 or animal BSL-3 enhanced (ABSL-3+) at the Lovelace Respiratory Research Institute in Albuquerque, New Mexico.

Ferret handling/care and infection

Castrated male ferrets (*Mustela putorius furo*), 11 – 14 weeks of age at the day of infection, weighing 0.7 to 1.0 kg, (supplied by Triple F Farms, Sayre, PA) were used for the studies. They were pre-screened by the supplier for H1 and H3 influenza A and influenza B seroconversion prior to shipment and similarly screened at LRRI within a week prior to infection. Ferrets were triple-housed throughout (including 14 days of quarantine and after viral challenge) in stainless steel cages and in separate BioBubbles® depending on H5N1 strain. Ferrets had access to food and water *ad libitum*. Temperature and humidity ranged 16 to 22°C and 30 to 65% respectively, and the light cycle was 12 hr on and 12 hr off. Ventilation in the study room was >15 air exchanges per hour. All ferret handlers were

vaccinated for circulating seasonal influenza strains and were not permitted to enter ferret quarters if they exhibited any symptoms of upper or lower respiratory infection.

Viral infection of ferrets

Ferrets were identified by an IPTT-300 Implantable Programmable Temperature and Identification Transponder; Bio Medic Data Systems, Inc, (BMDS) (Seaford, Delaware). These chips also provided subcutaneous body temperature data using a BMDS electronic proximity reader wand (WRS-6007; BMDS). Ferrets were anesthetized with an intramuscular injection of a ketamine/xylazine cocktail (20mg/kg of ketamine and 2 mg/kg of xylazine). Ferrets received 0.500 mL of pathogen or allantoic fluid per naris with a total of 1.0 mL delivered. Each subject was held upright for about one minute to ensure retention of the inoculum. Groups of ten ferrets were instilled with 10 PFU of VN1203 or HK483. An additional group of 18 ferrets was also infected with 10 PFU of HK483 and groups of six were sacrificed 4, 6, and 8 days post-infection for examination by virology and immunohistochemical assays.

Clinical observations were conducted twice daily and included temperature readings from the BMDS microchip and recording of clinical signs of disease. Study personnel were trained specifically in ferret handling procedures and the observation and recording of adverse signs and clinical symptoms in ferrets. Observations were recorded using an electronic data recording system. The onset, nature, severity, and duration of all visible changes such as abnormal respiration, excretions, behavioral, and neurological signs (*i.e.*, paresis, torticollis, seizures, and paralysis) were recorded as well as any observed coughing, sneezing, and nasal or ocular discharge. Additionally, an activity score was assigned at each

observation as follows: (0 = alert and playful, 1 = alert but playful only when stimulated, 2 = alert but not playful when stimulated, and 3 = neither alert nor playful when stimulated).

Cell culture and infection

Primary differentiated cells were isolated from the nasal turbinates of naïve ferrets and the protocol was adapted with minor modifications as described previously (13). Cells were rinsed from the tissue and plated directly onto collagen-coated 100mm tissue culture dishes. Cells were plated directly onto collagen coated transwell inserts (Corning Inc., Lowell, MA) with BEGM plus DMEM (Sigma-Aldrich Co. LLC., St. Louis, MO) media in the basolateral and apical chambers. Approximately seven days later, the media in the apical chamber was removed and the cells were maintained under air-liquid interface conditions. VN1203 and HK483 stocks were diluted in sterile 1X PBS to a multiplicity of infection of 0.001 in 100 μ L. A volume of 100 μ l of diluted virus or 1X PBS for control was applied to the apical surface of the cells and virus was allowed to penetrate the cells for one hour at 37°C and 5% CO₂. Following one hour of incubation, the inoculum was removed and cells were returned to the incubator until the next collection. The inoculum was titered to determine if there was a difference in adsorption between the two strains. Approximately 500 FFU/mL was delivered and 0 FFU/mL was recovered from the HK483 infected wells and an average of 5 FFU/mL was recovered from the VN1203 infected wells. Apical washes were collected by adding 200 μ L of 1X PBS onto the surface and pipetting five times. This was repeated for a total collection of 400 μ L. Apical washes were stored at -80C until viral titers were determined by an immunostaining foci-forming assay.

Real-time quantitative PCR analysis

Approximately 250 mg of ferret tissue was homogenized in 1mL of sterile 1X PBS at the time of collection and a 0.200 mL aliquot was added to Trizol® for a final volume of 1mL. Viral RNA was extracted using the Qiagen RNeasy kit and the Qiagen Universal Robot (Qiagen Inc., Valencia, CA). Amplification of the full viral coding sequence was done as previously described in (14). All assays were repeated in triplicate on the ABI 7300 real-time PCR system (Applied Biosystems, LifeTechnologies Corp., Carlsbad, CA). The quantitative PCR results were analyzed with the software provided.

Assay for viral titers

Viral titers from the apical wash of infected primary differentiated nasal turbinate cells and from ferret tissue homogenates were determined using the immunostaining foci-forming assay. Approximately 250 mg tissue sections were removed from the right caudal hilar, right caudal peripheral, left cranial hilar, and left cranial peripheral lung lobes, right nasal turbinate, olfactory bulb, cerebral cortex, and brain stem. These tissues were placed in 1 mL of sterile 1X PBS with one 5 mm stainless steel bead and homogenized with a Qiagen tissuelyser (Qiagen Inc., Valencia, CA) for 2 min at 30 Hz/sec. Viral titers were determined using the 96 well format previously described in (15). Virus present in the cells was stained with anti-influenza A antibody, MAB-8251, (Millipore, Billerica, MA), an anti-goat secondary antibody (Vector Laboratories Inc., Burlingame, CA), and detected with 3-Amino-9-ethylcarbazole (AEC) (Sigma-Aldrich Co. LLC., St. Louis, MO). Stained foci were counted and the titer was reported as foci-forming units per mL (FFU/mL).

Hematoxylin and eosin (H&E) stain and immunohistochemistry of ferret tissue sections

Lungs were inflation fixed at 15 cm of pressure with 10% neutral buffered formalin. The skull, lung, and brain were fixed in formalin for seven days then changed to 70%

ethanol. Fixed tissues were embedded in paraffin and tissue sections (4-6 μm) were stained by H&E for histopathological examination under light microscopy. Immunohistochemical staining was conducted using standard protocols. Briefly, endogenous peroxidases were blocked and antigen retrieval was performed using a citrate buffer. Avian influenza nucleoprotein was detected using IMG-5187A, (IMGENEX, San Diego, CA) (16), a biotinylated secondary antibody, and the ABC standard and DAB kits for detection (Vector Laboratories Inc., Burlingame, CA). Images were acquired using the Hamamatsu 2.0 NanoZoomer software (Hamamatsu Corp., Bridgewater, NJ). Histological determinations were made by a board-certified veterinary pathologist unfamiliar with the study design.

Statistical Analysis

GraphPad Prism 5, software version 5.04 (La Jolla, CA) was used to graph data and perform statistical analysis. The Kaplan Meier survival curve was used for the survival analysis, a Student's t-test was used for comparing two means, and an analysis of variance (ANOVA) was used for comparing multiple means. Mean \pm SEM is graphed and $p \leq .05$ was considered statistically significant.

Results

HPAI lethality and clinical signs

The neurotropism of HPAI viruses has been reported in human cases as well as in experimental animal models (4, 9, 10, 12, 17-21). Despite these reports, the neuropathogenesis of HPAI is poorly understood. To test the contribution of neurotropism to the lethality of two HPAI strains, low inoculating titers of A/Hong Kong/483/1997 (HK483) and A/Vietnam/1203/2004 (VN1203) were delivered by intranasal instillation to naïve ferrets using a dose of approximately 10 PFU to simulate the low amount of virus likely to be received in a natural infection. As reported previously, VN1203 is known to cause death at

lower inoculating titers than HK483 (7) and in this study VN1203 infection resulted in a significantly earlier median time to death (MTTD = 4 dpi) and 100% mortality ($n = 10$) within 6 days post-infection (dpi) whereas infection with 10 PFU of HK483 resulted in only 20% lethality ($n = 10$) (**Figure 1A**; Mantel Cox test, $p < .0001$, MTTD unable to be determined). Body weight was measured daily in all animals prior to and following infection (**Figure 1B**). Mock infected ferrets maintained body weight or increased over the twelve day study period, while all animals that received either VN1203 or HK483 declined in body weight. Of animals receiving HK483, survivors and non-survivors exhibited similar declines in body weight both in timing and magnitude, indicating progressing disease. Importantly, many ferrets receiving VN1203 succumbed prior to appreciable losses in body weight. There was no significant difference in weight loss post-infection with either VN1203 or HK483 at inoculating titers of 10 PFU and the eight surviving HK483 challenged ferrets began to gain weight by 12 dpi.

To assess clinical signs during infection with the two different strains, cage side observations were performed twice daily on ferrets following 10 PFU of VN1203 or HK483 infection ($n = 10$ per group). Seven ferrets instilled with VN1203 developed nasal discharge 3 dpi with 100% presenting nasal discharge by 4 dpi. Similarly, 100% of HK483 infected ferrets exhibited nasal discharge by 12 dpi with two subjects presenting symptoms as early as 3 dpi. Ocular discharge was noted between 3 and 6 dpi in two ferrets challenged with VN1203 and four ferrets challenged with HK483. These clinical signs indicated upper respiratory tract infection in the nose and conjunctiva. Eight of ten ferrets challenged with VN1203 developed neurological signs with four ferrets observed to have convulsions in the absence of fever 3 dpi, torticollis observed 5 dpi in one ferret, and paresis of musculoskeletal

dysfunction noted in three ferrets 6 dpi (**Table 1**). Of the two HK483 challenged ferrets that did not survive the study period, one died 6 dpi due to severe influenza-associated pneumonia and secondary bacterial lung infection as determined by histological examination and the second was humanely euthanized after losing more than 25% of its initial bodyweight by 11 dpi. Collectively, these findings indicated that a low dose of VN1203 produced more neurological signs, earlier time to death, and greater lethality compared to ferrets infected with HK483 while weight loss and symptoms in the respiratory tract were not key factors in lethality caused by VN1203.

HPAI infection in ferret nasal turbinates

Numerous reports suggest that virulence may be determined by replication kinetics in epithelial cells of the respiratory tract (20, 22-26). To determine if increased replication in the nasal epithelium contributed to the increased lethality of VN1203 in ferrets, primary differentiated ferret nasal turbinate cells were isolated from naïve ferrets, cultured, and subsequently infected with each H5N1 strain. In preliminary studies, isolated nasal turbinate epithelial cells grown at an air-liquid interface developed a characteristic polarized, pseudostratified morphology and were able to maintain trans-epithelial electrical potential and an air-liquid barrier for greater than two weeks following culture (data not shown). The appearance of multiple ciliary axonemes by microscopy and visible production of mucus are indicative of differentiated cultures similar to normal human bronchial epithelial cells that are routinely used in this laboratory (**Figure 2A**). Ferret nasal turbinate cultures were infected at a multiplicity of infection of 0.001 of VN1203 or HK483 to simulate the low inoculating titer of H5N1 infected ferrets *in vivo*. Viral titers were measured from the apical wash at 24, 48, and 72 hours post infection and infection followed the characteristic replication kinetics

observed for differentiated pulmonary epithelia as previously published by our group (26). As shown in **Figure 2B**, there was no significant difference (ANOVA, $F(1,6) = 1.88$, $p = .22$) in the viral replication of these two HPAI strains, suggesting that increased replication in this cell type is not a key contributor to pathogenesis in ferrets.

To further assess viral replication in the upper respiratory tract, viral load was measured in the nasal turbinates of ferrets infected with VN1203 or HK483. Nasal turbinate tissue was isolated from ferrets undergoing planned necropsies at 4 and 6 dpi and homogenized for analysis by an immunostaining foci-forming assay. Similar viral titers were measured in the nasal turbinates of HK483 and VN1203 challenged ferrets at 4 and 6 dpi (Student's t-test, $p = .42$) (**Figure 2C**). Further examination of viral load in the nasal turbinates was performed by H5N1-specific qRT-PCR analysis of RNA isolated from homogenized nasal turbinate tissue. PCR standards of RNA genomic copy numbers were used to determine the gene copy numbers of infected ferret nasal tissues. Consistent with the findings from viral titer studies, the viral gene copy number was not different between VN1203 and HK483 at either 4 or 6 dpi, and indicate that viral load of VN1203 and HK483 are similar in the nasal tissues of ferrets (data not shown).

Tissue sections of formalin-fixed, paraffin-embedded nasal turbinates from VN1203 or HK483 infected ferrets were examined by microscopy for histological changes and infection with HK483 produced focal areas of ulcerations of nasal epithelium and underlying tissue (**Figure 2E**). Ulcerations were observed in approximately 10% of each nasal cavity examined; whereas ulcerations and erosion was observed in approximately 95% of VN1203 infected nasal cavities. The epithelial barrier remained largely intact though inflammatory cells infiltrated the underlying stroma. The inflammatory response was more pronounced in

HK483 infection compared to VN1203 infection where inflammatory cell infiltration was not frequently observed. The nasal cavity of animals challenged with HK483 and examined 4, 6, and 8 dpi had fewer areas of ulceration in sensory epithelium, the sinuses, and epithelium lining the perimeter of the nasal cavity. In VN1203 infection, turbinate tissues showed larger and more numerous focal regions of epithelial changes (**Figure 2F**), although areas of normal appearance were present. Areas of histological changes were observed in more distal nares. Epithelial disruption and a discontinuous apical layer were characteristic of more severe regions with a loss of cellularity in the basolateral layer (**Figure 2F**). The presence of predominantly neutrophils in the submucosa was noted, as was neutrophil exudates in the nasal lumen. In HK483 infection, alterations of the nasal turbinates were milder at 4 dpi and increased by 6 and 8 dpi whereas histopathology of VN1203 were more numerous at 3 and 4 dpi. The distribution and severity of epithelial damage was milder in HK483 compared to VN1203 at all directly comparable time points. There was a pronounced acute inflammatory response associated with HK483 infection but was not a prominent feature in VN1203 infection.

Immunohistochemical analysis of influenza A NP (**Figure 2H,I**) indicated scattered focal areas of virus antigen detection in the olfactory neuroepithelial cells and in other cells in the intact epithelium of H5N1 infected ferrets as determined by the brown staining against the Luxol fast blue counterstain. The distribution and number of sites of virus expression in the nasal turbinates were variable between animals. Neuroepithelial staining exhibited a clustered appearance (**Figure 2I**) and this clustered staining was more apparent with VN1203 than HK483 infected nasal turbinates (**Figure 2H**).

Pathological observations and viral loads in the lung of HPAI infected ferrets

To assess the extent of respiratory infection concurrent with the lethality and neurological signs of infection, viral titers from homogenized lung tissue were determined by an immunostaining foci-forming assay in ferrets at 4 and 6 days following infection. High viral titers were measured in the lungs of infected ferrets at 4 and 6 dpi, and viral titers in the lung were similar between ferrets infected with HK483 or VN1203 (**Figure 3A**).

Additionally, there was no significant difference in the amount of viral RNA measured in the lung at 4 and 6 dpi for ferrets infected with either virus (**Figure 3B**). Consistent with the findings from nasal tissues, VN1203 and HK483 titers were not different in the lungs of infected ferrets.

Gross examination of lungs from HK483 or VN1203 infection was examined to assess infection-mediated lung disease in both HK483 and VN1203 infected ferrets. Large areas of dark reddish-purple consolidation were observed (**Figure 3D,E**) as compared to mock infected ferrets (**Figure 3C**). To investigate the histopathological changes in the lung of ferrets infected with VN1203 or HK483, randomized sections from four animals per group were stained with hematoxylin and eosin (H&E). Ferrets instilled with HK483 had few focal scattered areas of minimal to mild alveolitis and bronchiolitis on 4 dpi. Low numbers of epithelial cells detached into the lumen of alveolar spaces and there was infiltration of low numbers of neutrophils. There were peribronchiolar and scattered areas of alveolar parenchyma loss and infiltration of moderate numbers of neutrophil and mononuclear inflammatory cells 6 dpi. Locally extensive areas of bronchiolitis and peribronchiolar pneumonia, with localized loss of alveolar spaces in some animals were also observed (**Figure 3G**). The lung of ferrets challenged with VN1203 had multiple focal areas of pronounced cytopathology in the alveolar lining epithelium on 3 dpi. The severity of

epithelial loss and damage to the interalveolar wall resulted in fibrin and edema exudate and hemorrhage in these areas. There was infiltration of low numbers of neutrophil inflammatory cells, primarily in the interalveolar wall. Examination of lungs at 6 dpi showed multifocal areas with moderate neutrophil infiltration in the alveolar walls and alveolar spaces and minimal to mild edema exudate (**Figure 3H**). While the type of damage induced by each strain was distinct, the distribution of lung damage in the airways and alveoli were equivalent following either VN1203 or HK483 infection in ferrets.

HPAI viral load in the brain

Little is known regarding CNS involvement in the progression of HPAI disease. To determine the extent to which VN1203 and HK483 replicated in the olfactory bulb, tissue homogenates of the olfactory bulb were evaluated for viral titers. High viral titers were measured in the olfactory bulb of ferrets 3 to 6 days post challenge with VN1203. In contrast, no virus was recovered at 4, 6, or 8 dpi from the olfactory bulb of ferrets infected with HK483 (**Figure 4A**). To further assess more distal brain regions, viral titers from the cerebral cortex were also measured. Titers up to 10^7 foci forming units (FFU)/mL were detected in the cerebral cortex of ferrets that died of VN1203 infection while no virus was recovered from HK483 infected ferrets (**Figure 4C**) examined at the peak of infection. VN1203 infected ferrets had approximately 10^5 FFU/mL in the brain stem and viable virus was below the limit of detection (1 FFU/mL) in this tissue from ferrets infected with HK483 (**Figure 4E**). Typically, VN1203 was found at high levels in all animals at the time of death or euthanasia. In addition to high titers of viable VN1203 isolated from the brain sections, high copy numbers of viral RNA were also measured in the olfactory bulb, cerebral cortex, and brain stem of infected ferrets 3 to 6 days post challenge. Viral RNA copies were below the limit of

detection in the brain of HK483 infected ferrets at 4 dpi and significantly lower than those measured from VN1203 infected ferrets at later time points (**Figure 4B,D,F**, ANOVA, $p < .01$). Collectively, these data indicate that VN1203 replicated to a higher titer in the brains of ferrets compared to HK483 at similar time points following infection and HK483 entry into the brain was delayed and less severe compared with VN1203.

Localization of HPAI infection in the brain

Routes of infection in the CNS have been suggested (10-12, 21, 27); however, the dissemination of virus in the brain remains unknown. To localize VN1203 and HK483 antigen in the brain of ferrets, multiple 5 μ m sections of the frontal cortex, cerebrum, and cerebellum were obtained from formalin-fixed, paraffin-embedded brain tissues and examined by immunohistochemistry for avian influenza NP. Normal morphology was observed in the frontal cortex of mock-infected ferrets (**Figure 5A**) and HK483 NP antigen could not be detected from any brain section of ferrets challenged with HK483 and examined 4 dpi (**Figure 5B and 5E**). A single focus of staining was observed in the olfactory nucleus of one ferret each at 6 and 8 dpi (data not shown). Strikingly, numerous distinct foci of VN1203 NP expression were detected 3 dpi in the olfactory bulb and frontal cortex (**Figure 5C**) and similar expression was also observed 4 to 6 dpi. Foci were widespread and contained numerous nuclear-stained cells (**Figure 5F**).

Similar to observations in the frontal cortex, multiple foci of VN1203 were identified 3 dpi in the occipital cortex of the temporal lobe, the ectorhinal cortex, striatum, somatosensory area of the parietal lobe, the internal capsule, and the adjacent thalamus (**Figure 6A**). In contrast, no viral antigen was detected in these regions of ferrets infected with HK483 and examined at 4, 6, or 8 dpi (**Figure 6B**). Foci of VN1203 were numerous,

widespread, and concentric in appearance. Furthermore, virus was also identified in the dorsal cerebral cortex where no histologic alterations or inflammatory cell infiltration was observed (**Figure 6C**). VN1203 was observed in the internal capsule (**Figure 6D**) and the adjacent thalamus (**Figure 6E**), representing new areas of infection that have not been described previously. Foci in these regions were similar to those in other brain regions.

Hindbrain tissue sections were obtained from infected ferrets and assessed for HK483 and VN1203 at multiple time points. Hindbrain regions included the cerebellum, pons, medulla, and the most rostral aspects of the spinal cord (**Figure 7A**). Hind brains from HK483-injected ferrets appeared normal with an absence of any immunohistochemical staining for influenza NP at any time during the infection period and concurrent with active infection in the respiratory tract (**Figure 7C,D,I,J**). In contrast, viral antigen was observed in multiple regions of the brain stem, cerebellar peduncles, and cerebrotubular tracts in white and gray matter areas. More specifically, multiple foci of infection were identified in the Purkinje cells of the cerebellar foci (**Figure 7K,L**) with occasional staining extending into the granular layer, which is penetrated by Purkinje cell axons. Interestingly, the adjacent molecular layer that consists of dendrites extending from the Purkinje cells exhibited a complete lack of VN1203 staining, suggesting directional migration of VN1203 at least in the cerebellar folia. The widespread dissemination of VN1203 suggests that the virus did not spread from a single dissemination site.

Brain lesions during HPAI infection

Tissue sections from the forebrain, midbrain and hindbrain were randomly selected, stained by hematoxylin and eosin and examined under light microscopy for evidence of histological changes related to viral neuroinvasion. In contrast to ferrets infected with

VN1203 in which brain lesions were present on 3 dpi, there were no histological alterations in the brains of ferrets infected with HK483 examined on 4 dpi. Two of six HK483 infected animals examined on 6 dpi had acute neutrophil inflammatory cell infiltration in the olfactory system located in the olfactory nuclei in the frontal cortex (**Figure 8B,E**), the olfactory cortex in the temporal lobe, limbic system, and the somatosensory area in the parietal lobe. One of the two ferrets with observed inflammatory cell infiltration had viral antigen present in the olfactory nuclei while it was not detected elsewhere in the brain (data not shown). Two of six HK483 infected animals examined 8 dpi had more advanced mild to moderate acute inflammation limited to the olfactory system. Likewise, immunostaining was observed in only the olfactory nucleus in one HK483 infected ferret 8 dpi. Meningoencephalitis was pronounced in the olfactory system in a HK483 infected ferret that had lost more than 25% of its initial body weight, and had no neurological signs when examined 11 dpi.

Histological examination of ferrets infected with VN1203 on days 3-6 post challenge showed widespread lesions in gray and white matter areas in the frontal cortex (**Figure 8C,F**), thalamus, parietal and temporal lobes, midbrain/medulla (**Figure 8I,L**), and hind brain cerebellum folia (**Figure 8O**) in eight of ten animals, in sharp contrast to the brains of ferrets infected with HK483 where lesions were not observed (**Figure 8B,E,H,K,N**). **Figure 8A, D, G, J, and M** demonstrate healthy mock infected brain sections of ferrets. Low numbers of neutrophil infiltration in the olfactory bulb, and areas of cell death and/or loss of cellularity were evident in all brain regions of VN1203 infected ferrets. Microglial nodules were observed in regions near influenza foci (**Figure 8C,F**). Furthermore, inflammation of the meninges was evident in the frontal cortex consisting of increased cellular infiltration and increased size of the arachnoid space (**Figure 8C**). Lesions observed in the cerebrum and

cerebellum of VN1203 infected ferrets corresponded to regions of viral antigen detection by immunohistochemistry while HK483 infected ferrets did not have lesions or viral antigen detected in the cerebrum or cerebellum.

Discussion

Although neuropathogenesis and neurological sequelae have been recognized for HPAI infection, little is known about the contribution of neuroinvasion to lethality against the well-studied role of respiratory disease during influenza infection. Here we show that low infectious titers of distinct H5N1 HPAI viruses produce divergent disease outcomes amid distinct neurovirulence. We also show that neurological signs are important indicators of replicating virus in the brain and likely foretell morbidity and lethality in the ferret model. Infection with the clade I prototypic strain VN1203 at low inoculating titers led to substantial lethality and neurological signs, whereas the clade 0 prototypic strain, HK483, resulted in less lethality and no neurological sequelae. While cells of the lower respiratory tract are often the primary targets of influenza A virus, nasal turbinate cells including neuroepithelial bundles of the olfactory tract are also permissive to infection. In primary differentiated ferret nasal turbinate cells in culture, VN1203 and HK483 replicated to similar titers consistent with data obtained from the nasal turbinates of VN1203 or HK483 infected ferrets. Likewise, while the damage caused by each virus was distinct, the viral replication was similar in the lungs of ferrets infected with either VN1203 or HK483 suggesting that productive infection in the respiratory tract was an insufficient predictor of lethality in this model.

Remarkably, VN1203 infection was multifocal and widespread throughout the brain while HK483 was much less neurotropic with lesions limited to the olfactory system. The absence of neurological clinical signs in ferrets infected with HK483 correlated with

histopathological immunostaining that demonstrated virus was limited to the olfactory system. The restriction of virus primarily to the olfactory nucleus and olfactory cortex also correlated with the low viral RNA copy number in the brain. Viral RNA was detected in the olfactory bulb of approximately 75% of animals 6 and 8 dpi. All HK483 infected animals were negative on 4 dpi showing a delayed time course of transmission of virus to the olfactory bulb and brain in ferrets infected with HK483 compared to VN1203. These findings suggest differences in pathogenesis and neurotropism that correlated with the extent of dissemination within the CNS and are possibly indicative of differences in viral replication in the CNS. The prominent histological damage in the central olfactory system in the brain at 6 and 8 dpi in ferrets infected with HK483 were associated with marked inflammatory cell infiltration and showed HK483 induced alterations associated with only low levels of viral RNA detected in the brain by qRT-PCR. Multiple brain regions (forebrain, midbrain, and hindbrain) and several tissues within each region were found to have active VN1203 replication.

HK483 and A/Hong Kong/486/1997 have been used in murine models of infection to identify routes of neuroinvasion, and from these studies, the trigeminal, vagus, and sympathetic nerves (11, 12, 27) were identified in addition to the olfactory nerves. In the present study, virus expression was detected in the trigeminal and facial nuclei in the brainstem of ferrets infected with VN1203. Fibers from these nuclei are distributed in the reticular activating system and enter the cerebellum through the cerebellar peduncles. They also project to the thalamus and connect to the motor cortex via the corticobulbar tract. Ferrets had clinical signs of ocular discharge indicative of conjunctivitis, a possible site of entry into the terminal tributaries of the trigeminal nerve. The hypoglossal nerve innervates

the tongue and pharynx and the nucleus in the brainstem receives efferents from the sensory trigeminal nuclei. The data presented here indicate that the olfactory nerves may be an important conduit of neuroinvasion; however, other routes are plausible based on our findings of VN1203 replication and pathogenesis in multiple brain regions.

Other viruses such as JC virus, poliovirus, Epstein-Barr virus, mouse adenovirus 1, human T-lymphotropic virus type 1, and West Nile virus are known to infect the CNS through the vascular endothelium (28). HPAI has not been shown to enter the CNS through this route and virus was not detected in the CNS endothelium of the ferrets infected with VN1203 or HK483 in this study. A more likely method of CNS entry is through the peripheral nerves. It has been shown that poliovirus, adenoviruses, and rabies bind to neurons at the neuromuscular junction where specific receptors are expressed (28). While influenza receptors on neurons are not known, Jang *et al* (29) used microfluidic chambers to show VN1203 could be transported from the processes of freshly dissociated dorsal root ganglia cells of mice to the cell body in a separate compartment. This finding demonstrated that VN1203 traveled via the axons suggesting a method for transport of H5N1 to the CNS. Here, the distribution of virus antigen throughout various regions of the brain indicates that VN1203 may have entered the brain via multiple cranial nerves though the mechanism remains to be elucidated.

The infection of the olfactory region may be particularly important in the widespread infection observed in multiple brain regions prior to death. Cell death and ulceration of sensory epithelial cells with clinical signs of nasal discharge and viral expression strongly suggest that the nasal infection was the route of entry into the olfactory bulb and for subsequent dissemination in the central olfactory nervous system of both stains of virus.

Influenza has been shown to infect olfactory nerves (18, 19, 27) and immunostaining demonstrated virus expression in areas in the cerebrum in which mitral cells project from the olfactory bulb to synapse in the anterior olfactory nucleus, the olfactory cortex in the temporal lobe, the amygdala, the piriform cortex, and the entorhinal cortex. Multiple projections from the olfactory bulb may explain some of the widespread viral antigen observed in the cerebral cortex. The olfactory system is the only cranial sensory system that has direct projections into the cerebral cortex without relay in a thalamic nucleus. Also, the close neuroanatomical connections of the olfactory system to the limbic system help explain VN1203 distribution in the hippocampus and the striatum.

The nature of the neurological signs following VN1203 infection may have important implications for clinical evaluation of active H5N1 infection. Animals that succumbed to VN1203 infection at 3 dpi exhibited convulsions leading up to death. Consistent with these findings, VN1203 was isolated from the cerebral cortex from all animals that exhibited these signs. Further evidence of the link between viral localization and specific neurological signs can be observed in the later phase of lethality to VN1203. Ferrets that succumbed to infection at 5 or 6 dpi exhibited a lack of voluntary movement control and coordination. Upon analysis of viral localization in the brain, virus was isolated from the deep cerebellar nuclei, an area known to be important in motor control and gait. One important finding from the current studies is the elucidation of Purkinje cells of the cerebellar foci as a strongly permissive cell for H5N1 infection. Likewise, the granular layer, a region that receives axons from the Purkinje cells, but not the molecular layer, which consists of dendrites from Purkinje cells, was found to have substantial viral antigen staining and may indicate directional migration of H5N1 in neuronal tissues. Although further study is warranted, the notion that specific

neurological signs may be used to ascertain the presence of virus in various brain regions may become useful should therapeutics targeting neurological infection become available.

The neurovirulence and mechanisms of brain pathogenesis of HPAI H5N1 are not known and require further study. Clearly, viral determinants exist in different H5N1 viruses that lead to neurotropism in ferrets. Further studies to ascertain the mechanism by which H5N1 enters into and is disseminated throughout the brain will be important for identifying H5N1 viruses through global surveillance that may have enhanced pathogenesis in humans. Additionally, the route of infection and dissemination within the brain should be more clearly defined to provide clinicians with more markers of brain involvement in H5N1 infection and to identify novel areas as targets for therapeutics to prevent virus dissemination to the CNS. It is also unclear whether entry routes along different cranial nerves require specific receptors for viral entry, or if it is opportunistic in nature. Furthermore, therapeutic approaches that target influenza in the brain will likely need investigation in light of the rapid onset of neurological signs in human cases. While not widely appreciated outside of the influenza research community, the importance of neurological disease in HPAI should be emphasized in future public health initiatives.

Acknowledgments

The authors sincerely thank Richard Jaramillo for the primary differentiated ferret turbinate cells and Jesse van Westrienen for the qRT-PCR primers. Furthermore, we thank Zemmie Pollock for her help and guidance in performing the ferret studies and Drs. Heather Stout-Delgado, Dana Mitzel, and Chris Royer for their critical reading of this manuscript. Finally, we thank the ABSL3 animal resource staff and necropsy team for their assistance in collecting clinical observations and samples, the pathologist for assistance in reading the

slides, and the histology laboratory at LRRI for the H&E and Luxol Fast Blue staining of the ferret tissue sections.

References

1. **Gu, J., Z. Xie, Z. Gao, J. Liu, C. Korteweg, J. Ye, L. T. Lau, J. Lu, Z. Gao, B. Zhang, M. A. McNutt, M. Lu, V. M. Anderson, E. Gong, A. C. H. Yu, and W. I. Lipkin.** 2007. H5N1 infection of the respiratory tract and beyond: a molecular pathology study. *The Lancet*. **370**:1137-1145.
2. **Ng, W. F., and K. F. To.** 2007. Pathology of human H5N1 infection: new findings. *The Lancet*. **370**:1106-1108.
3. **Writing Committee of the Second World Health Organization Consultation on Clinical Aspects of Human Infection with Avian Influenza A (H5N1) Virus, A. N. Abdel-Ghafar, T. Chotpitayasunondh, Z. Gao, F. G. Hayden, D. H. Nguyen, M. D. de Jong, A. Naghdaliyev, J. S. Peiris, N. Shindo, S. Soeroso, and T. M. Uyeki.** 2008. Update on avian influenza A (H5N1) virus infection in humans. *N. Engl. J. Med.* **358**:261-273. doi: 10.1056/NEJMra0707279; 10.1056/NEJMra0707279.
4. **Belser, J. A., K. J. Szretter, J. M. Katz, and T. M. Tumpey.** 2009. Use of Animal Models to Understand the Pandemic Potential of Highly Pathogenic Avian Influenza Viruses. *Advances in Virus Research*. **73**:55-97; 55.
5. **Chan, M., C. Cheung, W. Chui, S. Tsao, J. Nicholls, Y. Chan, R. Chan, H. Long, L. Poon, Y. Guan, and J. Peiris.** 2005. Proinflammatory cytokine responses induced by influenza A (H5N1) viruses in primary human alveolar and bronchial epithelial cells. *Respiratory Research*. **6**:135-135-148.
6. **Graef, K. M., F. T. Vreede, Y. Lau, A. W. McCall, S. M. Carr, K. Subbarao, and E. Fodor.** 2010. The PB2 Subunit of the Influenza Virus RNA Polymerase Affects Virulence by Interacting with the Mitochondrial Antiviral Signaling Protein and Inhibiting Expression of Beta Interferon. **84**:8433-8445. doi: 10.1128/jvi.00879-10.
7. **Maines, T. R., X. H. Lu, S. M. Erb, L. Edwards, J. Guarner, P. W. Greer, D. C. Nguyen, K. J. Szretter, L. Chen, P. Thawatsupha, M. Chittaganpitch, S. Waicharoen, D. T. Nguyen, T. Nguyen, H. H. T. Nguyen, J. Kim, L. T. Hoang, C. Kang, L. S. Phuong, W. Lim, S. Zaki, R. O. Donis, N. J. Cox, J. M. Katz, and T. M. Tumpey.** 2005. Avian Influenza (H5N1) Viruses Isolated from Humans in Asia in 2004 Exhibit Increased Virulence in Mammals. *Journal of Virology*. **79**:11788-11800; 11788.
8. **Zitzow, L. A., T. Rowe, T. Morken, W. Shieh, S. Zaki, and J. M. Katz.** 2002. Pathogenesis of Avian Influenza A (H5N1) Viruses in Ferrets. *Journal of Virology*. **76**:4420-4429; 4420.
9. **de Jong, M. D., V. C. Bach, T. Q. Phan, M. H. Vo, T. T. Tran, B. H. Nguyen, M. Beld, T. P. Le, H. K. Truong, V. V. Nguyen, T. H. Tran, Q. H. Do, and J. Farrar.** 2005. Fatal avian influenza A (H5N1) in a child presenting with diarrhea followed by coma. *N Engl J Med*. **352**:686-91.

10. **Nishimura, H., S. Itamura, T. Iwasaki, T. Kurata, and M. Tashiro.** 2000. Characterization of human influenza A (H5N1) virus infection in mice: neuro-, pneumo- and adipotropic infection. **81**:2503-2510.
11. **Shinya, K., A. Makino, M. Hatta, S. Watanabe, J. H. Kim, Y. Hatta, P. Gao, M. Ozawa, Q. M. Le, and Y. Kawaoka.** Subclinical brain injury caused by H5N1 influenza virus infection. JVI.00239-11. doi: 10.1128/jvi.00239-11.
12. **Park, C. H., M. Ishinaka, A. Takada, H. Kida, T. Kimura, K. Ochiai, and T. Umemura.** 2002. The invasion routes of neurovirulent A/Hong Kong/483/97 (H5N1) influenza virus into the central nervous system after respiratory infection in mice. *Arch. Virol.* **147**:1425-1425-1436.
13. **You, Y., E. J. Richer, T. Huang, and S. L. Brody.** 2002. Growth and differentiation of mouse tracheal epithelial cells: selection of a proliferative population. *Am. J. Physiol. Lung Cell. Mol. Physiol.* **283**:L1315-21. doi: 10.1152/ajplung.00169.2002.
14. **Layton, R. C., A. Gigliotti, P. Armijo, L. Myers, J. Knight, N. Donart, J. Pyles, S. Vaughan, J. Plourde, N. Fomukong, K. S. Harrod, P. Gao, and F. Koster.** 2011. Enhanced immunogenicity, mortality protection, and reduced viral brain invasion by alum adjuvant with an H5N1 split-virion vaccine in the ferret. *PLoS One.* **6**:e20641. doi: 10.1371/journal.pone.0020641; 10.1371/journal.pone.0020641.
15. **Matrosovich, M., T. Matrosovich, W. Garten, and H. D. Klenk.** 2006. New low-viscosity overlay medium for viral plaque assays. *Virol. J.* **3**:63. doi: 10.1186/1743-422X-3-63.
16. **Thompson, C. I., W. S. Barclay, M. C. Zambon, and R. J. Pickles.** 2006. Infection of human airway epithelium by human and avian strains of influenza a virus. *J. Virol.* **80**:8060-8068. doi: 10.1128/JVI.00384-06.
17. **Govorkova, E. A., J. E. Rehg, S. Krauss, H. Yen, Y. Guan, M. Peiris, T. D. Nguyen, T. H. Hanh, P. Puthavathana, H. T. Long, C. Buranathai, W. Lim, R. G. Webster, and E. Hoffmann.** 2005. Lethality to Ferrets of H5N1 Influenza Viruses Isolated from Humans and Poultry in 2004. *Journal of Virology.* **79**:2191-2198; 2191.
18. **Mori, I., F. Goshima, Y. Imai, S. Kohsaka, T. Sugiyama, T. Yoshida, T. Yokochi, Y. Nishiyama, and Y. Kimura.** 2002. Olfactory receptor neurons prevent dissemination of neurovirulent influenza A virus into the brain by undergoing virus-induced apoptosis. **83**:2109-2116.
19. **Mori, I., Y. Nishiyama, T. Yokochi, and Y. Kimura.** 2005. Olfactory transmission of neurotropic viruses. *J. Neurovirol.* **11**:129-137. doi: 10.1080/13550280590922793.
20. **Shinya, K., M. Ebina, S. Yamada, M. Ono, N. Kasai, and Y. Kawaoka.** 2006. Avian flu: influenza virus receptors in the human airway. *Nature.* **440**:435-6.

21. **Tanaka, H., C. Park, A. Ninomiya, H. Ozaki, A. Takada, T. Umemura, and H. Kida.** 2003. Neurotropism of the 1997 Hong Kong H5N1 influenza virus in mice. *Vet Microbiol.* **95**:1-13.
22. **Chan, R. W. Y., K. M. Yuen, W. C. L. Yu, C. C. C. Ho, J. M. Nicholls, J. S. M. Peiris, and M. C. W. Chan.** 2010. Influenza H5N1 and H1N1 Virus Replication and Innate Immune Responses in Bronchial Epithelial Cells Are Influenced by the State of Differentiation. *PLoS One.* **5**:e8713.
23. **Chutinimitkul, S., D. van Riel, V. J. Munster, J. M. van den Brand, G. F. Rimmelzwaan, T. Kuiken, A. D. Osterhaus, R. A. Fouchier, and E. de Wit.** In vitro assessment of attachment pattern and replication efficiency of H5N1 influenza A viruses with altered receptor specificity. *J Virol.* **84**:6825-33.
24. **Ibricevic, A., A. Pekosz, M. J. Walter, C. Newby, J. T. Battaile, E. G. Brown, M. J. Holtzman, and S. L. Brody.** 2006. Influenza virus receptor specificity and cell tropism in mouse and human airway epithelial cells. *J Virol.* **80**:7469-80.
25. **van Riel, D., V. J. Munster, E. de Wit, G. F. Rimmelzwaan, R. A. Fouchier, A. D. Osterhaus, and T. Kuiken.** 2006. H5N1 Virus Attachment to Lower Respiratory Tract. *Science.* **312**:399.
26. **Mitchell, H., D. Levin, S. Forrest, C. A. Beauchemin, J. Tipper, J. Knight, N. Donart, R. C. Layton, J. Pyles, P. Gao, K. S. Harrod, A. S. Perelson, and F. Koster.** 2011. Higher level of replication efficiency of 2009 (H1N1) pandemic influenza virus than those of seasonal and avian strains: kinetics from epithelial cell culture and computational modeling. *J. Virol.* **85**:1125-1135. doi: 10.1128/JVI.01722-10; 10.1128/JVI.01722-10.
27. **Reinacher, M., J. Bonin, O. Narayan, and C. Scholtissek.** 1983. Pathogenesis of neurovirulent influenza A virus infection in mice. Route of entry of virus into brain determines infection of different populations of cells. *Lab. Invest.* **49**:686-692.
28. **McGavern, D. B., and S. S. Kang.** 2011. Illuminating viral infections in the nervous system. *Nat. Rev. Immunol.* **11**:318-329. doi: 10.1038/nri2971; 10.1038/nri2971.
29. **Jang, H., D. Boltz, K. Sturm-Ramirez, K. R. Shepherd, Y. Jiao, R. Webster, and R. J. Smeyne.** 2009. Highly pathogenic H5N1 influenza virus can enter the central nervous system and induce neuroinflammation and neurodegeneration. *Proceedings of the National Academy of Sciences of the United States of America.* **106**:14063-14068; 14063.

Figure Legends

Figure 1. VN1203 was more lethal than HK483 in ferrets despite similar weight loss in non-survivors. **A.** Survival of ferrets intranasally challenged with allantoic fluid (N = 2), A/Vietnam/1203/2004 (VN1203) (N = 10) or A/Hong Kong/483/1997 (HK483) N = 10, ***, $p < .0001$. **B.** Mean + SEM of bodyweight of ferrets instilled with VN1203 or HK483. N = 8 HK483 survivors, N = 2 HK483 non-survivors, N = 10 VN1203 non-survivors, N = 2 control.

Figure 2. VN1203 induced significant pathology despite similar nasal turbinate titers in ferrets infected with either virus. **A.** H&E stained section a primary differentiated ferret nasal turbinate cell monolayer. **B.** Primary differentiated ferret nasal turbinate cells were infected with VN1203 or HK483 at an MOI of 0.001. Mean + SEM of N = 4 samples per virus at each time point. **C.** Viral titers of homogenized nasal turbinates were graphed as mean + SEM for VN1203 or HK483 infected ferrets. **D-I.** Representative samples of nasal turbinate tissue of ferrets instilled with allantoic fluid (**D,G**), HK483 (**E,H**), or VN1203 (**F,I**). **D-F** were stained with H&E, **G-I** were stained with anti-avian influenza NP and counterstained with Luxol fast blue. **F.** # indicates inflammatory cells infiltrating the underlying stroma. **H,I.** Arrows point to H5N1 infected cells. Scale bars: **A**, 50 μ m; **D-F**, 300 μ m; **G-I**, 100 μ m.

Figure 3. Viral titers and histopathology were similar in the lung of H5N1 infected ferrets. **A.** Viral titers and **B.** viral RNA was measured from four sections of the lung per ferret. **A,B)** Data represents the mean + SEM from four lung regions of N = 1, VN1203 4 dpi, N = 3, VN1203 6 dpi, N = 6, HK483 4, 6, and 8 dpi. Dorsal view of ferret lung following intranasal instillation with allantoic fluid (**C**), HK483 (**D**), VN1203 (**E**). Lung

sections stained with H&E of ferrets instilled with allantoic fluid (**F**), HK483 (**G**), VN1203 (**H**). **F-H** scale bars = 600 μ m.

Figure 4. High viral titers were measured in the brain of VN1203 infected ferrets.

A,C,E) Viral titers were measured in three sections of the ferret brain. Titters were graphed as mean \pm SEM for VN1203 or HK483 infected ferret olfactory bulb (**A**), cerebral cortex (**C**), brain stem (**E**). Viral RNA was extracted from homogenized tissue and graphed as the mean \pm SEM of viral RNA copies per gram of tissue from VN1203 or HK483 infected ferrets' olfactory bulb (**B**), cerebral cortex (**D**), brain stem (**F**). White bars: HK483 infected ferrets, black bars: VN1203 infected ferrets. All mock infected ferrets were negative for virus. n.d. indicates virus or viral RNA was not detected. VN1203: N = 4, 3 dpi; N = 1, 4 dpi; N = 2, 5 dpi; N = 3, 6 dpi. HK483: N = 6; 4, 6 and 8 dpi.

Figure 5. VN1203 infection in the ferret brain was multifocal and evident in the olfactory tract.

Representative sections from the frontal lobe of ferrets intranasally instilled with allantoic fluid (**A,D**), on: olfactory nucleus, rf: rhinal fissure, HK483 (**B,E**) or VN1203 (**C,F**) were stained for viral antigen with IMGENEX 5187-A for avian influenza A NP and visualized with DAB. Brown stain indicates the presence of virus. Counterstained with Luxol fast blue. Scale bars: **A-C**) 5mm, **D-F**) 300 μ m.

Figure 6. VN1203 infection resulted in multifocal infection in the cerebral cortex of ferrets.

Representative sections of the cerebrum of ferrets intranasally instilled with VN1203 (**A, C-E**) and HK483 (**B**). Viral antigen was detected with IMGEX-5187A for avian influenza A NP and visualized with DAB. Brown stain indicates the presence of virus. Counterstained with Luxol fast blue. Scale bars represent 10 mm. cc: corpus collosum, ic: internal capsule, ot: optical tract, h: hippocampus, lv: lateral ventricle, oc: olfactory cortex, cp: cerebral peduncle.

Figure 7. VN1203 infected and replicated in Purkinje cells and deep cerebellar nuclei of the cerebellum.

Representative sections of the cerebellum of ferrets instilled with allantoic fluid (**A,B,G,H**), HK483 (**C,D,I,J**), VN1203 (**E,F,K,L**). Viral antigen was detected with IMGEX 5187-A for avian influenza A NP and visualized with DAB. Brown stain indicates the presence of virus. Counterstained with Luxol fast blue. (**B-F**) higher magnification of boxes in A-E respectively. H) White arrow indicates molecular layer, black arrow indicates granule layer, black arrowhead indicates a Purkinje cell, white arrowhead indicates Purkinje cell axons. L) Arrow indicates infected granule cell and arrowhead indicates infected Purkinje cell. Scale bars represent: **A,C,E,G,I,K**) 2mm; **B,D,F,H,J,L**) 300 μ m.

Figure 8. VN1203 resulted in severe and widespread brain lesions compared with HK483.

Representative sections from the olfactory nucleus (**A-F**), cerebrum (**G-L**), and cerebellum (**M-O**) were taken from ferrets instilled with allantoic fluid (**A,D,G,J,M**), HK483 (**B,E,H,K,N**), VN1203 (**C,F,I,L,O**) and stained with H&E for evaluation of histological alterations. **B**) Arrow points to meningeal inflammatory cell infiltration,

asterisk denotes infiltration of neutrophils. **D-F)** High magnification of boxes in A-C respectively. **O)** Asterisk denotes lesion. Scale bars: **A-C, J-L, M-O)** 1mm, **D-F)** 300 μ m, **G-I)** 5 mm.

Figures

Figure 1

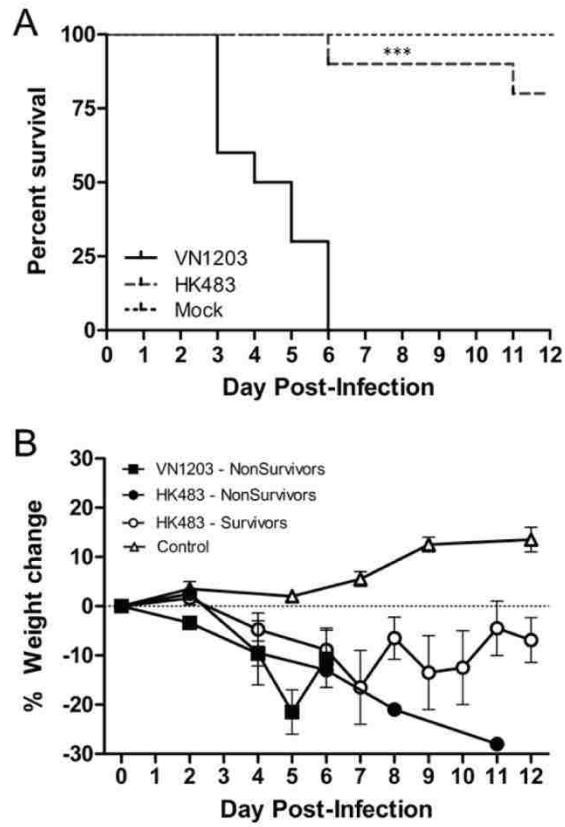


Figure 2

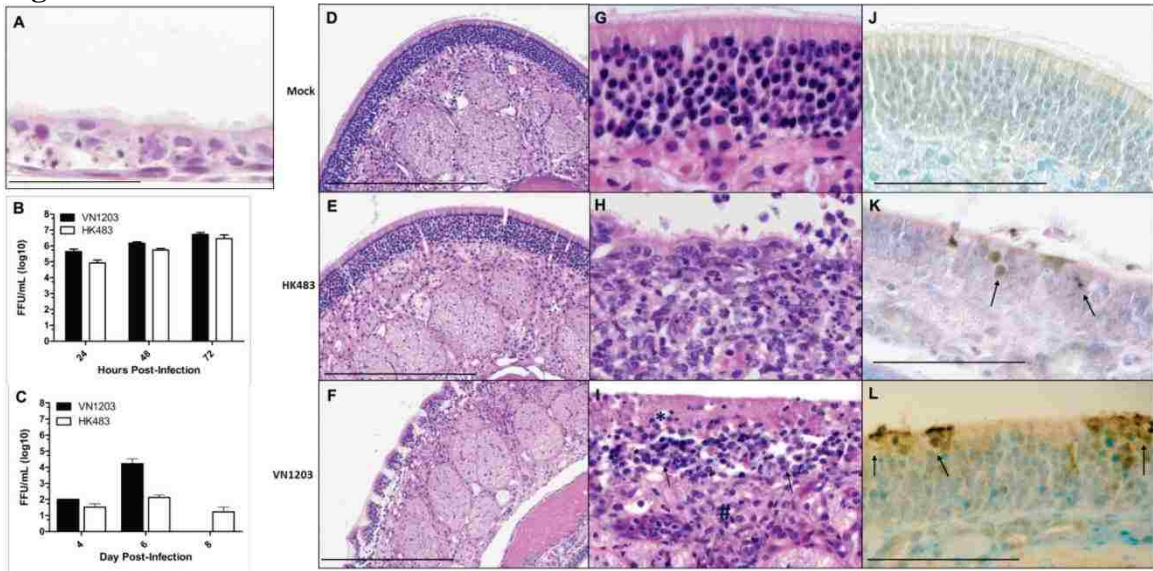


Figure 3

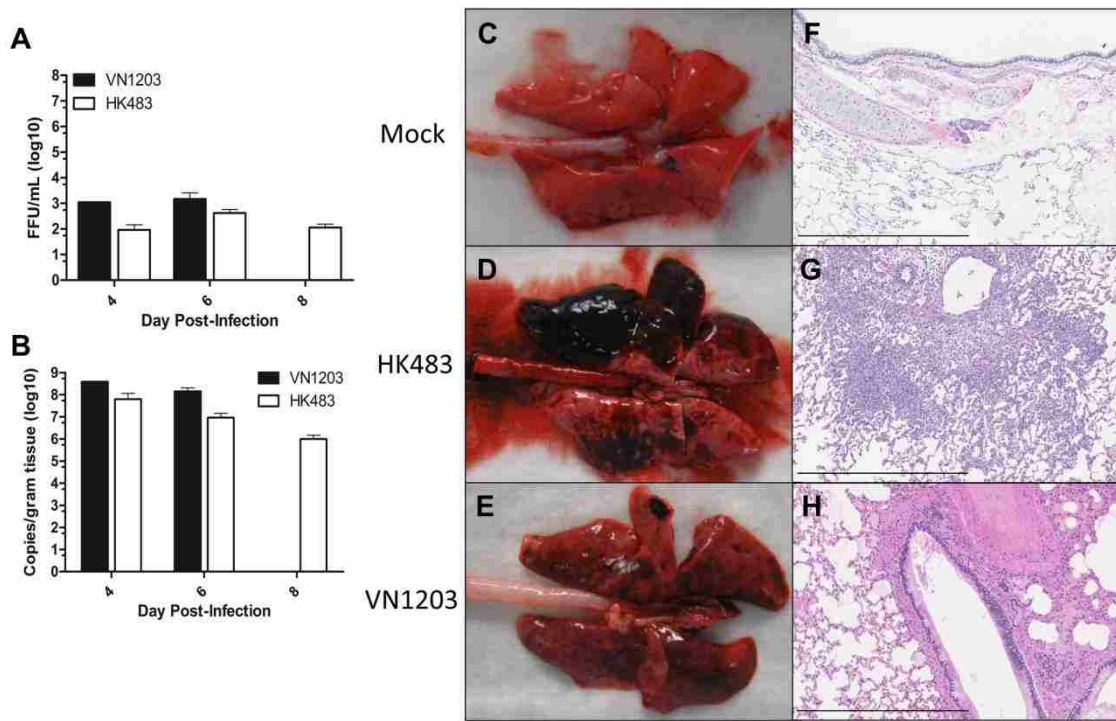


Figure 4

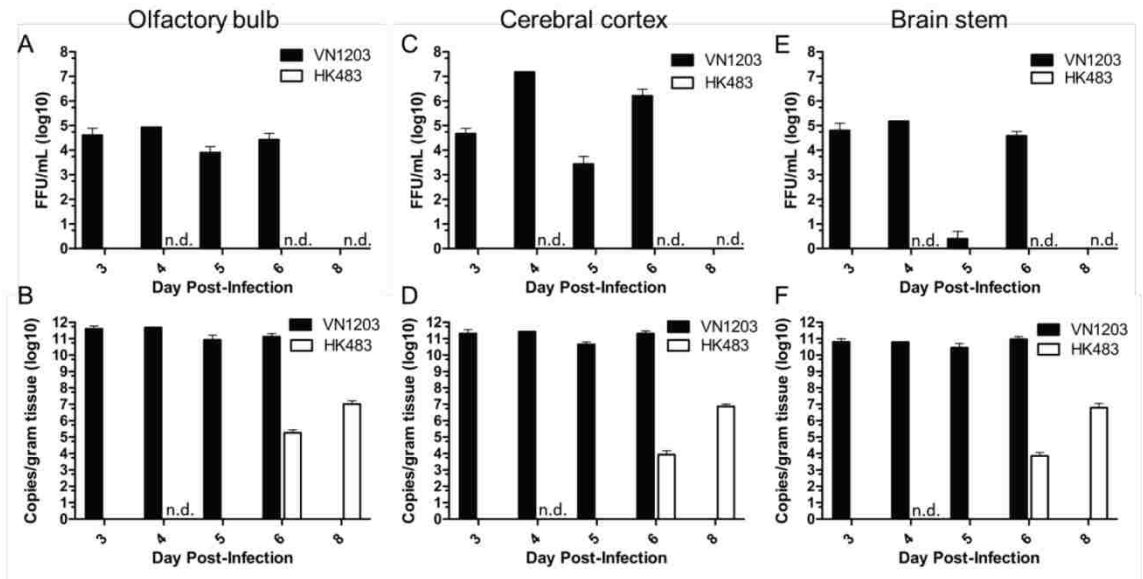


Figure 5

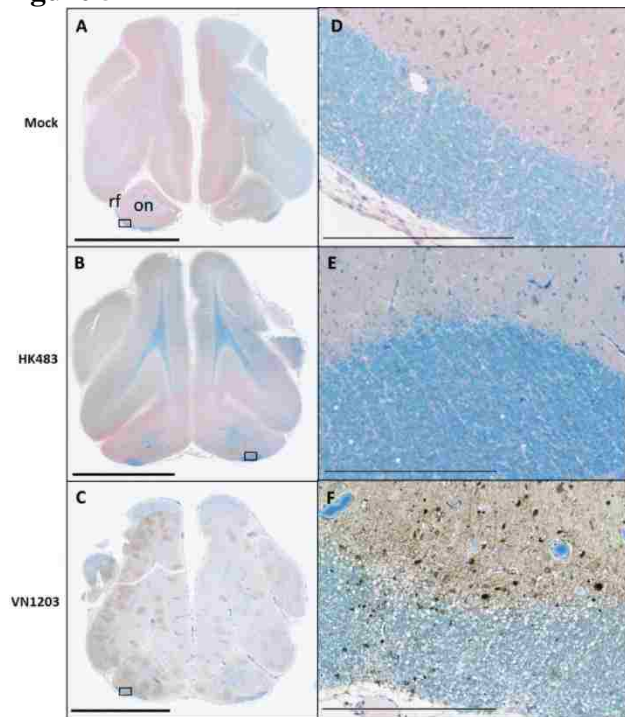


Figure 6

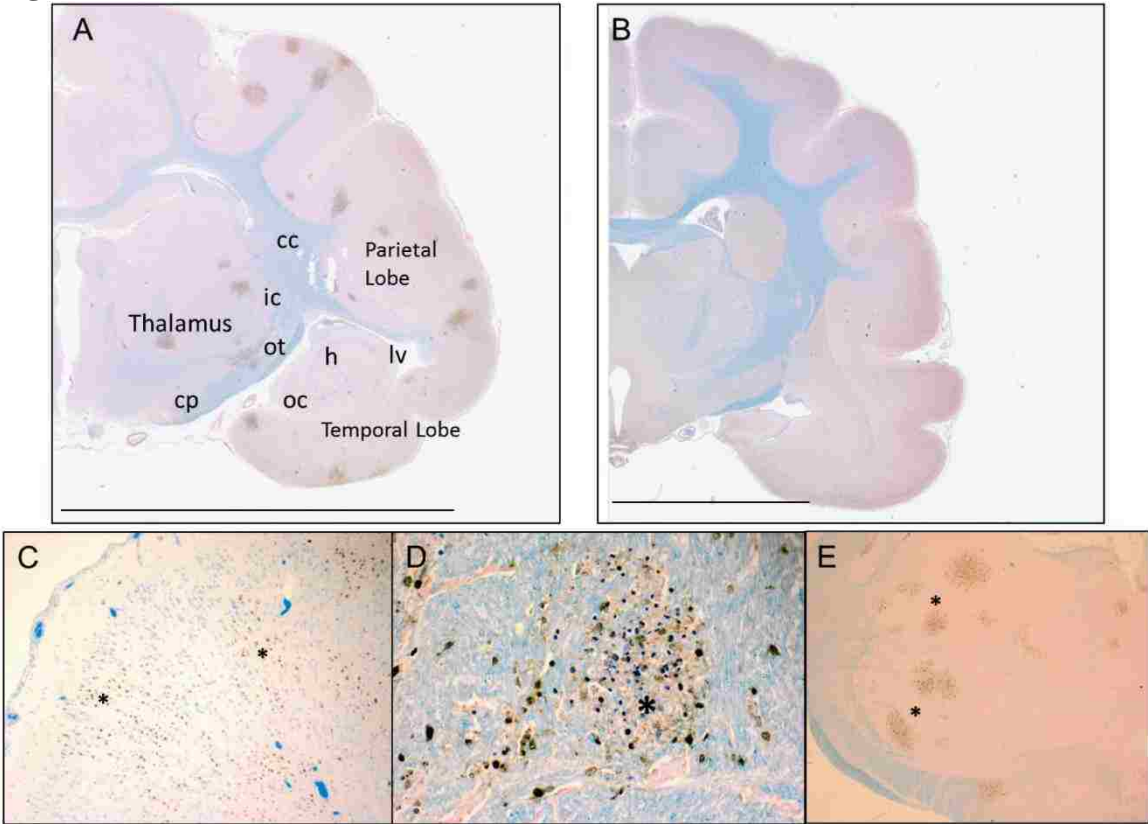


Figure 7

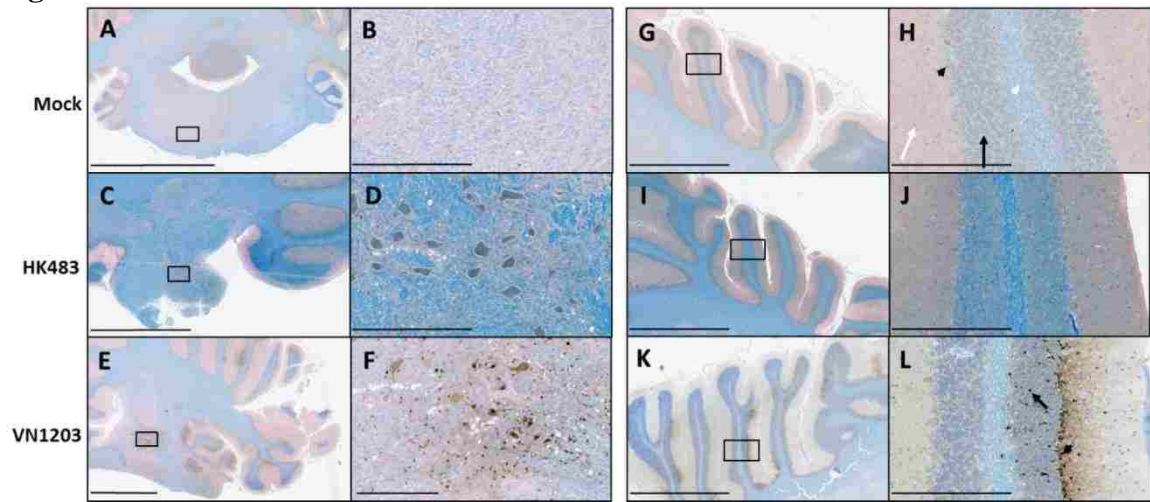
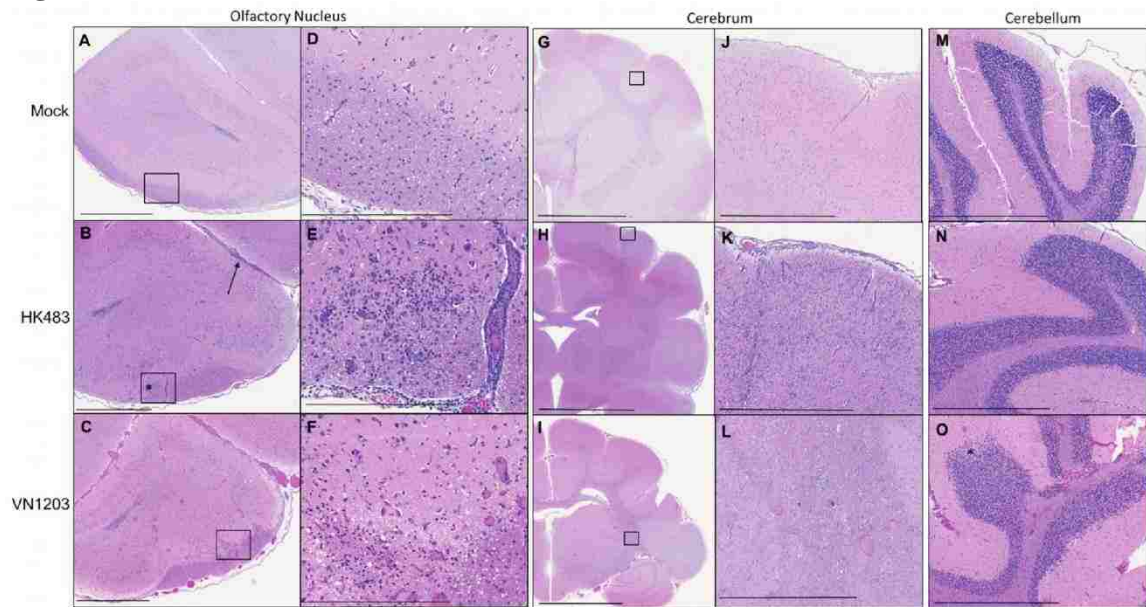


Figure 8



Table

Table 1. Clinical observations in ferrets post-challenge with VN1203 or HK483.

Number of ferrets with clinical symptoms (# with symptoms/total # in group)			
H5N1 strain	Nasal Discharge	Ocular Discharge	Neurological Symptoms
VN1203	10/10	2/10	8/10
HK483	10/10	4/10	0/10

Chapter Three: Aerosol Exposure to Low Doses of H5N1 Results in Widespread Infection and Neuroinflammation in the Ferret

Jennifer R. Plourde^{1,2}, Andrew Gigliotti³, Trevor Brasel⁴, Philip J. Kuehl⁵, Steve M. Storch⁵, Jennifer L. Tipper¹, and Kevin S. Harrod^{1,2,§}

¹Infectious Diseases Department, Lovelace Respiratory Research Institute, Albuquerque, NM

²Department of Pathology, Health Sciences Center, University of New Mexico, Albuquerque, NM

³Department of Pathology, Lovelace Respiratory Research Institute, Albuquerque, NM

⁴Institutional Office of Regulated Nonclinical Studies, University of Texas Medical Branch at Galveston, Galveston, TX

⁵Chemistry and Inhalation Exposure Program, Lovelace Respiratory Research Institute, Albuquerque, NM

[§]Corresponding author

Kevin S. Harrod , PhD

2425 Ridgecrest Dr SE, Albuquerque, NM 87108

Phone: 505-348-9488

Fax: 505-348-8567

Email: kharrod@lrri.org

Abstract

The aerobiology of influenza infection, including the highly pathogenic avian influenza (HPAI) H5N1 virus remains elusive. An increased understanding of the pathogenesis of infection by airborne influenza is critical to the understanding of human influenza disease. Herein, we elucidate unique sequelae of aerosolized influenza in an experimental model of infection. Following aerosol infection, viral antigen was widely disseminated throughout the central nervous system concomitant with lesions in the olfactory bulb, frontal lobe, cerebral cortex, thalamus, and brain stem. Lesions were commonly found in areas that could explain the neurological signs observed especially in the brain stem. This model more closely resembles natural human infection by exposing subjects to small particles of aerosolized influenza, which is how humans are generally exposed to the virus. Furthermore, the results of this study highlight that aerosolized HPAI can result in neuroinflammation and cause lesions in the brain and that neuropathogenesis is not a consequence of intranasal instillation. Such lesions could induce neurological signs that may be used by clinicians in the diagnosis of patients that present with atypical symptoms following HPAI exposure.

Introduction

Highly pathogenic avian influenza (HPAI) continues to infect humans with a high mortality rate. Since 2003, the World Health Organization has reported 608 confirmed human cases of HPAI subtype H5N1 and 359 deaths (http://www.who.int/influenza/human_animal_interface/EN_GIP_20121217CumulativeNumberH5N1cases.pdf, accessed 15 January 2013). The high mortality rate of this emerging virus emphasizes the need to study the pathogenesis of H5N1 infection to identify new targets for vaccines and therapeutics, increase the awareness of neurological signs and possible sequelae caused by HPAI infection, and aid clinicians in quickly diagnosing infection when patients present with non-respiratory symptoms.

Different routes of influenza exposure have recently been studied to identify differences in morbidity and lethality although more work needs to be done to characterize differences in pathogenesis of H5N1 infection following different routes of exposure to the virus (1). Ferrets are commonly used as a model for H5N1 infection and while intranasal instillation is often used as the means for infecting ferrets, studies have shown that aerosol exposure more closely represents the method by which humans typically become infected with airborne influenza virus (2-4). However, little is known regarding the neuropathogenesis of aerosolized H5N1 in mammals.

Neurotropism is a key feature of avian influenza in naturally susceptible populations of avian species (5, 6). Understanding the mechanism of how virus enters into the brain and disseminates so quickly is important for identifying outbreaks before entire flocks are destroyed and before humans become infected with newly emerging strains. Importantly, neurotropism has been recognized in several mammalian species

such as domestic cats, tigers and leopards, mice, and others (5-7). While limited autopsy information is available on fatal HPAI infection in humans, H5N1 has been detected in the brain and cerebrospinal fluid of some patients following clinical presentation of diarrhea, generalized convulsions, seizures, and ultimately coma (8-14). Neurological signs are not specific to H5N1 as a study of twelve major influenza pandemics in humans throughout the 20th and 21st centuries noted delirium, encephalitis, ocular abnormalities, amyotrophy, myelopathy, radiculopathy, ataxia, and seizures were reported as neurological manifestations of influenza infection (15).

In this study, we have developed a nose-only aerosol model that exposes naïve ferrets to H5N1 to represent the method by which mammals are naturally infected with influenza virus and to examine the neuropathogenesis of the virus at the time of death. It has been suggested that the neurotropism of H5N1 observed in experimentally infected animals is a result of intranasal instillation. In this paper, we show that exposure via aerosolized H5N1 leads to widespread multifocal infection throughout the brain with significant pathology concomitant with detectable infection and consistent with recorded neurological signs of infection.

Materials and Methods

Ethics statement

All animal procedures were conducted with the approval of the Institutional Animal Care and Use Committee (IACUC) and institutional biosafety committee of the Lovelace Respiratory Research Institute (LRRI), Albuquerque, NM. LRRI's animal facilities are accredited by the Association for Assessment and Accreditation of

Laboratory Animal Care International. Ferret experiments were conducted in the Animal Biosafety Level 3 (ABSL-3) enhanced facility.

Virus preparation

The highly pathogenic avian influenza A (HPAI) H5N1 virus, A/Vietnam/1203/2004 (VN1203) was isolated from a patient with a fatal case of influenza in 2004 and was obtained from the Centers for Disease Control and Prevention (Atlanta, GA). The virus was passaged once from the CDC stock in eggs, aliquoted, titrated by plaque assay on Madin-Darby Canine Kidney (MDCK) cells, and stored at -80°C. All manipulations with this virus strain were conducted under Biosafety Level 3 (BSL-3) conditions in the BSL-3 enhanced or animal BSL-3 enhanced (ABSL-3) facility at the Lovelace Respiratory Research Institute in Albuquerque, New Mexico.

Ferret handling/care and infection

Castrated male ferrets (*Mustela putorius furo*), approximately nine months of age, weighing ~1 kg, (supplied by Triple F Farms, Sayre, PA) were pre-screened by the supplier for H1 and H3 influenza A and influenza B seroconversion prior to shipment. Ferrets were triple-housed throughout quarantine (14 days) but single housed in stainless steel cages after virus challenge. Ferrets had access to food and water *ad libitum*. Temperature and humidity ranged 16 to 22°C and 30 to 65%, respectively and the light cycle was 12 hr on and 12 hr off. Ventilation in the study room was >15 air exchanges per hr. All ferret handlers had been vaccinated for circulating seasonal influenza strains and were not permitted to enter ferret quarters if they exhibited any symptoms of upper or lower respiratory infection.

Ferrets were anesthetized with an intramuscular injection of a ketamine/xylazine mixture (20mg/kg of ketamine and 4 mg/kg of xylazine) prior to implantation of two IPTT-300 Implantable Programmable Temperature and Identification Transponders (Bio Medic Data Systems, Inc, (BMDS) Seaford, Delaware). One microchip was implanted between the shoulders and one was implanted in a rear leg and both provided subcutaneous body temperature data throughout the study using a BMDS electronic proximity reader wand (WRS-6007; BMDS).

Viral infection procedures

Ferrets (n = 6) per group were challenged with the A/Vietnam/1203/2004 strain of H5N1 by nose only inhalation. Aerosols were generated with a Collison compressed air jet nebulizer (BIG Incorporated, Waltham, MA) from a suspension of virus in serum free media. Aerosols were characterized for viral concentration by collection into an all glass impinger (AGI). The AGI was filled (20 mL) with serum-free minimal essential medium (MEM) (Gibco # 42360-032) supplemented with 1X anti-mycotic, anti-biotic (Gibco # 15240) plus 8 drops of antifoam agent B. Particle size of the aerosol was measured with the GRIMM aerosol spectrometer (GRIMM Aerosol Technik GmbH & Co.). Particle size data were reduced to calculate the mass median aerodynamic diameter (MMAD, in μm) and geometric standard deviation (GSD).

Presented dose of the virus was determined by estimation of respiratory minute volume (16), measured aerosol concentration, and actual exposure time (17). All doses are reported as presented dose and therefore utilize a deposition fraction of 1.

Clinical observations

Clinical observations were conducted twice daily and included recording clinical signs of disease, body weights, and the monitoring of body temperature changes twice a day in response to infection via implanted BMDS microchips as described above. Study personnel were trained specifically in ferret handling procedures and the observation and recording of adverse signs and clinical symptoms in ferrets. Observations were recorded using the electronic Provantis system. The onset, nature, severity, and duration of all visible changes such as abnormal respiration, dehydration, emaciation, excretory, behavioral, and neurological signs (*i.e.*, paresis, torticollis, loss of righting or startle, head tilt, and paralysis) were recorded as well as any observed coughing, sneezing, and nasal or ocular discharge. Additionally, an activity score was assigned at each observation as follows: (0 = alert and playful, 1 = alert but playful only when stimulated, 2 = alert but not playful when stimulated, and 3 = neither alert nor playful when stimulated).

Moribund criteria were established in the approved IACUC protocol as body weight loss of more than 25% of their day 0 body weight, a decrease in body temperature to less than 92°F, indicative of shock, unresponsiveness to touch, self-mutilation, convulsions, paralysis or any movement disorder, or respiratory distress.

Histology and immunohistochemistry

Lungs (pressure fixed with 25 cm of hydrostatic pressure) and whole brain were fixed in 10% neutral buffered formalin for at least seven days and then changed to 70% ethanol. Representative samples of fixed tissues were trimmed, processed routinely, and embedded in paraffin. Tissue sections (4-6 µm) were cut and stained by H&E for histopathology examination. Immunohistochemical staining was conducted using

described protocols (18). Briefly, paraffin-embedded tissue sections were deparaffinized in xylene and decreasing concentrations of ethanol. Antigen retrieval was completed with a citrate buffer and endogenous peroxides were blocked with hydrogen peroxide in methanol. Slides were then incubated with 10% blocking buffer with goat serum, and the primary antibody (IMG-5187A, IMGENEX, San Diego, CA) was applied at a dilution of 1:800 overnight, 4°C. An anti-rabbit biotinylated secondary antibody (Vector Laboratories Inc., Burlingame, CA) was then applied at a dilution of 1:250 for one hour at room temperature. The ABC standard kit by Vectastain (Vector Laboratories Inc., Burlingame, CA) was used in conjunction with a DAB kit (Vector Laboratories Inc., Burlingame, CA) to detect antibody. Stained sections were then counterstained with hematoxylin, acid alcohol, and ammonium hydroxide, and rehydrated in increasing gradients of ethanol and xylene, and coverslipped. Images were acquired using the Hamamatsu 2.0 NanoZoomer software (Hamamatsu Corp., Bridgewater, NJ). Characterizations of histopathologic lesions were made with the assistance of a board-certified veterinary pathologist unfamiliar with the study design. Anatomic lesion distribution determinations were made by JRP with pathology consultation.

Statistical Analysis

GraphPad Prism 5, software version 5.04 (La Jolla, CA) was used to graph data and perform statistical analysis. The Kaplan Meier procedure was used for the survival analysis and an analysis of variance (ANOVA) was used for comparing multiple means. Mean \pm SEM is graphed and $p \leq .05$ was considered statistically significant.

Results

Survival and clinical signs of H5N1 infection in ferrets using aerosol delivery

Experimental studies of H5N1 infection in ferrets almost exclusively use intranasal instillation as the method for infection. However, natural exposure to influenza occurs via the presence of virus in aerosols that are inhaled and deposited in the upper respiratory tract. In this study, three groups (six ferrets per group) were exposed to varying quantities of aerosolized A/Vietnam/1203/2004 (VN1203), a highly pathogenic avian influenza (HPAI) strain shown to have high lethality in ferrets following intranasal instillation (19-21). Aerosolized VN1203 was presented to ferrets in nose-only exposure chambers to ensure the efficient delivery of the targeted amount of virus to the upper respiratory tract. The particle size of the viral aerosols were all $\sim 2.1 \mu\text{m}$ MMAD with GSD's of ~ 1.3 , which are highly respirable for ferrets. Concentrations of 0 to 2,561 plaque-forming units (PFU) per mL were utilized in the nebulizer, which resulted in presented doses of between 0 and 32 PFU.

Ferrets were humanely euthanized after meeting moribund criteria of the study as described in the methods between 4 and 8 days post-exposure (dpe). There was 100% lethality in the group of ferrets receiving the high dose of VN1203 (32 PFU) and the group exposed to the low dose of 0.2 PFU had 67% lethality (**Figure 1A**).

The median survival for both groups was 6.5 days. All six of the ferrets presented with the highest dose of 32 PFU developed neurological signs such as paralysis, loss of startle, twitching, head tilt, loss of righting, and torticollis between 5 and 8 dpe. One ferret in the group receiving 0.2 PFU was observed to be afflicted with paresis and torticollis at 8 dpe (**Table 1**).

Body temperature was obtained throughout the study from microchips implanted in the shoulder and leg of ferrets. Non-surviving ferrets developed a fever of two degrees elevated from their initial body temperature pre-exposure (**Figure 1B**). Similar to results in our laboratory following intranasal instillation at various doses, weight loss was not significantly different between groups suggesting weight loss was not dose dependent following aerosol infection of VN1203 (**Figure 1C**).

Aerosol exposure to VN1203 results in severe histopathology in the lung

Ferrets exposed to VN1203 via nose-only aerosol developed severe respiratory disease in the lung. Histological examination of lung sections showed widespread inflammation throughout the lung regardless of the amount of virus to which ferrets were exposed. In the most severely affected lungs, marked, widespread inflammatory infiltrates with edema and fibrin resulting in a loss of normal alveolar structure over large areas was observed. Intrapulmonary bronchioles were often obstructed by cellular debris and proteinaceous material (**Figure 2A and B**). In the mild to moderately diseased lungs, there was multifocal inflammation and the epithelial lining of the airways was disrupted (**Figure 2C**). Cells infected with VN1203 were identified through immunohistochemical staining with an antibody to avian influenza nucleoprotein and could be found throughout the damaged lung (**Figure 2D and E**). Cells positive for viral antigen were not commonly found along the damaged airway due to the loss of epithelial cells lining the airway.

H5N1 infection in the olfactory bulbs and frontal lobe of the ferret brain following aerosol exposure

H5N1 has been shown to cause neurological signs at low doses following intranasal instillation (19) and following nose-only aerosol delivery at higher doses (2, 3). However, the distribution of H5N1 in the brain following low dose aerosol delivery has not been studied. In this study, exposure to the lowest dose delivered resulted in virus distributed widely throughout the brain of ferrets. Viral antigen was consistently detected in the olfactory bulbs of ferrets at the time of death following exposure to the low or high dose (**Figure 3F-H**). Specifically, in the olfactory bulbs of infected ferrets, virus was detected in many of the cells surrounding the glomeruli in the glomerular layer (**Figure 3F and G**). The mitral cell layer and the granule cell layer also contained cells positive for H5N1; however the virus appeared to be more diffuse in these areas compared with the glomerular layer where staining intensity tended to be greater in the nuclei (**Figure 3H**).

Examination of the olfactory bulbs showed hemorrhage occurred in 40% of ferrets exposed to the low dose and 33% of those exposed to the high dose. When they occurred, hemorrhages were often observed in the external plexiform layer just deep to the glomerular layer, in the granule cell layer (**Figure 3B and C**), and in the accessory olfactory bulb. Lymphocytic inflammation in the glomerular layer with perivascular cuffing (meningoencephalitis) was also observed in the olfactory bulb of all ferrets examined (N = 6, high dose; N = 5, low dose).

VN1203 was widely distributed throughout the frontal lobe of ferrets exposed to the low or high dose of H5N1 as determined by immunohistochemical analysis. The viral distribution was multifocal with viral antigen found particularly in the grey matter and neuropil surrounding blood vessels although viral antigen was not detected within

endothelial cells or cells of the vascular tunics. Unlike the distinct circular areas of infected cells observed following intranasal instillation at low doses of VN1203 (19), virus was more widespread and diffuse following aerosol exposure with larger areas of infection detected (**Figure 4A and D**). On average, approximately 17% of the total frontal lobe section examined for each ferret was positive for influenza infection in ferrets exposed to either the low or high dose of H5N1 with as much as 34% of the frontal lobe containing positive cells in one ferret from the low dose group.

Meningoencephalitis, inflammation of the meninges concurrent with inflammation in the brain, was also observed in all ferrets examined with perivascular cuffing and lymphohistiocytic inflammation observed extending into the gray matter of the frontal lobe (**Figure 4B**). Karyorrhexis (fragmented nuclear debris) was commonly observed in areas with detectable virus in all animals and hemorrhage was observed in one ferret that was exposed to the higher dose of VN1203 (**Figure 4B, C, E**).

H5N1 was widely distributed throughout the cerebral cortex and hippocampus of ferrets following aerosol exposure

Ferrets exposed to VN1203 via aerosol also had moderate to severe inflammation in the meninges surrounding the cerebrum (**Figure 5A**). Similar to what was observed around the frontal lobe, perivascular cuffing and lymphocytic inflammation was also apparent in the cerebral cortex (**Figure 5B**). Karyorrhexis was consistently found in areas positive for viral antigen (**Figure 5B, C, E, and F**) and nuclear fragmentation and viral antigen were observed in the hippocampus (**Figure 5G-J**). Karyorrhexis was also found in the piriform lobe in conjunction with the detection of viral antigen.

In some ferrets, foci of VN1203 infection in the neocortex were discrete with distinct edges to the infected areas, similar to foci observed following intranasal infection with VN1203 at low doses. However, many ferrets exposed to low doses of VN1203 via aerosol exhibited viral distribution that was diffuse with virus found throughout the grey matter of the neocortex (**Figure 5D**).

Virus was widespread in the diencephalon of ferrets exposed to VN1203 via aerosol

Ferrets exposed to VN1203 via aerosol exhibited widespread multifocal infection throughout the thalamus, particularly in thalamic nuclei and infected areas ranged from multi-focal to diffuse regardless of exposure to the low or high dose (**Figure 6A and B**). Approximately 20 foci of viral antigen were detected in the thalamus per animal examined with infection detected throughout 34% of the thalamus. In contrast to viral antigen detection by immunohistochemical analysis, pathology observations were different between groups when H&E stained sections were examined. Exposure to the lower dose of VN1203 consistently resulted in distinct foci of karyorrhexis in the thalamic nuclei and in the tissue surrounding blood vessels in the thalamus. Mild to no inflammation was observed (**Figure 6C and D**) in conjunction with viral antigen detection. Lymphocytes and macrophages were marginated within the blood vessels of some ferrets exposed to the lower dose and hemorrhage was observed in one animal at the low dose.

Cell death was more widespread in the thalamus of ferrets exposed to the higher dose of VN1203 with moderate inflammation observed (**Figure 6E and F**). Discrete edges to the karyorrhectic areas often could not be identified in these ferrets with larger areas exhibiting widespread cell death than seen in low dose animals. Perivascular

cuffing was observed with lymphocytic inflammation extending from the vessels into the thalamus with lymphocytes and histiocytes often visible within the vessels. Hemorrhage was observed in one ferret exposed to the higher dose and it was more severe than the single instance of hemorrhage observed in the group exposed to the low dose of VN1203.

The habenular nuclei, located in the epithalamus, were positive for viral antigen with substantial cell death also observed. Interestingly, the endothelial and other vascular cells were negative by immunohistochemical staining while the cells within neuropil surrounding the vessels were positive (**Figure 6G and H**).

Immunopathology of VN1203 infection in the cerebellum and brain stem of ferrets following aerosol exposure

Virus was detected by immunohistochemical analysis in the Purkinje cells of the cerebellum in both groups of ferrets (**Figure 7D**). Rare foci of cellular debris were observed in areas of infected Purkinje cells (**Figure 7A**) and inflammation was not observed in any layer of the cerebellar cortex. Virus was also detected in the fastigial and interpositus nuclei of the cerebellum (**Figure 7E and F**) and significant cell death was observed in these areas by examination of H&E stained sections (**Figure 7B and C**).

H&E stained tissue sections that contained the brain stem at the levels of the cerebrum and cerebellum were examined and histological observations were recorded. Fifty percent of sections examined from the low dose group exhibited significant areas of cell death with karyorrhexis commonly observed (**Figure 8A**). The areas of cellular debris observed in the brain stem of ferrets exposed to the lower dose of VN1203 were much smaller than those observed in the high dose group. The foci of debris were discrete and widespread throughout the brain stem. In the group that received the high dose of

VN1203, 80% of sections examined contained areas of karyorrhexis that were widespread with discrete edges not well defined (**Figure 8B and C**). Most fields of cellular debris were large with foci infringing on each other to form large areas of damaged tissue. Perivascular cuffing was observed in 62% of brain stems examined from the group that received the low dose (**Figure 8A**) and in 80% from the group that received the high dose of VN1203 (**Figure 8D**). Infiltration of inflammatory cells was also more frequently observed in the brain stem of ferrets that received the high dose of VN1203 than those that received the low dose (**Figure 8D**). Significant hemorrhaging was observed in one ferret that received the high dose.

Viral antigen was consistently detected by immunohistochemistry in the same area as karyorrhexis and inflammation; however, it was not found in the ependymal cells, endothelial cells, or within the lumen of the blood vessels (**Figure 8E-H**). An average of 12 distinct foci including at least ten influenza infected cells per ferret were detected in the brain stem following exposure to either the low or high dose of H5N1. Approximately 11% of the area examined in the brain stem of low dose animals and approximately 6% of the area examined in the high dose group contained measurable foci of infected cells.

Discussion

Highly pathogenic avian influenza (HPAI) is commonly delivered intranasally to experimentally infected ferrets in order to efficiently deposit the desired quantity of virus to the upper respiratory tract. Other methods of HPAI instillation in ferrets have also been examined to determine effects of the chosen delivery method and to identify the route that results in pathogenesis most closely resembling what is observed in human cases of HPAI infection (2, 3).

In this study, aerosol exposure was used to study the pathogenesis of a more natural route of infection in ferrets. Nose-only chambers were used to reduce the amount of HPAI virus lost in large chambers or deposited on the ferrets' fur. Clinical signs of infection observed during the study period, morbidity, and analysis of histopathology confirm aerosolized HPAI was highly lethal and caused severe disease in the lungs and central nervous system. Compared to low doses of intranasally instilled VN1203, aerosol delivery resulted in a more widespread distribution of virus throughout the brain and substantially more inflammation than commonly observed in this laboratory following intranasal instillation of low doses of VN1203 (19).

The virus initially infects the nasal epithelium where it rapidly replicates and is likely disseminated to the CNS via nerves. The neuroepithelium of the nasal turbinates include olfactory nerve fascicles in the olfactory mucosa that extend through the cribriform plate to the main olfactory bulb (OB). The axons of olfactory receptor nerves and their glia pass through the olfactory nerve layer and synapse on the dendrites of mitral cells and tufted cells within the glomeruli of the olfactory bulbs. Both the mitral cell layer and glomeruli were consistently infected with HPAI at the time of death and significant pathology was observed in these areas.

From the main OBs, secondary projections extend directly to several regions within the basal telencephalon that comprise the olfactory cortex. The mitral cells of the OBs also project through the olfactory tract and lateral olfactory stria to the ipsilateral olfactory cortex over the piriform lobe, which also contained detectable virus and inflammation in this study. This suggests virus could pass directly from the OB to the piriform lobe via the axons by using inherent mechanisms of the cells (*e.g.*, anterograde

or retrograde transport. It is important to note these connections do not pass through thalamic nuclei.

Interestingly the thalamic nuclei were infected with HPAI and they receive axons only from other diencephalic and telencephalic sources and not from the olfactory tract. This suggests a route of CNS infection other than solely the olfactory tract. Some sources of input into the thalamic nuclei are primary relay thalamic nuclei, thalamic reticular system nuclei, the cingulate gyrus, and the frontal cortex, all of which were highly infected with HPAI.

Viral antigen and cell death were also observed in the fastigial nucleus of the cerebellum. This receives input from Purkinje cells and sends axons through the caudal cerebellar peduncle to the reticular formation and vestibular nuclei to regulate muscle tone and maintain balance. Each of these areas was also infected, which is consistent with virus utilizing axonal transport mechanisms of neuronal cells to disseminate throughout the CNS.

Many viruses have been shown to use axonal transport to impair neurological processes and induce severe pathologies (22). Rabies can induce neurodegeneration (23), Theiler's murine encephalomyelitis virus causes demyelination (24) and Borna disease virus can induce defects in synaptogenesis (25). Influenza infection has also been linked to Parkinson's disease due to inflammation caused by the infection (26). The connections between regions of the ferret brain that contain significant amounts of detectable viral antigen suggest that HPAI could be using the same mechanisms and routes as proteins that are continuously trafficking throughout the CNS.

Half of ferrets exposed to the low dose and all of those exposed to the high dose of aerosolized H5N1 exhibited neurological signs such as head tilt, shaking of limbs, loss of righting, loss of startle (which could indicate hearing loss), paralysis, torticollis, and twitching. Some ferrets appeared unsteady on their feet as if they were experiencing weakness (perhaps as a result of infection in the reticular formation of the brainstem). The head tilt observed in four of the six ferrets exposed to the higher dose of aerosolized H5N1 could be explained by the viral antigen and necrosis consistently found in the vestibular nuclei. Specifically, lesions in the vestibular division of the cranial nerve (CN) VIII typically manifest as head tilt toward the side of the lesion in affected animals. Furthermore, the “loss of startle” combined with the head tilt observed in fifty percent of ferrets exposed to the higher dose of H5N1 could be explained by damage to the vestibular and cochlear nerves.

Understanding the correlation between the localization of virus, lesions, and neurological signs observed during HPAI infections will help lead clinicians to more rapid diagnoses and treatment of patients who do not present with typical respiratory symptoms. Furthermore, elucidating the route HPAI takes to enter the CNS following aerosol exposure could provide insight into viral characteristics that could be exploited in the development of new vaccines, prophylactics, and therapeutics. Specific receptors or pathways could be temporarily inhibited to stop the virus from entering the CNS where it can induce severe disease, result in long-term illness, or result in death.

Acknowledgements

We would like to thank DARPA for funding this study and the Lovelace Respiratory Research Institute (LRRI) for intramural support. Thank you to Zemmie

Pollock who was the study coordinator and lead technician for this work. Special thanks to the comparative medicine veterinary staff at LRRI for technical support, and the Pathology department for trimming tissues and for processing and preparing the tissue sections for the H&E stains.

Competing interests

The authors have no competing interests to report.

Authors' contributions

JRP, JLT, and KSH wrote the paper. JLT, SMS, and PJK performed the experiments. JRP and AG analyzed the samples. JRP, JLT, TB, PJK, and KSH designed and conceived the experiments.

References

1. **Bodewes, R., J. H. C. M. Kreijtz, G. van Amerongen, R. A. M. Fouchier, A. D. M. E. Osterhaus, G. F. Rimmelzwaan, and T. Kuiken.** 2011. Pathogenesis of influenza A/H5N1 virus infection in ferrets differs between intranasal and intratracheal routes of inoculation. *Am J Pathol.* **179**:30-30-36. doi: 10.1016/j.ajpath.2011.03.026.
2. **Gustin, K. M., J. A. Belser, D. A. Wadford, M. B. Pearce, J. M. Katz, T. M. Tumpey, and T. R. Maines.** 2011. Influenza virus aerosol exposure and analytical system for ferrets. *Proceedings of the National Academy of Sciences.* **108**:8432-8437. doi: 10.1073/pnas.1100768108.
3. **Lednicky, J. A., S. B. Hamilton, R. S. Tuttle, W. A. Sosna, D. E. Daniels, and D. E. Swayne.** 2010. Ferrets develop fatal influenza after inhaling small particle aerosols of highly pathogenic avian influenza virus A/Vietnam/1203/2004 (H5N1). *Viol. J.* **7**:231-422X-7-231. doi: 10.1186/1743-422X-7-231; 10.1186/1743-422X-7-231.
4. **Tuttle, R. S., W. A. Sosna, D. E. Daniels, S. B. Hamilton, and J. A. Lednicky.** 2010. Design, assembly, and validation of a nose-only inhalation exposure system for studies of aerosolized viable influenza H5N1 virus in ferrets. *Viol. J.* **7**:135-422X-7-135. doi: 10.1186/1743-422X-7-135; 10.1186/1743-422X-7-135.
5. **Brojer, C., E. O. Agren, H. Uhlhorn, K. Bernodt, D. S. Jansson, and D. Gavier-Widen.** 2012. Characterization of encephalitis in wild birds naturally infected by highly pathogenic avian influenza H5N1. *Avian Dis.* **56**:144-152.
6. **Cardona, C. J., Z. Xing, C. E. Sandrock, and C. E. Davis.** 2009. Avian influenza in birds and mammals. *Comp Immunol Microbiol Infect Dis.* **32**:255-73.
7. **Hinshaw, V. S., W. J. Bean, J. Geraci, P. Fiorelli, G. Early, and R. G. Webster.** 1986. Characterization of two influenza A viruses from a pilot whale. *J Virol.* **58**:655-656.
8. **Zhang, Z., J. Zhang, K. Huang, K. S. Li, K. Y. Yuen, Y. Guan, H. Chen, and W. F. Ng.** 2009. Systemic infection of avian influenza A virus H5N1 subtype in humans. *Hum Pathol.* **40**:735-9.
9. **Korteweg, C., and J. Gu.** 2008. Pathology, molecular biology, and pathogenesis of avian influenza A (H5N1) infection in humans. *Am. J. Pathol.* **172**:1155-1170. doi: 10.2353/ajpath.2008.070791; 10.2353/ajpath.2008.070791.
10. **Gu, J., Z. Xie, Z. Gao, J. Liu, C. Korteweg, J. Ye, L. T. Lau, J. Lu, Z. Gao, B. Zhang, M. A. McNutt, M. Lu, V. M. Anderson, E. Gong, A. C. H. Yu, and W. I. Lipkin.** 2007. H5N1 infection of the respiratory tract and beyond: a molecular pathology study. *The Lancet.* **370**:1137-1145.

11. **de Jong, M. D., V. C. Bach, T. Q. Phan, M. H. Vo, T. T. Tran, B. H. Nguyen, M. Beld, T. P. Le, H. K. Truong, V. V. Nguyen, T. H. Tran, Q. H. Do, and J. Farrar.** 2005. Fatal avian influenza A (H5N1) in a child presenting with diarrhea followed by coma. *N. Engl. J. Med.* **352**:686-691. doi: 10.1056/NEJMoa044307.
12. **Gao, R., L. Dong, J. Dong, L. Wen, Y. Zhang, H. Yu, Z. Feng, M. Chen, Y. Tan, Z. Mo, H. Liu, Y. Fan, K. Li, C. K. Li, D. Li, W. Yang, and Y. Shu.** A systematic molecular pathology study of a laboratory confirmed H5N1 human case. *PLoS One.* **5**:e13315.
13. **Kuiken, T., J. van den Brand, D. van Riel, M. Pantin-Jackwood, and D. E. Swayne.** Comparative Pathology of Select Agent Influenza A Virus Infections. **47**:893-914. doi: 10.1177/0300985810378651.
14. **Studahl, M.** 2003. Influenza virus and CNS manifestations. *J. Clin. Virol.* **28**:225-232.
15. **Henry, J., R. J. Smeyne, H. Jang, B. Miller, and M. S. Okun.** Parkinsonism and neurological manifestations of influenza throughout the 20th and 21st centuries. *Parkinsonism Relat Disord.* **16**:566-71.
16. **Bide, R. W., S. J. Armour, and E. Yee.** 2000. Allometric respiration/body mass data for animals to be used for estimates of inhalation toxicity to young adult humans. *J. Appl. Toxicol.* **20**:273-290.
17. **Alexander, D. J., C. J. Collins, D. W. Coombs, I. S. Gilkison, C. J. Hardy, G. Healey, G. Karantabias, N. Johnson, A. Karlsson, J. D. Kilgour, and P. McDonald.** 2008. Association of Inhalation Toxicologists (AIT) working party recommendation for standard delivered dose calculation and expression in non-clinical aerosol inhalation toxicology studies with pharmaceuticals. *Inhal. Toxicol.* **20**:1179-1189. doi: 10.1080/08958370802207318; 10.1080/08958370802207318.
18. **Thompson, C. I., W. S. Barclay, M. C. Zambon, and R. J. Pickles.** 2006. Infection of human airway epithelium by human and avian strains of influenza a virus. *J. Virol.* **80**:8060-8068. doi: 10.1128/JVI.00384-06.
19. **Plourde, J. R., J. A. Pyles, R. C. Layton, S. E. Vaughan, J. L. Tipper, and K. S. Harrod.** 2012. Neurovirulence of H5N1 infection in ferrets is mediated by multifocal replication in distinct permissive neuronal cell regions. *PLoS One.* **7**:e46605. doi: 10.1371/journal.pone.0046605; 10.1371/journal.pone.0046605.
20. **Zitzow, L. A., T. Rowe, T. Morken, W. Shieh, S. Zaki, and J. M. Katz.** 2002. Pathogenesis of Avian Influenza A (H5N1) Viruses in Ferrets. *Journal of Virology.* **76**:4420-4429; 4420.

21. **Govorkova, E. A., J. E. Rehg, S. Krauss, H. Yen, Y. Guan, M. Peiris, T. D. Nguyen, T. H. Hanh, P. Puthavathana, H. T. Long, C. Buranathai, W. Lim, R. G. Webster, and E. Hoffmann.** 2005. Lethality to Ferrets of H5N1 Influenza Viruses Isolated from Humans and Poultry in 2004. *Journal of Virology*. **79**:2191-2198; 2191.
22. **Salinas, S., G. Schiavo, and E. J. Kremer.** 2010. A hitchhiker's guide to the nervous system: the complex journey of viruses and toxins. *Nat. Rev. Microbiol.* **8**:645-655. doi: 10.1038/nrmicro2395; 10.1038/nrmicro2395.
23. **Woldehiwet, Z.** 2002. Rabies: recent developments. *Res. Vet. Sci.* **73**:17-25.
24. **Brahic, M., J. F. Bureau, and T. Michiels.** 2005. The genetics of the persistent infection and demyelinating disease caused by Theiler's virus. *Annu. Rev. Microbiol.* **59**:279-298. doi: 10.1146/annurev.micro.59.030804.121242.
25. **Hans, A., J. J. Bajramovic, S. Syan, E. Perret, I. Dunia, M. Brahic, and D. Gonzalez-Dunia.** 2004. Persistent, noncytolytic infection of neurons by Borna disease virus interferes with ERK 1/2 signaling and abrogates BDNF-induced synaptogenesis. *FASEB J.* **18**:863-865. doi: 10.1096/fj.03-0764fje.
26. **Jang, H., D. Boltz, K. Sturm-Ramirez, K. R. Shepherd, Y. Jiao, R. Webster, and R. J. Smeyne.** 2009. Highly pathogenic H5N1 influenza virus can enter the central nervous system and induce neuroinflammation and neurodegeneration. *Proceedings of the National Academy of Sciences of the United States of America.* **106**:14063-14068; 14063.

Figure Legends

Figure 1. Survival, temperature, and bodyweight of ferrets following aerosolized H5N1 exposure.

A: Survival of ferrets exposed to 0 (dotted line), 0.2 (dashed line), or 31.88 (solid line) PFU of aerosolized A/Vietnam/1203/2004 (VN1203). **B:** Mean \pm SEM of temperature from the shoulder microchip; **C:** Mean \pm SEM of body weight change; **B, C:** Ferrets exposed to 0 PFU (open circles), 0.2 PFU (gray squares), or 31.88 PFU (black squares). **A-C:** N = 6 per group.

Figure 2. Ferrets suffer from severely damaged lungs following aerosol exposure to H5N1.

A-C: 5 μ m sections of inflation fixed, paraffin-embedded lungs stained with H&E. **B:** Higher magnification of box in panel A. **D-F:** Viral antigen was detected with IMGEX-5187A for avian influenza A NP and visualized with DAB. Brown stain indicates the presence of virus. **E:** Higher magnification of box in panel D. **E,F:** Arrows points to cells positive for viral antigen.

Figure 3. Pathological findings and H5N1 nucleoprotein are detected in the olfactory bulb of ferrets following aerosol exposure at a low dose.

A-D: 5 μ m sections of formalin fixed olfactory bulbs stained with H&E. **A,E:** Mock infected. **B-D, F-H:** Aerosol exposure to 0.2 PFU of VN1203. **C,G:** Higher magnification of box in panel B and F, respectively. Asterisk indicated glomeruli of the glomerular layer. **D:** MCL: mitral cell layer, GCL: granule cell layer.

Figure 4. Widespread distribution of H5N1 and inflammation in the frontal lobe following aerosol exposure in ferrets.

A,B: Viral antigen in the frontal lobe was detected with IMGEX-5187A for avian influenza A NP and visualized with DAB. Brown stain indicates the presence of virus. **B:** Higher magnification of box in panel A. **C:** H&E stained section of the frontal lobe. Inset is higher magnification of box.

Figure 5. Aerosol exposure to H5N1 results in perivascular cuffing, karyorrhexis, and widespread viral infection in the neocortex and hippocampus.

A-C: H&E stained sections of the cerebral cortex. **D-F:** Viral antigen in the cingulate gyrus was detected with IMGEX-5187A for avian influenza A NP and visualized with DAB. Brown stain indicates the presence of virus. **C,F:** Higher magnification of box in panel B and E, respectively. **C:** Arrows point to cellular debris. **F:** Arrow points to a blood vessel negative for viral antigen. **G-J:** Representative sections of the hippocampus. **G:** H&E stained section, **H:** viral antigen stained section of the hippocampus. **H, J:** Higher magnification of box in panel G. Higher magnification of box in panel G and I, respectively.

Figure 6. Aerosolized H5N1 results in widespread infection and pathological observations in the thalamus.

A,B: Viral antigen in the thalamus of ferrets exposed to 0.2 PFU was detected with IMGEX-5187A for avian influenza A NP and visualized with DAB. Brown stain indicates the presence of virus. **B:** Higher magnification of box in panel A. Asterisks denote foci of H5N1 infection. **C:** H&E stained section of the thalamus demonstrating perivascular cuffing around a blood vessel. **D:** Viral antigen was detected in the next

sequential section of panel C. Note the absence of positive staining in the vessel. **E:** Representative sections of the thalamus of ferrets exposed to 31.88 PFU of H5N1, stained with H&E. Arrows denote areas of inflammation. **F:** Higher magnification of box in panel E. **G:** H&E stained section of the epithalamus of a ferret exposed to the low dose of H5N1. **H:** Next sequential section of section in panel G, stained for viral antigen. Arrow denotes blood vessel negative for viral antigen among a foci of positive infection.

Figure 7. Viral antigen and cell death are detected in the cerebellum of ferrets following aerosol exposure.

Cerebellar sections stained with **A-C:** H&E or **D-F:** IMGENEX-5187A for avian influenza A NP and visualized with DAB. Brown stain indicates the presence of virus. **A:** Mild cellular debris was observed in the area of viral infection in the Purkinje cells of the cerebellum. **B:** Moderate cell death was observed in the fastigial (denoted by asterisk) and interpositus (denoted by pound sign) nuclei. **C:** Higher magnification of fastigial nucleus from B. Dashed arrow points to cellular debris. **D:** Area of positive infection in the Purkinje cell layer of the cerebellum. Arrow points to a Purkinje cell positive for viral antigen. **E:** The fastigial (denoted by asterisk) and interpositus (denoted by pound sign) nuclei were positive for viral antigen by immunohistochemistry. **F:** Higher magnification of avian influenza nucleoprotein positive area from panel D. Arrowhead points to a cell positive for viral antigen.

Figure 8. Aerosol exposure to H5N1 results in significant destruction in the brain stem of ferrets.

A-D: H&E stained sections of the brain stem of ferrets exposed H5N1 **A:** Circle identifies a nucleus with karyorrhexis and the arrow indicates perivascular cuffing of a

blood vessel. Ferret was exposed to 0.2 PFU of H5N1. **E:** Section subsequent to the H&E stained section in panel A with a circle indicating the same area and the arrow indicating the absence of positive staining in the blood vessel. **B:** Brain stem of a ferret exposed to the higher dose of H5N1. **C:** Higher magnification of the box in panel B. Arrows indicated cellular debris. **F:** Section subsequent to that in panel B stained for viral antigen. **G:** Higher magnification of box in panel F. **D:** Brain stem of a ferret exposed to the higher dose of H5N1 showing marked inflammation. **H:** Section subsequent to that in panel D stained for viral antigen.

Figures

Figure 1

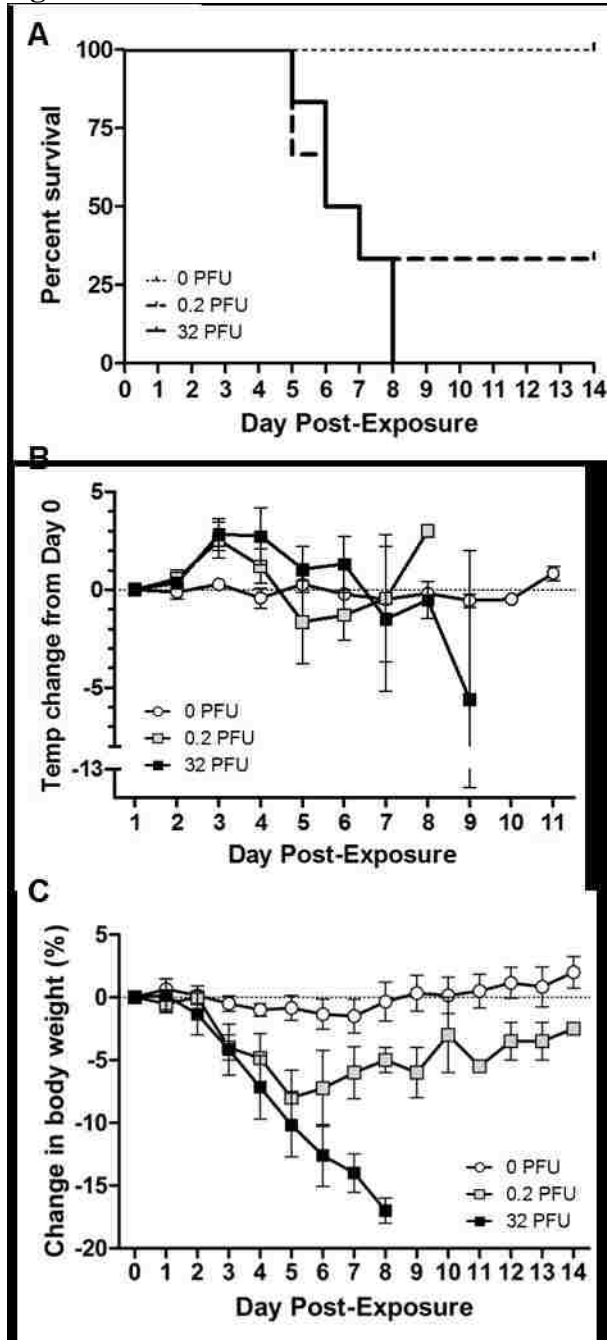


Figure 2

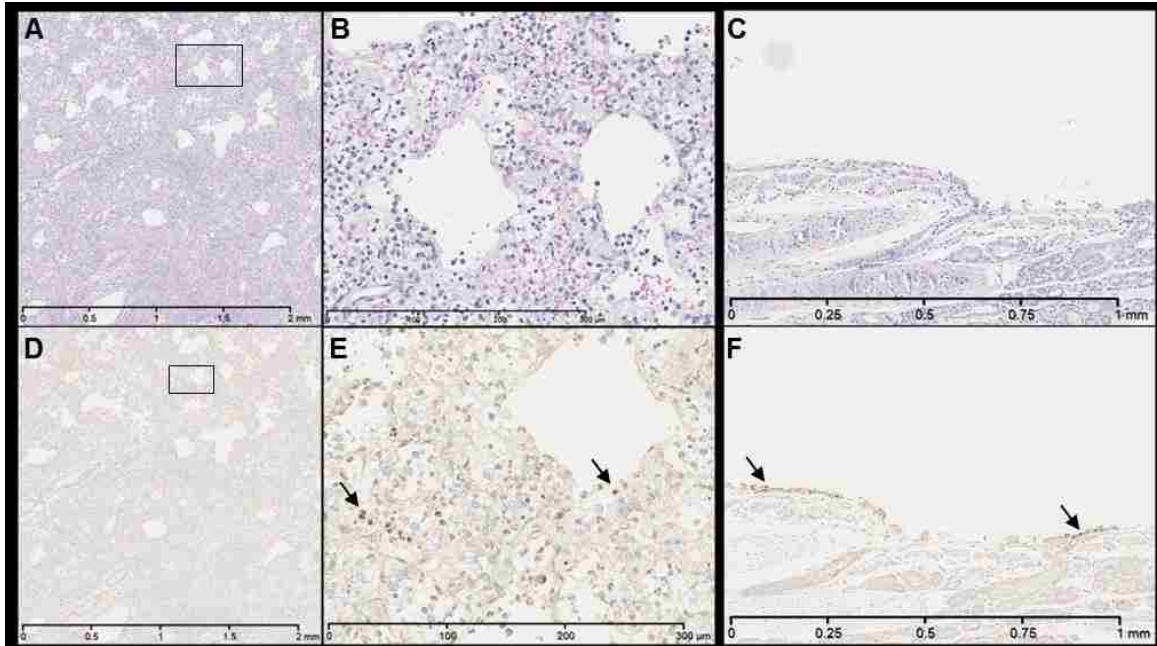


Figure 3

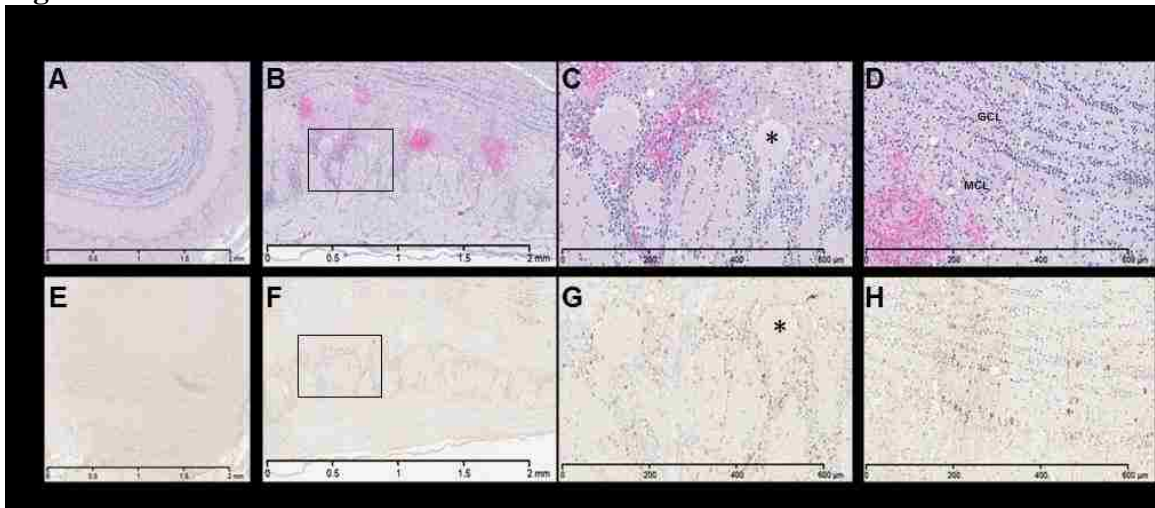


Figure 4

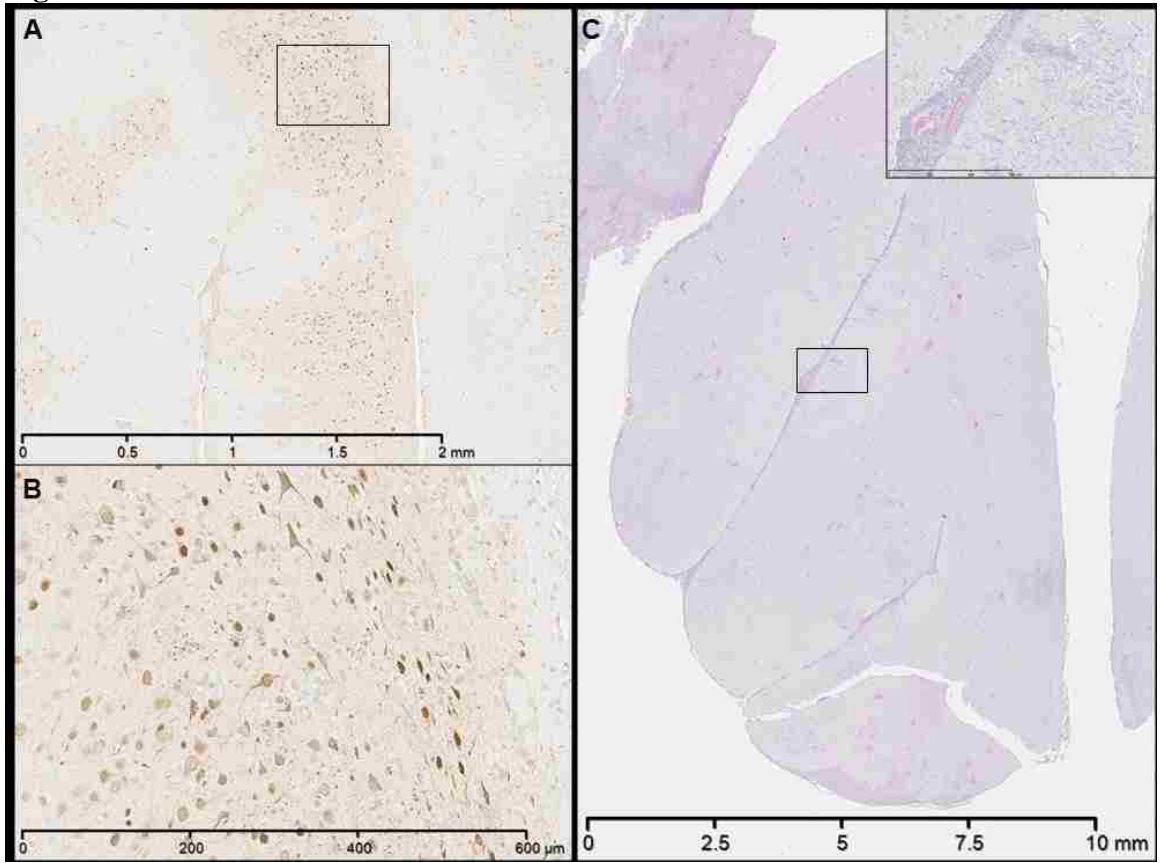


Figure 5

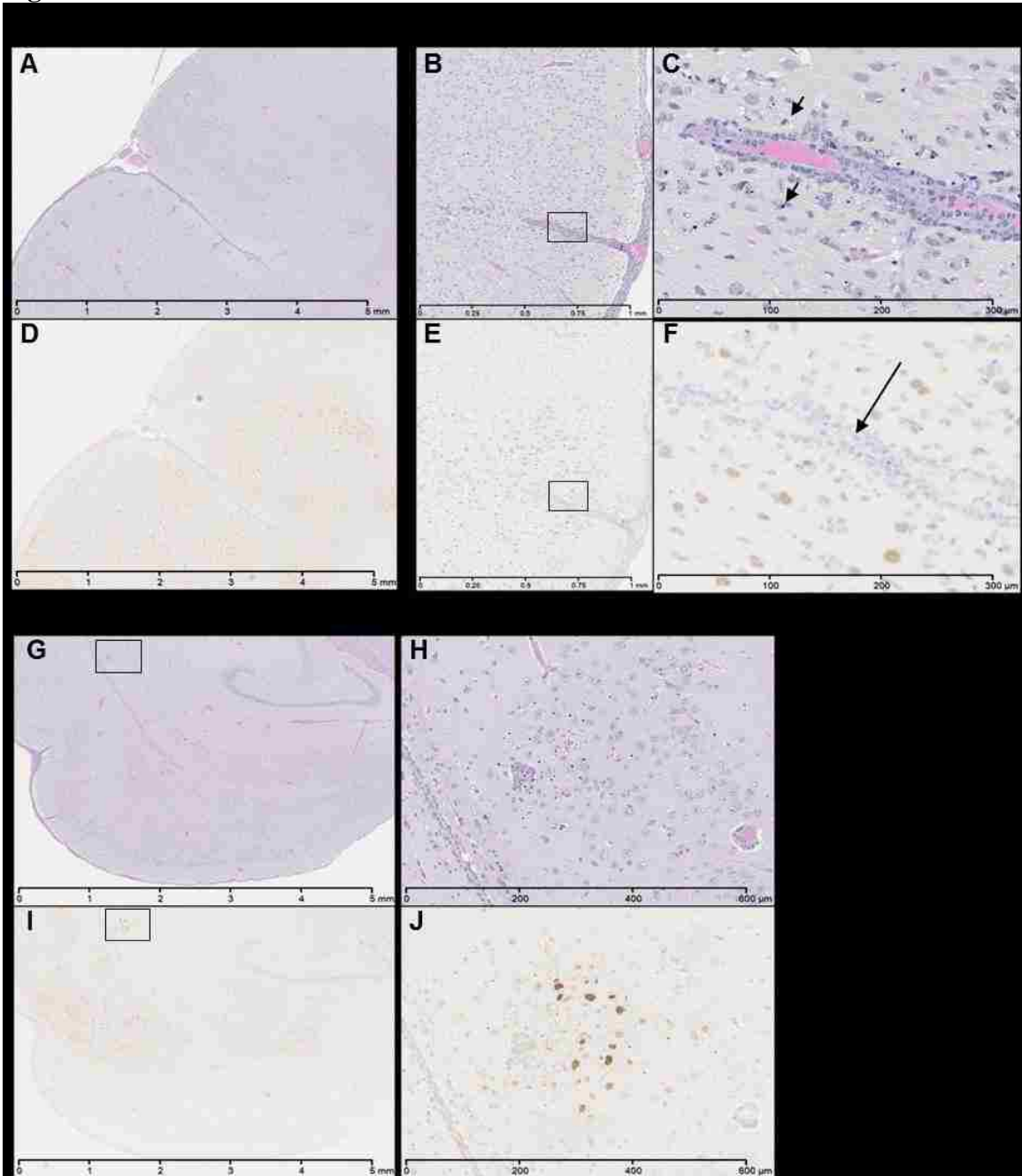


Figure 6

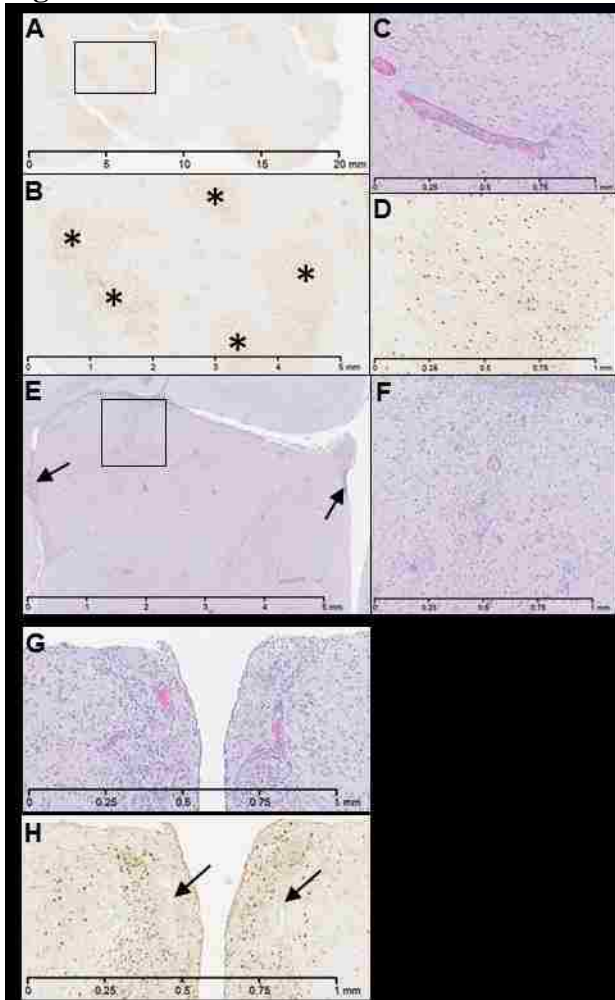


Figure 7

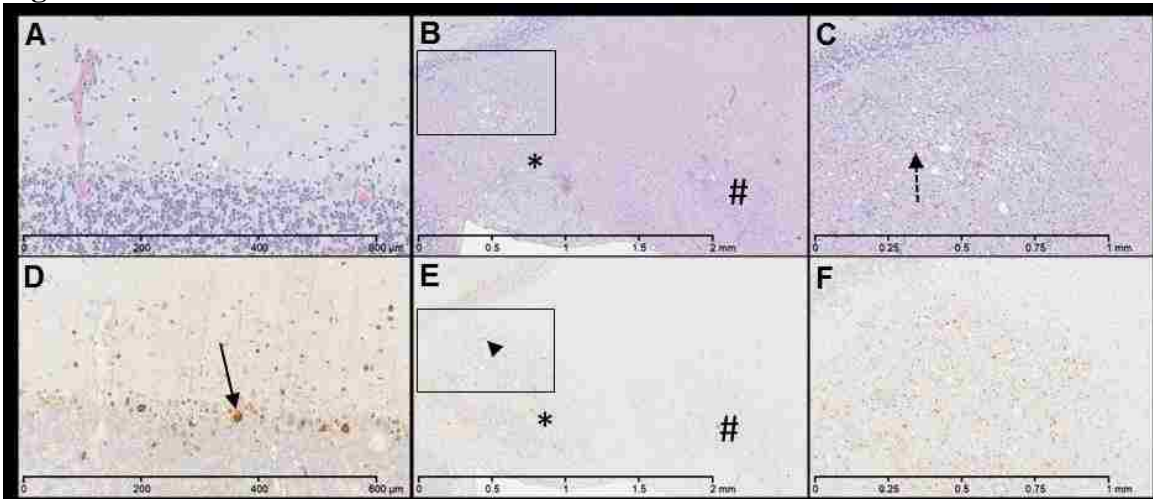
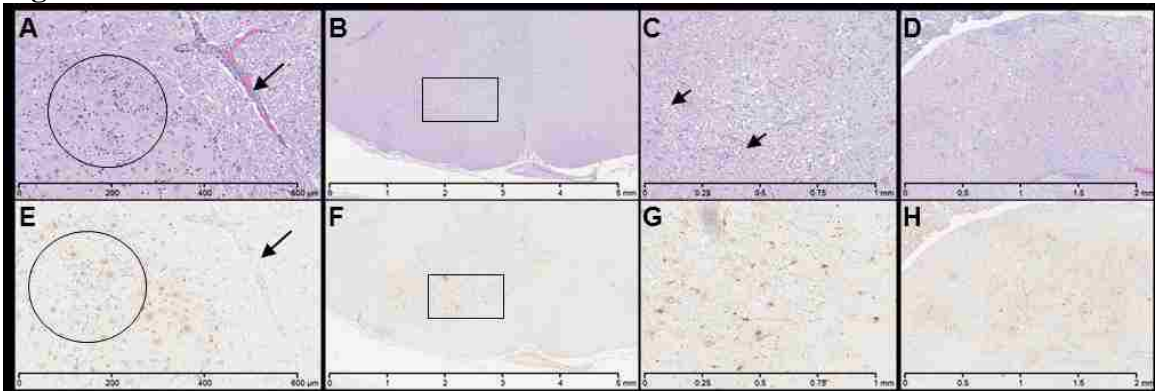


Figure 8



Table

Table 1. Prevalence of neurological signs in ferrets.

Dose (PFU)	Number of Ferrets with Neurological Signs/Total Ferrets in Group	Day of onset
0	0/6	NA
0.2	2/6	6, 7
32	6/6	5, 6, 7, 8

Chapter Four: Discussion

Summary of Studies

These studies sought to determine the spatial and temporal kinetics of the neuropathogenesis of highly pathogenic avian influenza (HPAI) in the ferret model following both nasal and deep lung deposition. Specifically, we examined neuroinvasion of HPAI into the ferret brain following infection and identified regions of the central nervous system (CNS) that are susceptible and permissive to HPAI infection. Furthermore, we correlated the neurological sequelae with neuroanatomical locations of lesions.

Two viruses, one isolated from the initial H5N1 outbreak in Hong Kong in 1997 (HK483) and one from the re-emergence in 2004 (VN1203) were introduced to ferrets at low doses to more closely represent natural infection in individuals. Investigating differences in neuropathogenesis between two well-characterized H5N1 viruses with differing lethality may guide future research in identifying viral determinants of neuropathogenesis. Furthermore, increased understanding of the correlations between the detection of virus outside of the respiratory tract with neurological signs observed during the course of disease may aid clinicians in the quick diagnosis of H5N1 in the absence of typical respiratory symptoms of infection. Importantly, we showed that HPAI deposition into the deep lung also results in neuroinvasion and clinical manifestations of CNS infection.

Intranasal instillation of low doses of VN1203 in ferrets resulted in 100% lethality with 80% of ferrets exhibiting neurological signs. Detailed examination of the neuropathogenesis of this virus revealed that VN1203 instillation resulted in widespread

multifocal infection in the brain with mild inflammation and focal areas of cell death as described by foci of nuclear debris – karyorrhexis. HK483 infection resulted in 20% lethality and no neurological signs of infection. Samples analyzed for viral load in the brain demonstrated VN1203 could replicate to high titers in the olfactory bulb, cerebral cortex, cerebellum, and brain stem while HK483 could not be isolated from these sections. Interestingly, viral RNA could be detected in the brains of HK483 infected ferrets, but at later time points (6 and 8 days post-infection). The differences in lethality could not be attributed to viral replication in the respiratory tract or differences in the lung pathology. We concluded that the increased lethality observed following intranasal instillation of a low dose of VN1203 was due to the neuropathogenesis of the virus and the inability of HK483 to replicate in the brain resulted in a more typical respiratory illness that the ferrets could clear and ultimately recover.

Comparable to observations following a low dose intranasal instillation of VN1203, aerosol exposure to a low dose of the same virus resulted in neurological signs of infection and 100% lethality although the mean time-to-death was delayed compared to intranasally instilled ferrets. The manifestation of neurological signs of infection suggests CNS involvement is not a consequence of intranasal delivery and virus delivered as an aerosol to the deep lung can also disseminate to and replicate in the brain. Furthermore, ferrets exposed via aerosol were found to have more inflammation than observed following intranasal instillation and foci of infection were observed to be more widespread and larger than those following intranasal instillation. Lesions in multiple areas of the CNS following aerosol exposure support multiple routes of neuroinvasion in the ferret.

Lethality is higher in cases of influenza infection that involve the CNS (1, 2); therefore it is important to understand where the virus is replicating in the brain, how it is getting there, and what neurological signs to look for as indications H5N1 has reached the brain. Further research in this area could identify aspects of the virus to target in order to prevent influenza from reaching the CNS and resulting in death.

Routes of H5N1 infection in the CNS

Despite the argument that H5N1 reaches the brain as a result of intranasal instillation, we showed widespread dissemination in the CNS of ferrets exposed to H5N1 via aerosol as well. The nose-only aerosol exposure model used in this study presented H5N1 particles that were approximately 2.1 μm mass median aerodynamic diameter (MMAD) which has been shown to be respirable for ferrets (3, 4). As the ferrets inspire small particles of aerosolized virus, the virus attaches to cells in the nasal epithelium where it can begin to replicate. Small particles are also inhaled into the lower respiratory tract and can replicate in the lung. There are several routes that have been suggested as possible ways virus can travel from the nose into the CNS (5, 6) and from the lung to the CNS (7).

The olfactory tract is the first route considered to be a major conduit of neuroinvasion (5, 7-9). The neuroepithelium of the nasal turbinates include olfactory nerve fascicles in the olfactory mucosa that extend through the cribriform plate to the main olfactory bulb (MOB), which we showed to have high titers of H5N1 at the time of death. Additionally, we showed *in situ* staining for viral antigen in the olfactory bulb and could describe specific areas of the olfactory bulb that were consistently infected. Consistent with the suggestion that virus travels via the olfactory nerves, virus was

detected in and around the glomeruli which are found in the MOB. The glomeruli contain mitral cells and tufted cells whose dendrites synapse with the axons of olfactory receptor nerves and whose glia pass through the olfactory nerve layer. Not surprisingly, mitral cells were also commonly infected.

Secondary projections from the MOB to the olfactory cortex provide a plausible route of further dissemination in the CNS. Mitral cells also project through the olfactory tract and lateral olfactory stria to the ipsilateral olfactory cortex over the piriform lobe. Following both intranasal instillation and aerosol exposure, viral antigen was detected in the olfactory cortex and piriform lobe consistent with the olfactory nerve as a route of infection. Lesions and viral antigen in the piriform lobe could affect a ferret's olfactory sensation leading to an inability to locate food resulting in weight loss.

Notably, the connections from the mitral cells of the MOB to the piriform lobe, located caudally to the MOB, do not pass through the thalamic nuclei, which were also infected with H5N1 following both methods of virus exposure. However, there appeared to be more foci of infection in the thalamus of ferrets exposed to aerosolized H5N1. The thalamic nuclei only receive axons from other diencephalic and telencephalic sources and not from the olfactory tract. Possible origins of the virus that reach the thalamus could be the cingulate gyrus and the frontal cortex; both of which contained multifocal and widespread H5N1 infection following both routes of exposure.

The trigeminal nerve (cranial nerve (CN) V) has also been suggested as a route of infection into the CNS (7). This nerve innervates the face and is responsible for facial sensations and mastication. Mouse studies of H5N1 infection suggested virus could travel via the trigeminal nerve from the face due to the close proximity to the nose where virus

is typically presented (7). Following both intranasal instillation and aerosol exposure in the studies discussed here, viral antigen was detected by immunohistochemistry in the spinal tract of CN V, supporting the possibility that the virus could reach the CNS via the trigeminal nerve in addition to the olfactory nerve. Importantly, the trigeminal nerve does not traverse the brain via the same path as the olfactory nerve and enters the pons through the caudolateral part of the transverse fibers of the pons.

The cell bodies of the glossopharyngeal (CN IX), vagus (CN X), and accessory (CN XI) nerves are located in the nucleus ambiguus, which is found in the brain stem. The vagus nerve reaches through the neck and thorax and branches to innervate the esophageal muscles, larynx, trachea, and bronchi as well as the heart and other viscera. Since influenza viruses are known to infect and replicate in the respiratory tract, the complex innervations of the lung by the vagus nerve provide a route for the virus to reach the CNS without passing through the olfactory or trigeminal nerves. The brain stem of ferrets in these studies, regardless of the exposure method, was widely infected with H5N1 as determined by immunohistochemistry. While the nucleus ambiguus was not specifically examined, more detailed analysis of brain stem sections from future studies could describe whether or not the vagus nerve was likely a route of infection by H5N1 in these models. Finally, the nerves of the sympathetic nervous system have been suggested as routes of H5N1 infection in the brain using a mouse model of infection (7). The studies presented here did not examine the sympathetic nerve ganglia; however, future studies could ascertain whether or not H5N1 can travel up the sympathetic nerve in the ferret model of intranasal or aerosol infection.

Correlation of neurological signs of infection with lesions in the CNS

Understanding the correlation of neurological signs observed during the course of infection could aid clinicians in a quicker diagnosis of avian influenza infection when patients present without the typical respiratory symptoms or with neurological signs in addition to respiratory symptoms. Lesions in discrete and identifiable areas of the brain with described functions could result in neurological sequelae that could be used in differential diagnoses and treatment plans (10). Clinical signs of damage to various areas of the CNS have been characterized for the cerebrum, diencephalon, mesencephalon, cerebellum, vestibular system, and brain stem (10). Using these described clinical signs, we could identify regions of the brain to examine for lesions caused by H5N1 infection that could explain the neurological signs observed.

VN1203 infection resulted in widespread and severe cytopathology in the neuroepithelium of the nasal turbinates. Lesions in this area are known to result in altered perception, particularly as an olfactory deficit (10). An inability to smell food could hinder the infected ferrets from eating and could contribute to some of the weight loss observed during the studies. In addition to the disrupted neuroepithelium following intranasal instillation with H5N1, exposure to aerosolized VN1203 resulted in widespread inflammation and hemorrhaging in the olfactory bulb of infected ferrets. Nuclear debris was consistently observed around the glomeruli and throughout the various layers of the main olfactory bulb. These lesions and the moderate inflammation apparent in this area could also impair the ferrets' ability to smell and find food.

Widespread and multifocal inflammation was also observed throughout the cerebral cortex. Additionally, we observed areas of distinct karyorrhexis in the cerebral

cortex that were also positive for viral antigen in sequentially cut sections. The damage to this area could explain the paresis and paralysis observed following both methods of exposure (10).

Within the diencephalon, widespread lesions and inflammation were observed, especially in areas positive for virus. Damage to the thalamus and hypothalamus could also explain weight loss due to a “deranged appetite” – anorexia, and disrupted thermoregulation, which was more evident following aerosol exposure. Additionally, inflammation in the thalamus appeared to be more widespread with more foci of infection and lesions after aerosol exposure than following intranasal instillation. The observed convulsions could have been seizures although a diagnosis of seizures could not be confirmed with the techniques used on these studies. Lesions to the thalamus could result in seizures (10) and future studies should be designed to look for neurological signs specific to damage in the thalamus and more thoroughly studied.

Some ferrets experienced what was described as “shaking or shivering,” which could have been tremors or chills, during the course of infection and this sign could be attributed to damage in the cerebellum (10). In these studies, the Purkinje cells of the cerebellar cortex were widely infected with VN1203, regardless of the infection method, and lesions and viral antigen were detected in the deep cerebellar nuclei. The fastigial nuclei are connected to the vestibular nuclei and damage to this connection could interfere with hearing. Hearing loss could explain the “loss of startle” observed in ferrets exposed to aerosolized VN1203. The dentate nuclei of the cerebellum are partially responsible for controlling voluntary movement and the lesions observed in this area could have resulted in the ferrets’ inability to control movement.

Widespread inflammation and lesions were observed in the brain stem of infected ferrets and damage to the reticular formation of the brain stem could result in lameness, paresis and paralysis, and weakness. Viral antigen and lesions were consistently found in this structure of the brain stem following VN1203 infection.

Lesions to the cranial nerves could also result in many neurological signs of infection. Damage to CN III, CN IV, CN V, CN VI, CN VII, CN X could also explain paresis and paralysis. Lesions in CN VIII could cause head tilt, which was observed following infection with VN1203. More detailed studies designed to examine these specific cranial nerves should be conducted to further investigate which nerve(s) are involved in the neurological signs recorded following VN1203 infection.

While we did not look specifically at viremia as contributing to CNS infection, it is plausible that HPAI viruses, which bind to red blood cells, could infect extrapulmonary organs via the hematogenous route (11, 12). However, we did examine blood vessels in formalin-fixed paraffin embedded tissue sections that were probed for HPAI antigen and did not find any indication of HPAI virus in the endothelial cells or cells in the lumen of the vessels. This route should be further explored in future studies of HPAI infection in ferrets.

Limitations of the Study

While ferrets provide an excellent model for studying the pathogenesis of influenza viruses, cost, care, and ethical considerations typically limit the number of animals available and allowed on a study. Also, the outbred nature of the subjects limits the reproducibility that is available for inbred mouse models, permitting variation between animals that cannot be controlled. While care was taken to take samples

consistently between studies and trim formalin-fixed paraffin embedded sections uniformly, the inherent anatomical variation between subjects did not always permit this. Organ weights and sizes varied between animals so standard sampling techniques did not always account for these variations (*e.g.*, a specific weight of tissue was removed for virus cultures; however this may not have been the same percentage of the weight of each respective organ between animals).

More detailed tracking of the routes of neuroinvasion could be accomplished using a fluorescently tagged HPAI virus and appropriate imaging platforms. Live tracking studies would provide further details on the route(s) HPAI viruses utilize to disseminate from the respiratory tract to extrapulmonary tissues. Furthermore, direct inoculation of HPAI virus (neurovirulent and non-neurovirulent) into the brain would distinguish whether less lethal, non-neurovirulent strains could replicate in neuronal tissue but lack a mechanism for disseminating to the CNS or if the deficiency is in the viral replication process in neuronal cells. We pursued intracranial inoculations but due to ethical and logistical constraints, this route of exposure could not be examined.

While these limitations exist with utilizing the ferret model, they are carefully considered during the study design, sampling process, and analysis. They are consistent between studies and controlled for as much as possible.

Future Studies

The nose-only aerosol method of H5N1 exposure in ferrets is an invaluable model for studying the effects of HPAI infection in a physiologically relevant way. Low doses of virus should continue to be used to better represent the amount of virus a human would be exposed to as an aerosol in a natural infection.

The findings of these studies have provided great insight into the neuropathogenesis of H5N1, specifically the lethal strain, VN1203. While we have identified brain regions that are susceptible and permissive to VN1203 infection, future studies should be designed to examine detailed routes of infection as well as be designed to study specific basal nuclei in the brain.

Time-course studies that seek to model the route of neuropathogenesis in the ferret following aerosol exposure to HPAI should be designed to take frequent samples for measuring viral load in the CNS, other extra-pulmonary regions, and the respiratory tract. Fixed samples should be trimmed with precision to allow for identical slides to be cut from multiple animals for more exact comparisons and power in statistically analyzing differences in localization, and confidently identifying specific brain regions.

The reverse genetics system has been established and optimized for influenza research and many studies have used the system to discover viral determinants of lethality (12-23). Studies that seek to identify viral determinants of neuropathogenesis in an aerosol model of infection would be greatly beneficial in identifying new virulence markers that could enhance surveillance of newly emerging HPAI viruses. Of particular interest are the segments that comprise the ribonucleoprotein (*i.e.*, PB1, PB2, and PA). We can hypothesize that differences in these segments permit VN1203 to replicate to high titers in the brain and result in severe lesions that cause enough damage to manifest as neurological signs. Another segment of interest is the HA of neurovirulent strains. This surface glycoprotein may enhance attachment and entry into neuronal cells permitting replication and dissemination throughout the CNS. Finally, the NS segment would be

interesting to study in order to determine if differences in the immune response contribute to the increased lethality in the neuropathogenic strains of HPAI.

Conclusions

In the first study described in this dissertation, we sought to identify determinants of lethality for a virulent H5N1 strain from 2004 (VN1203) and for a less virulent isolate from 1997 (HK483) following intranasal instillation of a low dose in ferrets. We concluded the increased lethality of VN1203 was due to the neuropathogenesis of the virus. High viral loads in the olfactory bulb, cerebral cortex, cerebellum, and brain stem were measured by microplaque assays and visualized by immunohistochemical staining for viral antigen. These analyses resulted in identifying specific regions of the brain as susceptible and permissive to infection by VN1203.

The second study highlights the neurological sequelae of VN1203 infection following aerosol exposure of a low dose deep into the lung. We showed aerosolized VN1203 resulted in widespread infection with more foci of infection and more severe inflammation than observed following intranasal instillation. The widespread and multifocal nature of the infection aided in our analysis of identifying lesions in specific neuroanatomical regions that correlated with neurological signs of infection. Importantly, this study showed that H5N1 infection could still result in neurological manifestations of disease when ferrets were exposed to the more natural route of infection.

Mouse models of HPAI infection are often used to examine the neuropathogenesis of HPAI viruses because many more H5N1 strains are neuroinvasive to mice (7, 9, 24-28). To our knowledge these are the first studies describing brain regions susceptible and permissive to VN1203 replication in the ferret model, particularly

following low dose aerosol exposure, which is a more physiologically relevant model than intranasal instillation. Widespread CNS involvement and the consistent observation of neurological signs of infection following aerosol exposure support the argument that H5N1 can reach the brain via several routes of infection and it is not a consequence of intranasal instillation. Furthermore, the manifestation of neurological signs in ferrets following aerosol exposure recapitulate observations of CNS involvement in humans following infection with human influenza strains as reported over the last century (1, 29-36).

Importantly, increased understanding of the correlation between neurological signs of infection, the localization of neuroanatomical lesions, and viral antigen, may provide clinicians with more markers of avian influenza infection when presented with cases of atypical symptoms. Finally, as more information on mechanisms of neuropathogenesis of the virus is reported and routes of infection are better understood, drugs aimed at blocking those specific pathways could prevent the virus from entering the CNS and could increase survival rates following HPAI infection.

References

1. **Okabe, N., K. Yamashita, K. Taniguchi, and S. Inouye.** 2000. Influenza surveillance system of Japan and acute encephalitis and encephalopathy in the influenza season. *Pediatr. Int.* **42**:187-191.
2. **Jang, H., D. Boltz, K. Sturm-Ramirez, K. R. Shepherd, Y. Jiao, R. Webster, and R. J. Smeyne.** 2009. Highly pathogenic H5N1 influenza virus can enter the central nervous system and induce neuroinflammation and neurodegeneration. *Proc. Natl. Acad. Sci. U. S. A.* **106**:14063-14068; 14063.
3. **Alexander, D. J., C. J. Collins, D. W. Coombs, I. S. Gilkison, C. J. Hardy, G. Healey, G. Karantabias, N. Johnson, A. Karlsson, J. D. Kilgour, and P. McDonald.** 2008. Association of Inhalation Toxicologists (AIT) working party recommendation for standard delivered dose calculation and expression in non-clinical aerosol inhalation toxicology studies with pharmaceuticals. *Inhal. Toxicol.* **20**:1179-1189. doi: 10.1080/08958370802207318; 10.1080/08958370802207318.
4. **Bide, R. W., S. J. Armour, and E. Yee.** 2000. Allometric respiration/body mass data for animals to be used for estimates of inhalation toxicity to young adult humans. *J. Appl. Toxicol.* **20**:273-290.
5. **Shinya, K., A. Makino, M. Hatta, S. Watanabe, J. H. Kim, Y. Hatta, P. Gao, M. Ozawa, Q. M. Le, and Y. Kawaoka.** 2011. Subclinical brain injury caused by H5N1 influenza virus infection. *J. Virol.* **85**:5202-5207. doi: 10.1128/jvi.00239-11.
6. **Mori, I., T. Yokochi, and Y. Kimura.** 2002. Role of influenza A virus hemagglutinin in neurovirulence for mammals. *Med. Microbiol. Immunol.* **191**:1-4.
7. **Park, C. H., M. Ishinaka, A. Takada, H. Kida, T. Kimura, K. Ochiai, and T. Umemura.** 2002. The invasion routes of neurovirulent A/Hong Kong/483/97 (H5N1) influenza virus into the central nervous system after respiratory infection in mice. *Archives of Virology.* **147**:1425-1425-1436.
8. **Mori, I., Y. Nishiyama, T. Yokochi, and Y. Kimura.** 2005. Olfactory transmission of neurotropic viruses. *J. Neurovirol.* **11**:129-137. doi: 10.1080/13550280590922793.
9. **Tanaka, H., C. Park, A. Ninomiya, H. Ozaki, A. Takada, T. Umemura, and H. Kida.** 2003. Neurotropism of the 1997 Hong Kong H5N1 influenza virus in mice. *Vet. Microbiol.* **95**:1-13.
10. **Bolon, B., and M. T. Butt (eds.),** 2011. *Fundamental Neuropathology for Pathologists and Toxicologists.* Wiley & Sons, Inc., New Jersey.
11. **Wang, X., J. Zhao, S. Tang, Z. Ye, and I. Hewlett.** 2010. Viremia associated with fatal outcomes in ferrets infected with avian H5N1 influenza virus. *PLoS One.* **5**:e12099.

12. **Maines, T. R., X. H. Lu, S. M. Erb, L. Edwards, J. Guarner, P. W. Greer, D. C. Nguyen, K. J. Szretter, L. Chen, P. Thawatsupha, M. Chittaganpitch, S. Waicharoen, D. T. Nguyen, T. Nguyen, H. H. T. Nguyen, J. Kim, L. T. Hoang, C. Kang, L. S. Phuong, W. Lim, S. Zaki, R. O. Donis, N. J. Cox, J. M. Katz, and T. M. Tumpey.** 2005. Avian Influenza (H5N1) Viruses Isolated from Humans in Asia in 2004 Exhibit Increased Virulence in Mammals. *J. Virol.* **79**:11788-11800. doi: 10.1128/jvi.79.18.11788-11800.2005.
13. **Govorkova, E. A., J. E. Rehg, S. Krauss, H. L. Yen, Y. Guan, M. Peiris, T. D. Nguyen, T. H. Hanh, P. Puthavathana, H. T. Long, C. Buranathai, W. Lim, R. G. Webster, and E. Hoffmann.** 2005. Lethality to ferrets of H5N1 influenza viruses isolated from humans and poultry in 2004. *J. Virol.* **79**:2191-8.
14. **Hoffmann, E., S. Krauss, D. Perez, R. Webby, and R. G. Webster.** 2002. Eight-plasmid system for rapid generation of influenza virus vaccines. *Vaccine.* **20**:3165-70.
15. **Hoffmann, E., G. Neumann, Y. Kawaoka, G. Hobom, and R. G. Webster.** 2000. A DNA transfection system for generation of influenza A virus from eight plasmids. *Proc. Natl. Acad. Sci. U. S. A.* **97**:6108-6113; 6108.
16. **Imai, H., K. Shinya, R. Takano, M. Kiso, Y. Muramoto, S. Sakabe, S. Murakami, M. Ito, S. Yamada, M. t. Q. Le, C. A. Nidom, Y. Sakai-Tagawa, K. Takahashi, Y. Omori, T. Noda, M. Shimojima, S. Kakugawa, H. Goto, K. Iwatsuki-Horimoto, T. Horimoto, and Y. Kawaoka.** 2010. The HA and NS Genes of Human H5N1 Influenza A Virus Contribute to High Virulence in Ferrets. *PLoS Pathog.* **6**:e1001106.
17. **Katz, J. M., X. Lu, T. M. Tumpey, C. B. Smith, M. W. Shaw, and K. Subbarao.** 2000. Molecular correlates of influenza A H5N1 virus pathogenesis in mice. *J Virol.* **74**:10807-10.
18. **Long, J., D. Peng, Y. Liu, T. Wu, and X. Liu.** 2008. Virulence of H5N1 avian influenza virus enhanced by a 15-nucleotide deletion in the viral nonstructural gene. *Virus Genes.* **36**:471-478; 471.
19. **Neumann, G., M. Hatta, and Y. Kawaoka.** 2003. Reverse genetics for the control of avian influenza. *Avian Dis.* **47**:882-7.
20. **Noah, D. L., R. M. Krug, and a. A. J. S. Karl Maramorosch.** 2005. Influenza Virus Virulence and Its Molecular Determinants. *Adv. Virus Res.* **65**: 121-145.
21. **Pleschka, S., S. R. Jaskunas, O. G. Engelhardt, T. Zu'rcher, P. Palese, and A. Garcí'a-Sastre.** 1996. A Plasmid-Based Reverse Genetics System for Influenza A Virus. *J. Virol.* **70**:4188-4192; 4188.

22. **Wasilenko, J. L., C. W. Lee, L. Sarmiento, E. Spackman, D. R. Kapczynski, D. L. Suarez, and M. J. Pantin-Jackwood.** 2008. NP, PB1, and PB2 Viral Genes Contribute to Altered Replication of H5N1 Avian Influenza Viruses in Chickens. *J. Virol.* **82**:4544-4553. doi: 10.1128/jvi.02642-07.
23. **Wit, E. d., M. I. J. Spronken, G. Vervaet, G. F. Rimmelzwaan, A. D. M. E. Osterhaus, and R. A. M. Fouchier.** 2007. A reverse-genetics system for *Influenza A virus* using T7 RNA polymerase. *J. Gen. Virol.* **88**:1281-1287.
24. **Barnard, D. L.** 2009. Animal models for the study of influenza pathogenesis and therapy. *Antiviral Res.* **82**:A110-22.
25. **Iwasaki, T., S. Itamura, H. Nishimura, Y. Sato, M. Tashiro, T. Hashikawa, and T. Kurata.** 2004. Productive infection in the murine central nervous system with avian influenza virus A (H5N1) after intranasal inoculation. *Acta Neuropathol.* **108**:485-92.
26. **Lipatov, A. S., S. Krauss, Y. Guan, M. Peiris, J. E. Rehg, D. R. Perez, and R. G. Webster.** 2003. Neurovirulence in mice of H5N1 influenza virus genotypes isolated from Hong Kong poultry in 2001. *J. Virol.* **77**:3816-23.
27. **Lu, X., T. M. Tumpey, T. Morken, S. R. Zaki, N. J. Cox, and J. M. Katz.** 1999. A mouse model for the evaluation of pathogenesis and immunity to influenza A (H5N1) viruses isolated from humans. *J. Virol.* **73**:5903-11.
28. **Rowe, T., D. S. Cho, R. A. Bright, L. A. Zitzow, and J. M. Katz.** 2003. Neurological Manifestations of Avian Influenza Viruses in Mammals. *Avian Diseases.* **47**:1122-1126.
29. **Abrahams, A.** 1919. Discussion on Influenza. *Proc. R. Soc. Med.* **12**:97-102.
30. **Hamer, W. H.** 1919. Discussion on Influenza. *Proc. R. Soc. Med.* **12**:24-26.
31. **Kapila, C. C., S. Kaul, S. C. Kapur, T. S. Kalayanam, and D. Banderjee.** 1958. Neurological and hepatic disorders associated with influenza. *Br. Med. J.* **2**:1311-1314.
32. **Turner, E. B.** 1919. Discussion on Influenza. *Proc. R. Soc. Med.* **12**:76-90.
33. **Gu, J., Z. Xie, Z. Gao, J. Liu, C. Korteweg, J. Ye, L. T. Lau, J. Lu, Z. Gao, B. Zhang, M. A. McNutt, M. Lu, V. M. Anderson, E. Gong, A. C. H. Yu, and W. I. Lipkin.** 2007. H5N1 infection of the respiratory tract and beyond: a molecular pathology study. *The Lancet.* **370**:1137-1145.
34. **de Jong, M. D., B. V. Cam, P. T. Qui, V. M. Hien, T. T. Thanh, N. B. Hue, M. Beld, L. T. Phuong, T. H. Khanh, N. V. V. Chau, T. T. Hien, D. Q. Ha, and J. Farrar.** 2005. Fatal Avian Influenza A (H5N1) in a Child Presenting with Diarrhea Followed by Coma. *N. Engl. J. Med.* **352**:686-691. doi: doi:10.1056/NEJMoa044307.

35. 1970. Neurological complications of influenza. *Br. Med. J.* **1**:248-249.
36. **Glaser, C. A., K. Winter, K. DuBray, K. Harriman, T. M. Uyeki, J. Sejvar, S. Gilliam, and J. K. Louie.** 2012. A population-based study of neurologic manifestations of severe influenza A(H1N1)pdm09 in California. *Clin. Infect. Dis.* **55**:514-520. doi: 10.1093/cid/cis454; 10.1093/cid/cis454.